FINAL REPORT

Identifying Indicators of State Change and Forecasting Future Vulnerability in Alaskan Boreal Ecosystems

SERDP Project RC-2109

AUGUST 2016

Dr. Edward Schuur
A. David McGuire
Jill Johnstone
Michelle Mack
Scott Rupp
Eugenie Euskirchen

Post-Doctoral Associates
April Melvin
Helene Genet
Amy Breen

Graduate Students
Xanthe Walker
Mélanie Jean
Matthew Frey
University of Florida

SERDP
DOD ▪ EPA ▪ DOE

Page Intentionally Left Blank

Page Intentionally Left Blank

REPORT DOCUMENTATION PAGE

Form Approved
OMB No. 0704-0188

1. REPORT DATE *(DD-MM-YYYY)*	**2. REPORT TYPE**	**3. DATES COVERED** *(From - To)*
21-11-2016	Final	Mar 2011-Nov 2016

4. TITLE AND SUBTITLE
Identifying Indicators of State Change and Forecasting Future Vulnerability in Alaskan Boreal Ecosystems

5a. CONTRACT NUMBER
SERDP #2109

5b. GRANT NUMBER

5c. PROGRAM ELEMENT NUMBER

6. AUTHOR(S)
Schuur, Edward, A.G.; McGuire, Anthony, D.; Mack, Michelle, C. Rupp, Scott; Johnstone, Jill; Euskirchen, Eugenie; Melvin, April; Genet, Helene; Breen, Amy; Walker, Xanthe; Jean, Melanie; Frey, Matthew

5d. PROJECT NUMBER

5e. TASK NUMBER

5f. WORK UNIT NUMBER

7. PERFORMING ORGANIZATION NAME(S) AND ADDRESS(ES)
University of Florida
219 Grinter Hall, Box 115500

8. PERFORMING ORGANIZATION REPORT NUMBER

9. SPONSORING / MONITORING AGENCY NAME(S) AND ADDRESS(ES)
Strategic Environmental Research and Developmental Program
901 N. Stuart St. Suite 103
Arlington, VA, 22203

10. SPONSOR/MONITOR'S ACRONYM(S)
SERDP

11. SPONSOR/MONITOR'S REPORT NUMBER(S)

12. DISTRIBUTION / AVAILABILITY STATEMENT

13. SUPPLEMENTARY NOTES

14. ABSTRACT
This report summarizes empirical and modeling studies to improve understanding of the mechanistic linkages among fire, vegetation, the soil organic layer, and permafrost thaw across interior Alaska. Primary objectives: (1) Determine mechanistic links among fire, soils, permafrost, and vegetation succession in order to develop and test field-based ecosystem indicators that can be used to directly predict ecosystem vulnerability to state change and (2) Forecast landscape change in response to projected changes in climate, fire regime, and fire management. Results show that increased wildfire severity increases permafrost thaw in the near-term and influences seedling establishment and successional trajectories, shifting forest composition from black spruce ecosystems to those comprised of deciduous tree species. Long term, this shift has consequences for understory moss growth and organic soil re-accumulation, thereby directly influencing permafrost recovery. Forest management approaches employed will also impact successional trajectories and vulnerability of permafrost to thaw

15. SUBJECT TERMS
Alaska, boreal forest, permafrost, vulnerability, fire management, modeling, soil

16. SECURITY CLASSIFICATION OF:			**17. LIMITATION OF ABSTRACT**	**18. NUMBER OF PAGES**	**19a. NAME OF RESPONSIBLE PERSON**
a. REPORT	**b. ABSTRACT**	**c. THIS PAGE**			Edward Schuur
					19b. TELEPHONE NUMBER *(include area code)* 928-523-3559

Standard Form 298 (Rev. 8-98)
Prescribed by ANSI Std. Z39.18

Page Intentionally Left Blank

Table of Contents

List of Tables (Numbered by Task)

List of Figures (Numbered by Task)

List of Acronyms

ALD	Active layer depth
ALFRESCO	Alaska Frame-Based Ecosystem Code
ALT	Active layer thickness
AR	Autocorrelation
BD	Basal diameter
BRT	Boosted regression tree
C	Carbon
Ca	Calcium
CCCMA	Canadian Centre for Climate Modeling and Analysis
CCSM4	Community Climate System Model 4.0
CMI	Climate moisture index
CMIP3	Coupled model intercomparison project phase 3
CO_2	Carbon dioxide
CPCRW	Caribou Poker Creeks Research Watershed
CWD	Coarse woody debris
cv	cross validation
D	Dry upland
DBH	Diameter at breast height
DoD	Department of Defense
DOS-TEM	Dynamic Organic Soil version of the Terrestrial Ecosystem Model
ECHAM	European Centre Hamburg Model
FMO	Fire management officers
FMPO	Fire management planning options
GCM	Global climate model
GIPL	Geophysical Institute Permafrost Laboratory
GWP	Global warming potential
HR	Heterotrophic respiration
HSD	Honest significant difference
K	Potassium
KCl	Potassium chloride
LOESS	Locally weighted scatterplot smoothing
LTER	Long-term ecological research
M	Moist lowland
MCMC	Markov Chain Monte Carlo
Mg	Magnesium
MRI-CGCM3	Meteorological Research Institute Coupled General Circulation Model v3.0
MS	Mean sensitivity
N	Nitrogen
NDVI	Normalized difference vegetation index
NECB	Net ecosystem carbon balance
Nf	North facing midslope
NH_4	Ammonium
NMDS	Non-metric multidimensional scaling
NO_3	Nitrate
NPP	Net primary productivity

NSF	National Science Foundation
NSP	Near-surface permafrost
OM	Organic matter
P	Phosphorus
PB	Paper birch/black spruce stands
PET	Potential evapotranspiration
PFRR	Poker Flats Research Range
PO_4^{2-}	Phosphate
PRISM	Parameter-elevation regressions on independent slopes model
PSM	Plant-soil-microbial
R	Correlation between trees
RCP	Representative concentration pathway
ROL	Residual organic layer
S	South facing midslope
SC	Stuart Creek
SERDP	Strategic Environmental Research and Development Program
SLA	Specific leaf area
SNAP	Scenarios Network for Alaska and Arctic Planning
SNR	Signal to noise ratio
SOL	Soil organic layer
SON	Statement of need
SRES	Special Report on Emissions Scenarios
TA	Trembling aspen/black spruce stands
TSLF	Time since last fire
USGS	United States Geological Survey
VPDB	Vienna PeeDee belemnite
WC	Willow Creek
ZIP	Zero-inflated Poisson

Keywords

Alaska paper birch, base cations, *Betula neoalaskana*, black spruce, boreal forest, carbon, climate change, dendroclimatology, drought stress, ecological modeling, feedbacks, fire, fire effects, fire management, fire severity, forest regeneration, growth-climate responses, invasive species, model coupling, nitrogen, nutrient cycling, permafrost, *Picea mariana*, plant-soil-microbial feedbacks, radiocarbon, stable carbon isotopes, seedling establishment, succession, soil, succession, tree-rings, tree species, vegetation dynamics

Acknowledgements

We thank the Northern Scientific Training Program of Indian and Northern Affairs Canada, the Natural Science and Engineering Council of Canada, the Bonanza Creek LTER (NSF), the Alaska Land Carbon Program (USGS) and the Integrated Ecosystem Model for Alaska and Northwest Canada Project (USGS and U.S. Fish and Wildlife Service) for providing additional support. We thank Gordon Amundson, Brian Young, Dan Rees, Randi Jandt, and Eric Miller for assistance in identifying and accessing fire management areas. Grace Crummer and Julia Reiskind provided analytical assistance, Heather Alexander generously shared unpublished tree carbon and nitrogen concentration data, and Rosvel Bracho provided guidance in setting up the incubation experiment and processing acquired data. We also thank Camilo Mojica, Simon McClung, Peter Ganzlin, Demetra Panos, Bethany Avera, Alicia Sendrowski, Samantha Miller, Fraser Baalim, Nicolas Boldt, Scott Dudiak, Dominik Oliver, and Patricia Tomchuk for assistance with fieldwork, as well as others in the Northern Plant Ecology Lab and additional undergraduate laboratory assistants and the University of Florida.

Abstract

The boreal region of Interior Alaska is changing. Greater occurrence of high severity fires is shifting forests from mono-dominant black spruce stands to deciduous and mixed forest ecosystems. This shift is altering the relationships between vegetation, soils and permafrost stability, and may lead to long-term changes in ecosystem structure and function.

Objectives: In this report, we summarize an extensive suite of empirical studies with modeling to improve understanding of the mechanistic linkages among fire, vegetation, the soil organic layer (SOL), and permafrost thaw across interior Alaska. Our primary objectives include: (1) Determine mechanistic links among fire, soils, permafrost, and vegetation succession in order to develop and test field-based ecosystem indicators that can be used to directly predict ecosystem vulnerability to state change and (2) Forecast landscape change in response to projected changes in climate, fire regime, and fire management.

Technical Approach: We conducted fieldwork across interior Alaska in numerous burned sites of varying ages that spanned a wide range of forest tree species and understory composition to address specific tasks outlined in the original grant proposal. These empirical studies included quantification of aboveground tree biomass, tree seedling germination and establishment, understory moss growth, understory vegetation composition, SOL mass and carbon (C) and nutrient cycling and pool sizes and fluxes, permafrost thaw, and impacts of forest management on ecosystem processes. These analyses relied primarily on existing methodologies that have been shown previously to be effective in evaluating similar research questions. Results of these studies informed the development of a predictive model of post-fire reduction in SOL thickness, and incorporation of this model into an existing model (Dynamic Organic Soil version of the Terrestrial Ecosystem Model, DOS-TEM), to improve understanding of the combustion of the SOL and permafrost degradation following fire, vegetation succession following fire, and post-fire soil organic layer recovery and relationship to permafrost thaw. A model framework was then developed to couple the Alaska Frame-Based Ecosystem Code (ALFRESCO) with DOS-TEM. ALFRESCO was then used to investigate how changing fire management planning options within military training lands would influence the future fire regime and concurrent boreal forest vegetation dynamics.

Results: Results of our study support and expand upon the understanding of the linkages among fire, soils, permafrost, and vegetation succession across multiple analytical scales. Our seedling establishment study showed that seedling germination post-fire is affected by complex interactions among moisture, seed size, elevation and latitude, post-fire SOL thickness, and time since the last fire. Seed germination trials showed consistently high germination on mineral soil substrate.

Our study also highlighted large differences in ecosystem C and nutrient distribution and cycling in deciduous and conifer stands. Black spruce and Alaska paper birch forest exhibited similar ecosystem C stocks, however black spruce contained greater C in soils while birch contained larger quantities in aboveground tree biomass. Generally, nutrient cycling was much faster in the birch stands relative to spruce. For the moss transplants and litter manipulation study conducted at this site, we observed after one year that the marked mosses had adapted their growth form to the environmental conditions associated with their new stand, and after two years of treatments

we were able to detect impacts of the leaf litter treatments in both forest types, with larger litter inputs resulting in less moss growth. This result suggests that shifts towards greater deciduous tree species dominance may reduce understory moss cover, reducing SOL accumulation and increasing vulnerability of permafrost to thaw. Further, a divergence in total bryophyte cover across a mix of stand types and successional stages showed a divergence between the coniferous (spruce) and deciduous (birch and aspen) successional trajectories that occurred between 20 and 40 years since fire. This divergence seemed to coincide with major changes in leaf litter cover associated with the canopy type.

We observed a decrease in the proportion of spruce relative to total trees from the pre-fire to the post-fire stand in nearly all examined stands, indicating shifts from black spruce dominated stands to mixed or deciduous dominated stands. Forest stands most likely to show the largest change in black spruce dominance were those that had relatively thin post-fire SOL depths and showed dendroclimatic indications of recent drought stress. These sites were generally located at warmer and drier landscape positions, suggesting a landscape pattern of lower resilience to disturbance compared to sites in cool and moist locations.

Management practices designed to reduce the likelihood of fire spread into inhabited areas reduce ecosystem C pools, especially when shearblading methods were used. The greatest C losses were from aboveground pools, however the practice was also associated with high deciduous tree species establishment in areas previously dominated by black spruce and an increase in thaw depth. Thinning also impacted ecosystem processes, but with moderate impacts. These results suggest increased use of shearblading could contribute further to shifts successional trajectories across interior Alaska.

Our predictive model of SOL combustion identified landscape drainage as the primary driver of the relative amount of SOL burned during fire, with permafrost thaw initiating with smaller SOL losses in upland sites than lowland sites. When SOL was allowed to re-accumulate post-fire, less permafrost degradation occurred and at the lowland site, full recovery of initial thermal state was regained within 40 years. Wildfire modeling showed that fire frequency and extent are projected to increase across the majority of future climate combinations for the northern boreal forest region of Alaska, despite the increase of less flammable deciduous vegetation and the reduction of more flammable late successional spruce forest. Concurrently, the distribution of near surface permafrost is projected to decrease in the region, driven primarily by the effect of warming and fire disturbance on permafrost thaw. Modeling an experimental alternative fire management planning scenario showed that changing all military lands within the study area from limited to full protection led to a consistent increase in the number of fires, yet a decrease in the amount of area burned through 2100 compared to the status quo. This led to an increase in the amount of late successional coniferous forest present on the landscape, in contrast to maintaining the current fire management scenario, which leads to more early successional deciduous forest on the landscape through the end of the century

Benefits: Collectively, our results support the understanding that increased wildfire severity and loss of the SOL increases permafrost thaw in the near-term and influences seedling establishment and successional trajectories, shifting forest composition from black spruce dominated ecosystems to those comprised of deciduous tree species. In the longer-term, this shift has

consequences for understory moss growth and SOL re-accumulation, thereby directly influencing permafrost recovery post-fire. Change in tree species composition also alters C and nutrient cycling rates and the partitioning of ecosystem C stocks into above and belowground pools. Finally, forest management approaches employed will further impact successional trajectories and vulnerability of permafrost to thaw.

Objectives

This research was designed to improve understanding of the mechanistic connections among vegetation, the (SOL), and permafrost ground stability in Alaskan boreal ecosystems. Understanding these linkages is critical for projecting the impact of climate change on permafrost in ecosystems that are subject to abrupt anthropogenic and natural disturbances (fire) to the organic layer. This research responds to several elements within the SERDP Statement of Need (SON) by using Department of Defense (DoD) and surrounding lands in Interior Alaska to explore and test the conceptual and mechanistic basis for threshold change and regime shift in the Alaskan boreal forest **(SON 4)**. The primary objectives of this study were to (**1) Determine mechanistic links among fire, soils, permafrost, and vegetation succession in order to develop and test field-based ecosystem indicators that can be used to directly predict ecosystem vulnerability to state change** and (**2) Forecast landscape change in response to projected changes in climate, fire regime, and fire management.**

We hypothesized that major threshold change is more likely to occur in ecosystems that are already at the margins - forests that, historically, are already stressed - and where fires are at the extremes in terms of size or severity. We expected that severe fires occurring in forest stands that have not experienced deep burning as part of the recent fire cycle would consume a larger proportion of the SOL and have the greatest potential for permafrost destabilization. We also hypothesized that drought-stressed forest stands were more likely to shift to an alternate, deciduous, successional trajectory after fire and that moss percent cover and organic soil re-accumulation would be negatively related to the percent cover of deciduous canopy tree species.

Based on the understanding of these mechanisms developed from field measurements, we then used spatially explicit numerical modeling to predict the response of permafrost ground and disturbance regimes to projected changes in climate **(SON 2)**. These modeling approaches provide a dynamic mapping tool to help land managers identify those DoD lands that are resistant and those that are vulnerable to permafrost degradation under scenarios of disturbance and climate change **(SON 1, 3)**. In addition, these approaches will allow land managers to explore the consequences of interactive changes in climate and management for vegetation composition, establishment of invasive species, fire dynamics, and ecosystem structure and function **(SON 3)**.

Background

The boreal region of Interior Alaska comprises a mosaic of evergreen, deciduous, and mixed forest ecosystems interspersed with herbaceous or shrubby wetlands. These ecosystems are often underlain by perennially frozen permafrost soils, and range across gradients of soil moisture that vary with topography, from very poorly drained to well drained soils. Evergreen stands dominated by black spruce (*Picea mariana*) are the most abundant forest type in Interior Alaska and are frequently underlain by permafrost (Van Cleve et al., 1991). Black spruce forests are highly flammable and typically burn during stand replacing fires every 70-130 years (Johnstone et al., 2010a). Fire offers an opportunity for plant community reorganization that can be strongly influenced by fire characteristics (Chapin et al. 2006). After high severity fires, mono-dominant spruce stands can give way to fully deciduous stands where permafrost degrades or is lost completely. After less-severe fires, spruce replaces itself and permafrost can stabilize and recover over succession. Stable cycles of fire disturbance and spruce self-replacement have persisted for over 8kya, since black spruce came to dominate the evergreen forests of Interior Alaska (Chapin et al. 2006). Forecasted changes in future climate, however, could affect the stability of boreal ecosystems directly, by warming permafrost in undisturbed ecosystems, and indirectly, through an increase in fire size and severity (Kasischke and Turetsky, 2006). These direct and indirect effects of climate warming could, together, drive a regional fire regime shift and alter the distribution of boreal ecosystems, changing the landscape of Interior Alaska and the goods and services it provides to humans (Chapin et al., 2008).

Understanding permafrost dynamics is central for evaluating potential threshold change faced by boreal ecosystems (Schuur et al. 2008). Because permafrost ground includes large volumes of ice, permafrost thaw can trigger major changes in surface topography- known as thermokarst - as ice melts and the ground surface subsides (Shur and Jorgenson 2007). As the freezing point threshold is passed, permafrost thaw and ground subsidence can have profound biological and physical effects on natural ecosystems. Vegetation is dependent on the surface water table created by permafrost, so much so that ground subsidence and redistribution of soil moisture can have much larger effects on ecological functioning than changes in ground temperature alone (Schuur et al., 2009). In addition, changes in the ground structure due to loss of ground ice have catastrophic effects on facilities, infrastructure, and military testing and training. Permafrost temperature, thickness, and geographic continuity are controlled to a large extent by the surface energy balance and thus vary strongly with latitude (Brown et al. 1998). Interior Alaska lies within the discontinuous permafrost zone, where regional temperature is not low enough to sustain permafrost everywhere and existing permafrost is especially susceptible to observed and anticipated climate warming (Hinzman et al. 2005). Here, permafrost stability and distribution is a function of local factors including the vegetation structure and, in particular, by the characteristics of the thick organic soil layer present in many boreal ecosystems. Organic soil layers buffer the response of permafrost to climate variability and delay heat propagation into the soil (Osterkamp et al. 1994). Thus, ecosystem structure, particularly the thickness of the soil organic layer as well as rapid changes in that layer via fire or human activities, can have profound effects on permafrost stability and its degradation in a changing climate.

Plant-soil-microbial (PSM) feedbacks between vascular plants, mosses, and microbial decomposition maintain deep organic soils in the black spruce forests and wetlands of Interior Alaska. This internal feedback has been a key source of ecosystem resilience under the historical

fire regime; moist, cold soils, poorly drained due to permafrost, burn at low severity and create a seedbed that favors the re-establishment of black spruce (Johnstone and Chapin, 2006) and the recovery of the organic soil layer. In extreme fires, however, these soils can burn deeply (Boby et al., 2010). When less than ~5 cm of organic soil remains after fire, deciduous tree species such as aspen and birch establish at high densities (Johnstone et al., 2010b) and catalyze a switch to alternate plant successional trajectories that are dominated or co-dominated by deciduous trees. Here, a new PSM feedback domain emerges where shallow organic soils are maintained by rapidly decomposing litter from highly productive deciduous species. Degradation and loss of permafrost is likely once this threshold is reached (Yoshikawa et al., 2002), leading to a state change that permanently alters ecosystem structure and function. Shifts between domains of spruce vs. deciduous dominance and the resulting effects on permafrost have large implications for ecosystem productivity and carbon storage (Mack et al., 2008), feedbacks to regional climate (Randerson et al., 2006), the goods and services that boreal ecosystems provide to humans (Chapin et al., 2008), including ecosystem resilience to anthropogenic activities such as those related to military operations. In addition, fire and shifts in PSM feedbacks may also create new opportunities for the spread of invasive plant species that capitalize on soil disturbance and associated warming and reduced acidity of the soil (Conn et al. 2008). Because the organic soil layer plays this dual role, mediating climate effects on the ground thermal regime and controlling vegetation successional dynamics, it is a key indicator for understanding resilience and state change of boreal ecosystems on permafrost soils.

Managing interactions among fire, vegetation, and permafrost: Fire management has the potential to influence the natural fire regime by determining the spatial patterning and timing of fire occurrence, and thus the successional state of the ecosystems within the management area. Controlled burning of selected evergreen stands can increase deciduous stand frequency on the landscape with the potential for altering spread of natural wildfires because of the differential flammability of boreal ecosystems (Chapin et al. 2006). White spruce is generally less flammable than black spruce, as illustrated by a long history during the Holocene of white spruce dominance (8-10 kya) with low fire frequency (Higuera et al. 2009). However, the juxtaposition of black and white spruce forest stands on the landscape means that white spruce often burns in tandem within the fire regime of black spruce, as do shrubby or herbaceous wetlands where surface organic soils can serve as a ground fuel to carry fire during dry months (Turetsky et al. 2002). In contrast, deciduous or early successional stands have little ground fuel and while they can burn, they often reduce the spread of fire relative to other ecosystem types (Cumming, 2001). Human manipulation of the fire cycle via lower intensity controlled burns has the potential to reduce the risk of high intensity large fires - the type most likely to burn the organic soil deeply and cause threshold changes in permafrost and vegetation - by creating a patchwork of early successional vegetation that could reduce fire spread under some conditions. However, fire management also includes the installation of fire containment lines (firebreaks). Although these affect a smaller area than controlled burns, containment lines can be a much more intense disturbance of the vegetation and the organic soil layer, causing threshold changes in permafrost that could alter landscape patterns of drainage (L. A. Viereck, unpublished data). In sum, fire management has the potential to reduce the risk of the severe fires that are most likely to cause future state changes in boreal ecosystems, but has associated localized disturbances that are potentially novel to these ecosystems.

The DoD manages approximately 7,200 km^2 of land in the State of Alaska. Over 95% of Alaskan military land is located in the boreal forest of Interior Alaska, associated with Fort Wainwright and Eielson Air Force Base near the city of Fairbanks, and with Fort Greeley near the city of Delta Junction. These lands cross two ecologically, economically, and culturally important boreal eco-regions: the Tanana-Kuskokwim Lowlands, which covers about 52,000 km2 of Interior Alaska, and the Yukon-Tanana Uplands, which covers about 102,000 km^2. Fire is the most widespread natural disturbance in these regions. The Yukon-Tanana Uplands have the highest incidence of lightning strikes in Alaska and the Yukon Territory (Dissing and Verbyla 2003). In addition to high natural sources of ignition, these military lands also experience high human ignition pressures due to their proximity to the road system and urban areas, and the frequency of military testing and training activities. Thus, these military lands are designated in a distinct fire management zone by the Alaska Interagency Coordination Center so that local fire management officers (FMO) can address the unique needs of military land management. Because of this fire management designation, DoD lands offer the potential to understand both the threshold changes associated with severe fires, and the potential for fire management to either contribute to or mitigate vulnerability of DoD lands to threshold change in ecosystem state.

Task Description: Methods, Results, and Discussion

Task 1: Field sampling of wildfire site network

T1: Materials and methods

Field sampling wildfire plots for permafrost, soils, seedlings

In summer 2011, our field crew resampled the black spruce wildfire network that was established following the 2004 severe fire year in Alaska. The study area consisted of three large burn complexes located in interior Alaska. The burns originated from multiple fire starts that occurred during the hot and dry summer of 2004. In the year after the fire, we selected 38 stands that were dominated by black spruce prior to burning for detailed experiments on post-fire regeneration, including addition of boreal tree seed and outplantings of seedlings started in the greenhouse. Measurements of environmental characteristics, fire severity (Boby et al., 2010), post-fire seed rain (Johnstone et al. 2009), and initial plant recovery were made at the sites in 2005-2008 (Johnstone et al., 2010b; Bernhardt et al., 2011). Because these sites span a wide range of soil moisture (from sub-xeric to sub-hygric), elevation (lowland valley forests to alpine treeline) and fire severity (~0 to ~100% SOL consumption), they provide an excellent suite of sites to test and quantify the effects of fire severity on plant and soil processes across broad landscape gradients. Our initial measurements indicated that severe burning at many sites has interrupted the feedbacks that favor black spruce stand replacement, and stimulated the initiation of alternative successional trajectories via increased recruitment of deciduous tree species (Johnstone et al., 2010b). However, it remains unclear whether the patterns of initial seedling recruitment are likely to be maintained, augmented, or diluted by longer-term effects of site conditions and fire severity on soil thermal regime, nutrient pool sizes, rates of nutrient cycling, and multi-year growth and survival of tree seedlings after fire.

Sampling activities for this SERDP project built off the previous records of environmental conditions at the sites and included re-measurements of SOL and active layer depth along permanent monitoring transects, assessment of tree seedling recruitment, survival, growth, and nutrient status, as well as harvest of an outplanting experiment to test for controls over establishment of dominant tree species.

Depth of the SOL and depth to permafrost were re-measured at 5 m intervals along two 25 m transects at each site. To measure SOL depth, a knife was used to remove a ~10 cm x 10 cm intact square of organic material, then a ruler was used to measure the depth of each horizon. Depth to permafrost was estimated at a location adjacent to the organic soil measurement by inserting a 2 m steel probe into the ground and recording the depth at which frozen soil was encountered.

Laboratory preparation and analysis of samples

In 2011-2012, we processed ~10,000 seedlings from the outplanting experiment in the lab, separating and weighing biomass in categories of current year and previous year tissues to obtain estimates of annual and total growth. Foliage samples from harvested seedlings of 5 tree species were ground and analyzed for C and N concentration.

We combined our seedling count data with another, similar dataset from similar black spruce forests in Yukon Territory (Brown 2011). This provided us with a broad, regional dataset of 55 sites with experimental seeding treatments (Table 1.1). We characterized variations in environmental factors at each site based on measured variables of latitude, elevation, and soil moisture availability. We characterized vegetation legacies and the influence of fire history on seed availability based on seeding treatments, and by measuring a) basal area of pre-fire tree species (an indicator of the size of the black spruce aerial seedbank; Greene et al. 1999), b) distances from unburned edges (an indicator of potential seed dispersal from unburned stands; Greene and Johnson 2000), and c) the age of the stand when it burned (a measure of regeneration potential; Viglas et al. 2013). We estimated pre-fire stand age as a proxy for time since the last fire (TSLF) based on averaged basal ring counts of 5 randomly selected trees at each site. Finally, we characterized post-fire seedbed conditions based on site-level estimates of SOL thickness.

Data analysis and synthesis

Data representing seedling counts, size, and harvested biomass were assembled and catalogued for all years of available data (2005-2011). We used seedling counts and size measurements obtained in 2011 to verify and quality check counts from previous years in 2005, 2006, and 2008. We systematically checked all of the seedling data for inconsistencies and errors by plotting observed data points in relation to year of sampling or field measurements of seedling size, and examining residuals from predictive models for each species and year. Any observed outliers were double-checked against the original field notes and raw data records. If a mistake was found, it was corrected and noted in the data file. Data points with irreconcilable errors were removed and noted (< 1% of total data points); some negative values for seedling size were removed because they represented dieback, and these are also noted in the data files.

We developed allometric equations to predict biomass of all unharvested individuals for each measurement year from field measurements of tree seedling diameter and height. Allometric equations were developed using log transformed data to linearize relationships between diameter or height and biomass; for new growth, this was log(x+c) to deal with zero values, where c is the minimum non-zero value observed. We fit linear models using the 'lm' function in the base package of R statistical software (version 3.0.3; R Core Team 2014), and the best fits were selected based on AIC, F statistic, and residual standard error values (Tables 1.2 and 1.3). For 2006 and 2008 biomass estimations, we used allometric equations containing only diameter measurements; however for 2011 biomass we used allometric equations that included both diameter and height. This was because new growth height was measured in 2006 and 2008, and total height was measured in 2011. Using our model coefficients and fitted values, estimated current year and total aboveground biomass (g dry mass) for each species in every measurement year. Biomass predictions were based on field measurements of stem diameter and height, and allowed us to estimate seedling growth from the initial measurements in 2006 to the harvest in 2011. These equations are of high accuracy, with R^2 values generally above 0.8 (Tables 1.2 and 1.3).

Our primary analysis assessed the relative importance of vegetation legacies (seed availability), environmental conditions, and fire history on patterns of post-fire seedling recruitment. The response data of interest in our analyses were counts of tree seedlings that germinated and

survived the first 3 years after fire in experimental plots (seedling recruits). Analyses of the seedling count data required statistical models that accounted for zero-inflation, and the multi-level structure of the data (experimental plots nested within sites). In addition, we had multiple potential predictor variables that could be included as covariates in a model, and wished to select the important ones. Given the complexity of our analyses and characteristics of our data, we collaborated with statisticians to develop zero-inflated models using novel approaches for variable selection and a Bayesian estimation of model parameters (Brown et al. 2015). We used a generalized model based on the Poisson distribution, and added a zero-inflation component to account for zeros observed in excess of those expected under the Poisson model (Zuur et al. 2009). In the resulting zero-inflated Poisson (ZIP) mixed model, zeros are modeled as a result of two separate processes, those arising from the logistic model of zero-inflation and those arising from the Poisson count model. Site-specific random effects were included in the ZIP models to account for heterogeneity among different sites and the dependence between the plots nested within the same site. We used a Lasso method (Tibshirani 1996) to select the variables in the Poisson and zero-inflation portions of the mixed models. All covariates were transformed to z-scores prior to model selection to facilitate comparison of model coefficients. We then used Bayesian Markov Chain Monte Carlo (MCMC) to conduct model estimation (Ellison 2004). Our analyses were performed in R (version 3.0.3; R Core Team 2014); further details may be found in Brown et al. (2015).

Given the substantial time investment in completing the seedling recruitment analyses, we have not yet compiled a formal analysis of the seedling biomass and nutrient content data for publication. Our plan is to use structural equation modeling to estimate the relative influence of site environmental conditions, residual SOL depth, and soil nutrient availability on seedling growth and foliar nutrient content for the four tree species used in our outplanting experiments. Co-I Johnstone will lead these analyses and development of an associated peer-reviewed publication during an upcoming research sabbatical in July-December 2016.

T1: Results and discussion

Across the sites measured in 2005 and 2011, the mean organic layer depth was 3 cm less in 2011 and the thaw depth had increased by 17 cm (Figure 1.1). These results suggest that in the 6 years following the severe 2004 fire year, there has been no re-accumulation of soil organic matter and possibly a small loss. In general, there has also been permafrost thaw. We are continuing to explore the relationship between SOL depth and permafrost across sites using statistical models that will allow us to assess inter-site variability in responses, with a focus on important environmental variables including the proportion of organic material lost during the fire and site drainage class.

Analyses of seedling biomass demonstrate a large range of variation in total and new (current year) biomass among species and individual seedlings (Figure 1.2). This puts us in a very good situation to explore the factors that are likely to explain this variation, including hypothesized effects of fire severity and post-fire organic layer depth on seedling growth. Due to time constraints, these analyses will be completed later in 2016.

Our analyses of seedling recruitment after fire demonstrate multiple effects of pre-fire legacies and environmental factors on post-fire recruitment and hence, initial assembly of the boreal tree

community (Brown et al. 2015). Replicated seeding experiments were broadly distributed across environmental and disturbance gradients and allowed us to separate legacy effects on seed availability from environmental constraints that shape potential tree recruitment after fire. We found that legacy effects played a dominant role in determining potential tree recruitment following disturbance. For example, most obvious feature of observed seedling counts was the high proportion of zero counts among both seeded and control plots for all species. However, adding seed reduced the probability of zeros (logistic models) and increased recruitment (count models) of all species (Figure 1.3, Table 1.4). Seed addition treatments had the strongest effect on overall probability of occurrence for black spruce and Alaskan birch, and the least effect on white spruce. In the absence of experimental seed, the probability of seedlings recruiting in a 50 cm x 50 cm plot was about 30% for spruce (with most natural seedlings likely black spruce), 20% for Alaskan birch, and 10% for aspen (Figure 1.3). Consistent responses to seed addition provide evidence that seed limitation is likely to affect recovery patterns of all four tree species, despite expectations of black spruce deriving ample seed from serotinous cones of the pre-fire stand (e.g. Greene et al. 1999). Our results indicate that available safe sites for seedling recruitment are not saturated even for the most locally abundant species.

When constraints on seed availability were relaxed, environmental filtering of species-specific regeneration niches determined patterns of recruitment, with each species showing shared and unique responses to environmental factors (Figure 1.4, Table 1.4). The probability of seedling occurrence was positively correlated with moisture for all four species, in that wetter areas had fewer zeros than drier areas (Figure 1.4A,B). Moisture was also an important predictor of black spruce counts, but did not predict counts of other species (Table 1.4A). The sensitivity of boreal tree species to moisture in our study covaried with seed size: small-seeded species (aspen) were more sensitive than large-seeded species (white & black spruce) to variations in moisture. All species responded in the same direction, however, indicating that access to soil moisture is a common constraint among species. Increased sensitivity of small seeded species to moisture limitation likely reflects a reduced ability to reach stable moisture supplies in deeper organic soils (Hesketh et al. 2009). Interestingly, this sensitivity does not reflect landscape sorting of forest types dominated by these different species. Mapped distributions of trembling aspen in Alaska show a preference for warmer, drier sites (which our models suggest should have lower recruitment potential) while black spruce dominates in cooler, moister sites (e.g. Calef et al. 2005). The difference in species sorting between early assembly and observed landscape distributions suggests that landscape patterns derive from subsequent filters that affect growth and survival (including biotic interactions, which we did not test here), or alternatively, are maintained by legacy effects such as those related to seed availability.

In contrast to moisture, we observed seedling recruitment responses to gradients in elevation and latitude that were consistent with sorting patterns of established forest communities. The probability of seedling occurrence was negatively correlated with elevation for all species except black spruce, in that higher elevation areas had more zeros than lower areas (Table 1.4). The effects of latitude were qualitatively different between deciduous versus spruce species. For trembling aspen and Alaskan birch, latitude was positively correlated with the occurrence of zeros in the logistic models but was not a variable of importance in the count models. Latitude was not important in the logistic models for black and white spruce, but was positively correlated

with spruce seedling counts. Thus, more northerly sites had higher densities of spruce seedlings and fewer observations of deciduous seedlings (Figure 1.4C,D).

Two environmental factors in our suite of potential covariates represent additional effects of fire characteristics that modify environmental and pre-fire legacy effects: post-fire thickness of the SOL, which affects seedbed conditions through the combined influence of fire severity and pre-fire thickness, and time-since-last-fire (TSLF), a measure of fire return interval that affects the reproductive potential of a stand. Sites with a thick SOL after fire were more likely to have zero observations of aspen and birch (Figure 1.4E,F, Table 1.4C,D). Although SOL did not affect the number of excess zeros in the spruce seedling counts, SOL thickness was negatively correlated with the count of black spruce seedlings, with fewer seedlings occurring on deep organic layers (Table 1.4A,B). Overall, our models indicate that the presence of a thick SOL after fire restricts recruitment of small-seeded, deciduous species compared to spruce, consistent with our hypothesis that low severity fires that leave the SOL intact will favor the long-term dominance of black spruce (Johnstone et al. 2010b).

In response to TSLF, stands with a short fire return interval had a greater probability of zero observations of spruce seedlings than those with longer fire return intervals, even when seeded. TSLF did not influence the occurrence of zeros in the trembling aspen and Alaskan birch logistic models, and was not an important parameter in any of the count models. The effect of TSLF on black spruce recruitment likely represents an effect of disturbance on seed availability. Like many serotinous conifers, black spruce reproduction after fire depends on seed dispersed from sealed cones held on-site in an aerial seedbank (Greene et al. 1999). Northern stands of black spruce require at least 50 years to accumulate sufficient seed for stand self-replacement after fire (Viglas et al. 2013), making them vulnerable to severe seed limitation of recruitment following a short fire return interval (Brown and Johnstone 2012).

Table 1.1 Characteristics of experimental seeding treatments used in the analysis of seedling recruitment following the 2004 fires in Alaska and 2005 fires in Eagle Plains, Yukon. Number of viable seeds sown was estimated as % seed germination based on seed germination trials. Seedling:seed ratios are calculated as the number of emerged seedlings divided by estimates of viable seeds planted. Table from Brown et al. (2015).

Species	Region	Seed Provenance	Weight of seed sown (g plot^{-1})	Estimated# of viable seeds sown (seeds plot^{-1})	Viability (mean, SE)	Seedling:seed ratio (mean, SE)
Picea mariana	Alaska	Delta Jct., AK 63°55'N, 145°44'W	0.17	75	60% (4)	0.052 (0.0082)
	Eagle Plains	Same as Alaska	0.30	150		0.040 (0.0061)
Picea glauca	Alaska	Tok, AK 63°19'N, 142°58'W	0.23	75	90% (2)	0.014 (0.0024)
	Eagle Plains	Eagle Plains 64°09'37"N, 138°32'54"W	0.50	150	60% (2)	0.017 (0.0023)
Betula neoalaskana	Alaska	Fairbanks, AK 64°51'N, 147°48'W	0.81	250	23% (1)	0.015 (0.0027)
	Eagle Plains	Same as Alaska	0.03	25		0.071 (0.013)
Populus tremuloides	Alaska	Fairbanks, AK 64°51'N, 147°48'W	0.20	1500	95% (1)	0.0018 (0.00031)
	Eagle Plains	N/A	-	-	-	-

Table 1.2 Model fit summary table for total biomass using 2011 harvest data. SE = standard error, DF = degrees of freedom.

Species	Model covariates	Adjusted R^2	P value	Residual SE	F statistic	DF
Paper birch	diameter*height	0.9617	<0.001	0.1385	394.7	44
Paper birch	diameter	0.9535	<0.001	0.1705	926.2	46
Black spruce	diameter*height	0.9356	<0.001	0.1431	1124	229
Black spruce	diameter	0.8974	<0.001	0.1805	2031	231
Lodgepole pine	diameter*height	0.9804	<0.001	0.123	3565	211
Lodgepole pine	diameter	0.9703	<0.001	0.1514	6992	213
Trembling aspen	diameter*height	0.9695	<0.001	0.1239	2176	202
Trembling aspen	diameter	0.9336	<0.001	0.183	2883	204
White spruce	diameter*height	0.9014	<0.001	0.2014	689.8	223
White spruce	diameter	0.8335	<0.001	0.2617	1132	225

Table 1.3. Model fit summary table for new (current year) biomass using 2011 harvest data. SE = standard error, DF = degrees of freedom.

Species	Model covariates	Adjusted R^2	P value	Residual SE	F statistic	DF
Paper birch	diameter*height	0.9441	<0.001	0.1655	265.8	44
Paper birch	diameter	0.9332	<0.001	0.181	657.3	46
Black spruce	diameter*height	0.8596	<0.001	0.2123	474.5	229
Black spruce	diameter	0.823	<0.001	0.2384	1080	231
Lodgepole pine	diameter*height	0.9424	<0.001	0.2052	1168	211
Lodgepole pine	diameter	0.9359	<0.001	0.2166	3123	213
Trembling aspen	diameter*height	0.9203	<0.001	0.1934	789.6	202
Trembling aspen	diameter	0.9056	<0.001	0.2103	1969	204
White spruce	diameter*height	0.815	<0.001	0.2724	332.9	223
White spruce	diameter	0.7734	<0.001	0.3015	772.3	225

Table 1.4. Parameter estimates (with 95% credible intervals) from count and logistic zero-inflation models of seedling recruitment for (a) black spruce, (b) white spruce, (c) trembling aspen, and (d) Alaskan birch. Blank cells indicate environmental covariates that were eliminated through model selection. Dashes indicate covariates not included in the full model.

	(a) Black spruce		(b) White spruce	
	Count □	Zero-inflated □	Count□	Zero-inflated□
Intercept	-0.38 (-0.81,0.02)	0.24 (-0.04,0.52)	-0.01 (-0.42,0.35)	0.45 (0.17,0.73)
Organic layer (cm)	-0.76 (-1.27,-0.26)			
Moisture (%)	1.10 (0.58,1.67)	-0.37 (-0.61,-0.14)		-0.46 (-0.72,-0.21)
Seed addition (Y/N)	1.24 (1.11,1.36)	-1.15 (-1.57,-0.73)	0.39 (0.24,0.54)	-0.64 (-1.04,-0.25)
Latitude (˚)	0.83 (0.42,1.25)		0.67 (0.30,1.07)	
Elevation (m)				0.46 (0.19,0.74)
TSLF* (years)		-0.58 (-0.79,-0.38)		-0.29 (-0.47,-0.11)
Basal area (m^2 ha^{-1})			-	-
Nearest stand (distance class)			-	-

	(c) Trembling aspen		(d) Alaskan birch	
	Count □	Zero-inflated □	Count□	Zero-inflated□
Intercept	0.75 (0.06,1.32)	1.29 (0.88,1.70)	-0.04 (-0.82,0.64)	1.93 (1.51,2.38)
Organic layer		1.69 (1.24,2.21)		0.92 (0.50,1.35)
Moisture		-1.37 (-1.88,-0.94)		-0.85 (-1.24,-0.48)
Seed addition	0.24 (0.13,0.36)	-1.15 (-1.75,-0.57)	0.54 (0.43,0.64)	-1.89 (-2.48,-1.34)
Latitude		0.58 (0.20,0.99)		0.81 (0.50,1.14)
Elevation		1.66 (1.23,2.12)		1.67 (1.31,2.06)
TSLF*				

*TSLF = Time since last fire

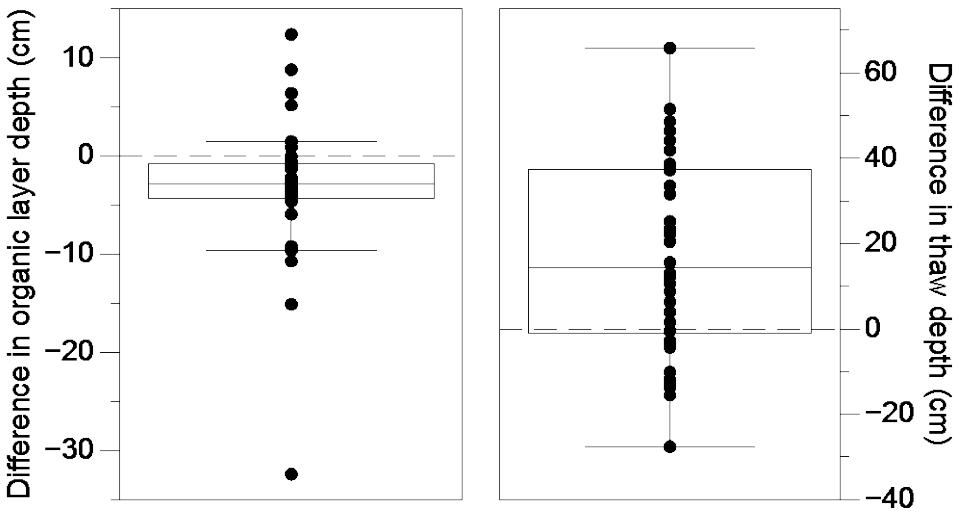

Figure 1.1 Change in organic layer and thaw depths for 6 years following the 2004 severe fire year.

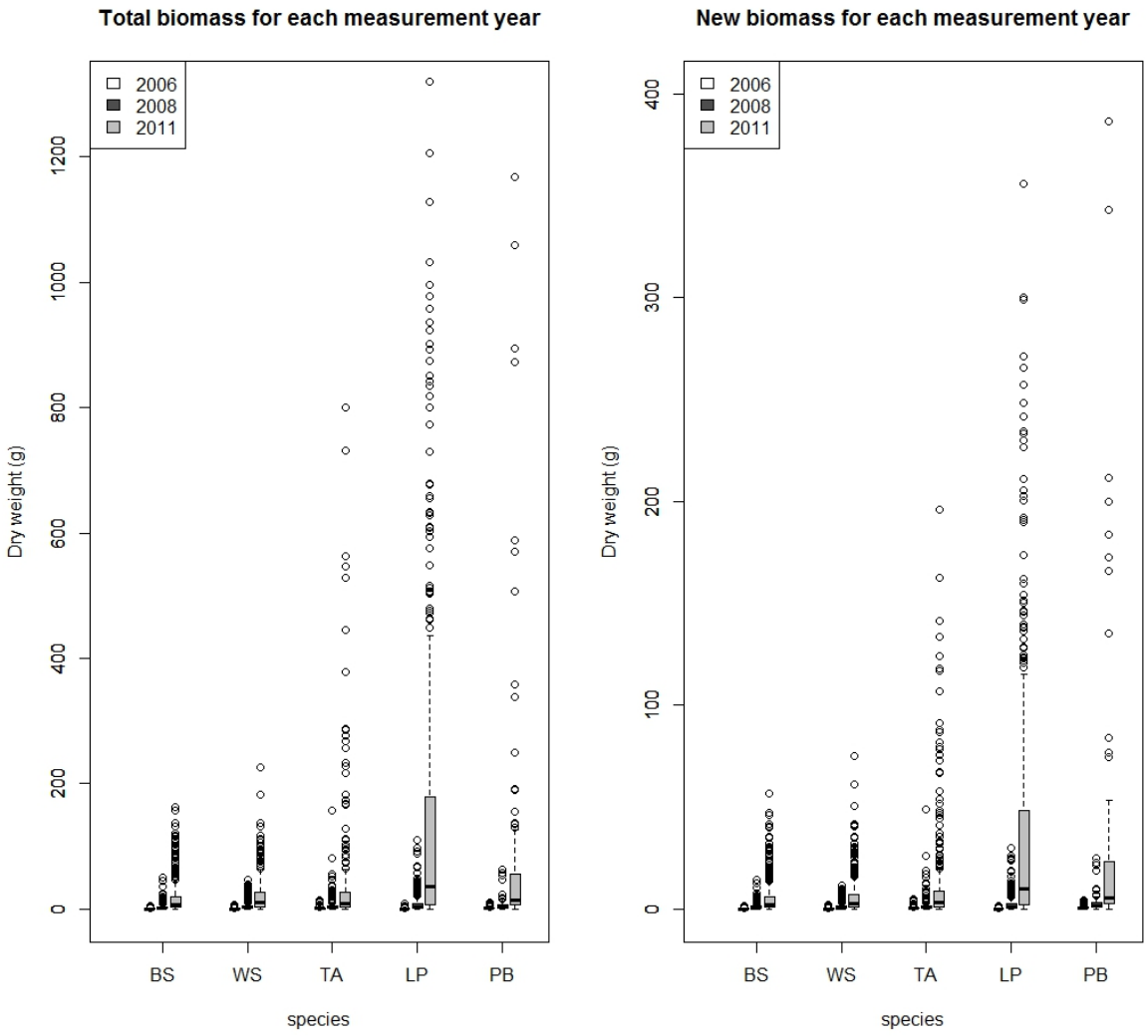

Figure 1.2. Boxplots representing total biomass (left panel) and new growth biomass (right panel) of each species outplanted in the intensive study sites in the Alaska 2004 burns. Data are sorted by species (BS = black spruce, WS = white spruce, TA = trembling aspen, LP = lodgepole pine, PB = paper birch). Box shading indicates different years of field measurement. Boxes encompass the 25%–75% quartiles of the data, with the median indicated by the thick line through the center of each box. Whiskers extending from the box encompass the 95% quartiles, and extreme observations are shown as black open circles. Values for unharvested trees were obtained using allometric equations created from 2011 harvested trees. Note that the axes are different for each panel.

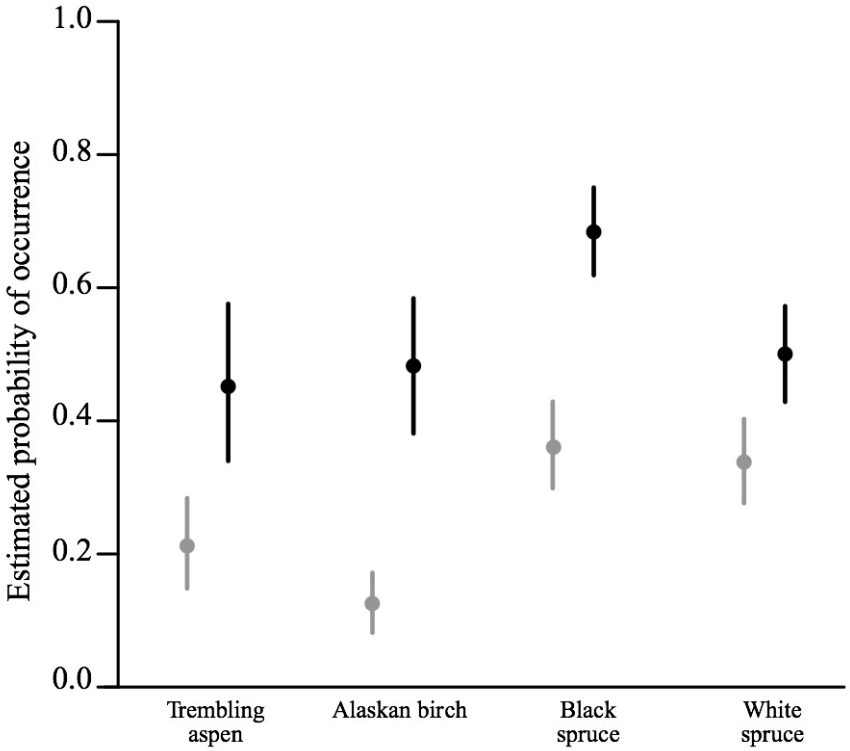

Figure 1.3. Probability of seedling occurrence in the absence (grey bars) and presence (black bars) of seed application estimated from our Bayesian analyses of four tree species in seeding experiments following 2004 fires in Alaska and 2005 fires in adjacent Yukon Territory. Species are ordered according to increasing seed size: trembling aspen, Alaskan birch, black spruce, and white spruce. Error bars indicate a 95% credible interval. Figure from Brown et al. (2015).

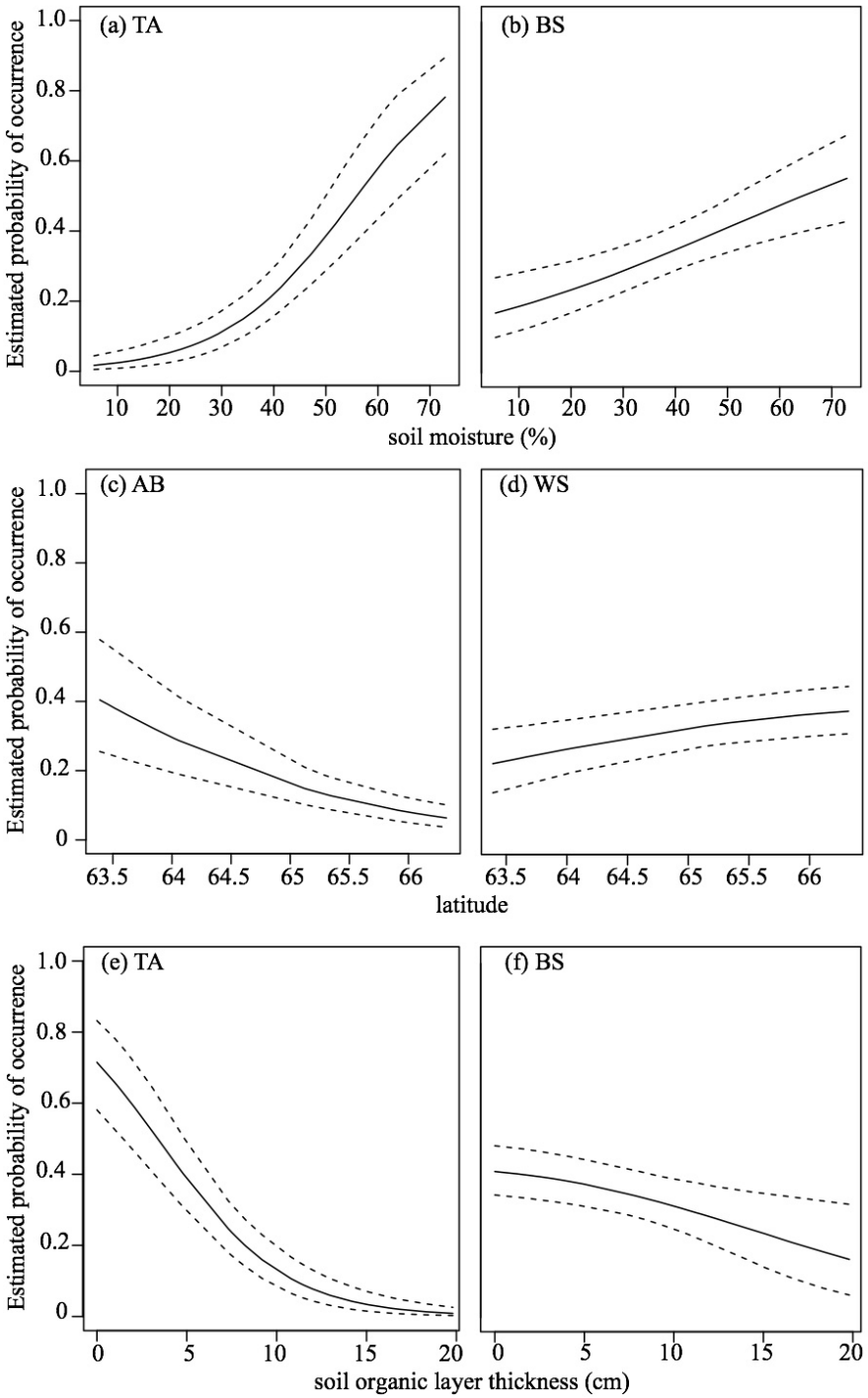

Figure 1.4. Estimated probability of occurrence of the species used in the seeding experiments based on (a,b) site-level soil moisture, (c,d) latitude, and (e,f) residual organic layer (ROL) thickness. Solid lines represent posterior medians from the Bayesian analysis and dashed lines indicate a 95% credible band. Plots in each row are arranged with smaller-seeded species on the left and larger-seeded species on the right. Species are: TA=trembling aspen, AB=Alaskan birch, BS=black spruce, and WS=white spruce. Figure from Brown et al. (2015).

Task 2: Identification and sampling of new wildfire plots and unburned control plots

T2: Materials and methods

To extend our understanding of the impacts of wildfire on the SOL, permafrost, and vegetation beyond recently burned black spruce stands, we identified burned/unburned pairs of sites composed of either a mixture of deciduous and conifer species or dominated by deciduous hardwoods. These sites were used for estimation of age of SOL material consumed during fire, and instrumented with sensors to monitor long-term change in permafrost. In 2011, SOL samples were collected from 7 burned black spruce stands varying in slope, aspect, and drainage class, to quantify C losses following fire across different landscape positions and fire severity. Estimates of SOL depth were also collected in adjacent unburned stands. At each site, one 30 m transect was established and SOL depth by horizon was recorded every 3 m. At 6 m intervals, the SOL was removed in a ~10 cm x 10 cm intact block and returned to the lab for analysis of the ^{14}C in decomposing moss bodies buried in the SOL (methods detailed in Mack et al. (2011)). The ^{14}C signature of the moss is an indicator of the ^{14}C composition of the atmosphere at the time the moss was alive and fixing C. This information allows us to estimate the age of buried moss and in areas that have recently burned tells us how old the organic material was that was consumed during the fire.

Also in 2011, we identified and sampled fire severity, combustion losses, and tree seedling establishment in 12 burned/unburned pairs of mixed and hardwood dominated stands. At each site, one 100 m transect was established. All trees rooted within 1 m of either side of the transect were measured over ten, 10-m intervals for the length of the transect (totaling 100 m^2 sampled per transect). All trees > 1.4 m in height were measured at diameter at breast height (DBH, 1.4 m). For trees < 1.4 m tall, a basal diameter measurement was taken. Tree species and percent combustion of aboveground biomass were also recorded. The SOL depth was measured using a knife to remove a ~10 cm x 10 cm intact square of organic material every 5 m along the transect and a ruler was used to estimate depths of each horizon.

To monitor changes in permafrost following fire, we identified 3 burned/unburned pairs of black spruce sites in 2012 and 2013 and instrumented each site with thermistor temperature sensors to a depth of 1.5 m. These sites included forests burned in 2004, 2010, and 2013, two of which are located in fire scars extending onto military lands at Eielson Air Force Base and Fort Wainwright. At each site, a 1.5 m drill bit was used to drill a hole in the soil. A 1.5 m probe containing the temperature sensors was then inserted into the hole so that the top of the probe was level with the SOL surface. The thermistor wires were inserted into a Campbell Scientific multiplexer and CR1000 datalogger and the datalogger was attached to a battery and solar panel power supply. This automated system records the temperature of each sensor every hour and provides a continuous measurement of differences in permafrost between burned and adjacent unburned forest.

T2: Results and discussion

For the hardwood stands included in the burned/unburned pair study, the organic layer was reduced by a mean of 7 cm during fire, resulting in a (ROL) organic layer that was 1-3 cm thick. Aboveground live tree biomass losses with fire varied between the hardwood stands, with one

site showing complete tree mortality and the second site losing 30% of live tree biomass relative to adjacent unburned forest. Both burned areas showed very high combustion rates, with < 5% of fine branch material remaining on all measured trees.

Across black spruce stands of varying topographic positions, we found that fires rarely consumed C that had accumulated longer than 10-20 years ago (Figure 2.1). At the organic layer-mineral soil interface, the age of C ranged from 150 to > 600 years old, suggesting that in the boreal forest at least a portion of the organic layer may be retained through numerous fire cycles.

The soil temperature in burned and unburned pairs instrumented with sensors was generally higher in burned relative to unburned areas (Figures 2.2 and 2.3). The difference in soil temperature was typically highest in the summer months and extended to depth in the Stuart Creek (SC) and Willow Creek (WC) sites. This pattern is likely the result of the loss of the SOL during the fire, thereby removing the insulation, which would moderate changes in soil temperatures during the summer months.

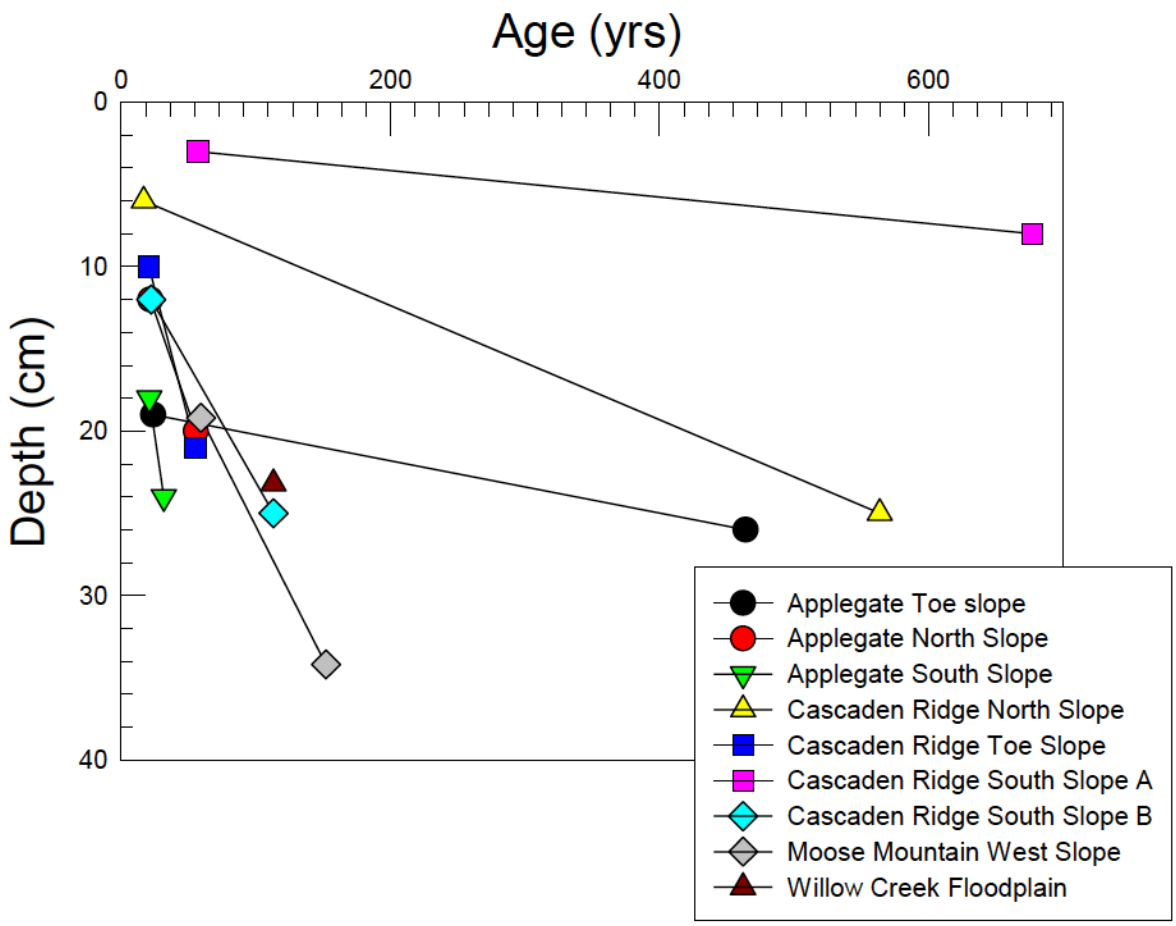

Figure 2.1. Estimated age of the organic layer surface and deepest organic soils for 9 cores sampled across 4 recent fires in interior Alaska.

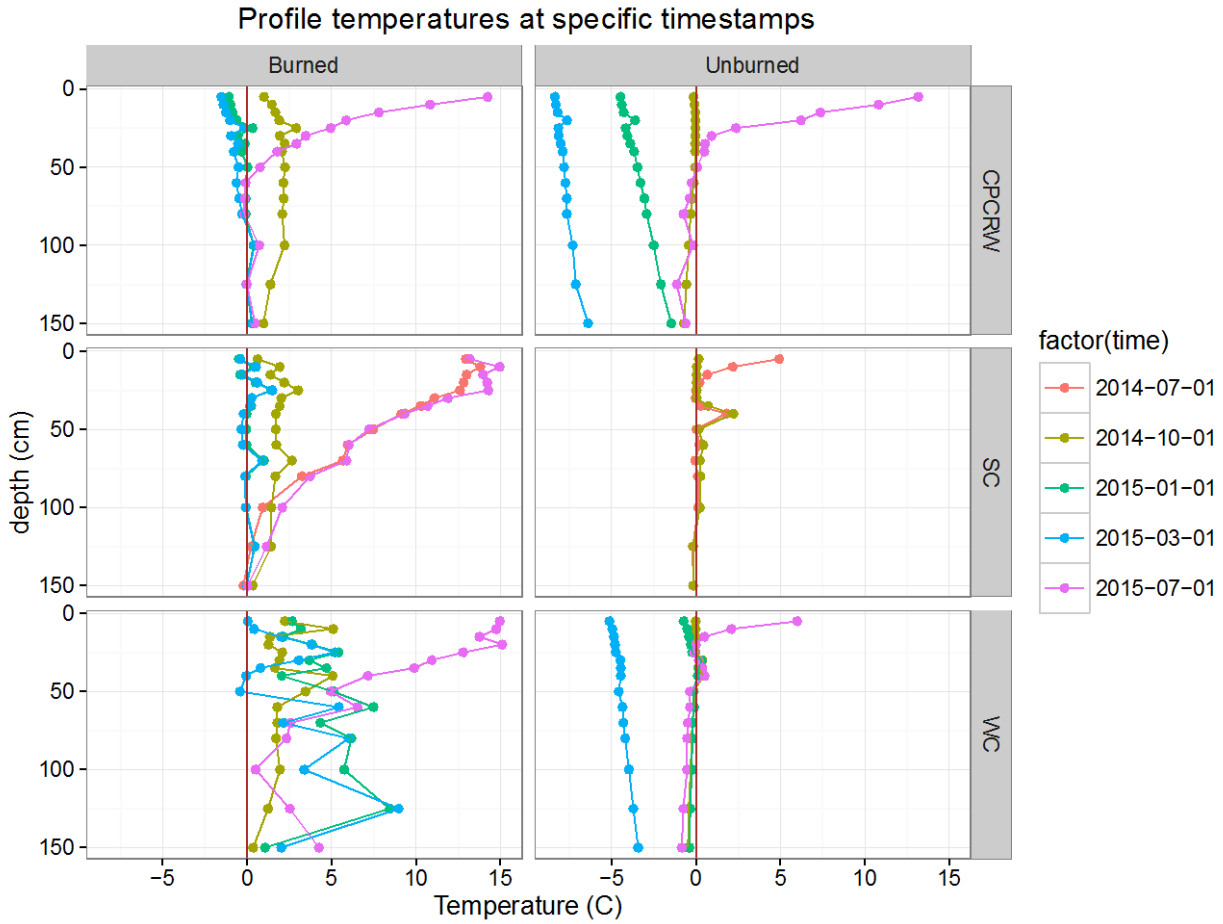

Figure 2.2. Temperature profiles for three burned-unburned paired sites. Data represents temperature for specific timestamps during different months in 2014-2015.

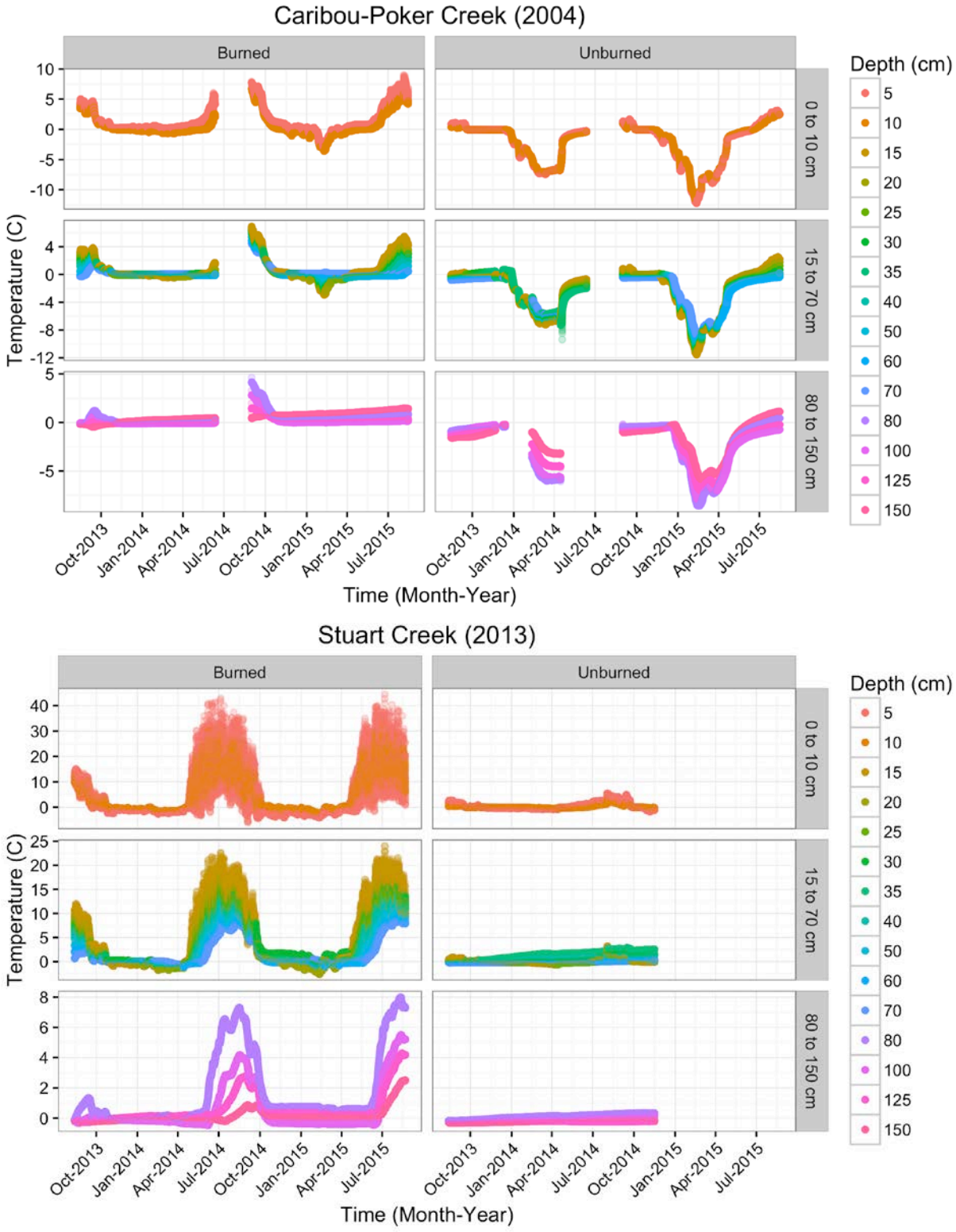
Caribou-Poker Creek (2004)
Burned
Unburned
0 to 10 cm
15 to 70 cm
80 to 150 cm
Temperature (C)
Time (Month-Year)
Depth (cm)
5
10
15
20
25
30
35
40
50
60
70
80
100
125
150
Oct-2013
Jan-2014
Apr-2014
Jul-2014
Oct-2014
Jan-2015
Apr-2015
Jul-2015
Stuart Creek (2013)
Burned
Unburned
0 to 10 cm
15 to 70 cm
80 to 150 cm
Temperature (C)
Time (Month-Year)
Depth (cm)
5
10
15
20
25
30
35
40
50
60
70
80
100
125
150
Oct-2013
Jan-2014
Apr-2014
Jul-2014
Oct-2014
Jan-2015
Apr-2015
Jul-2015

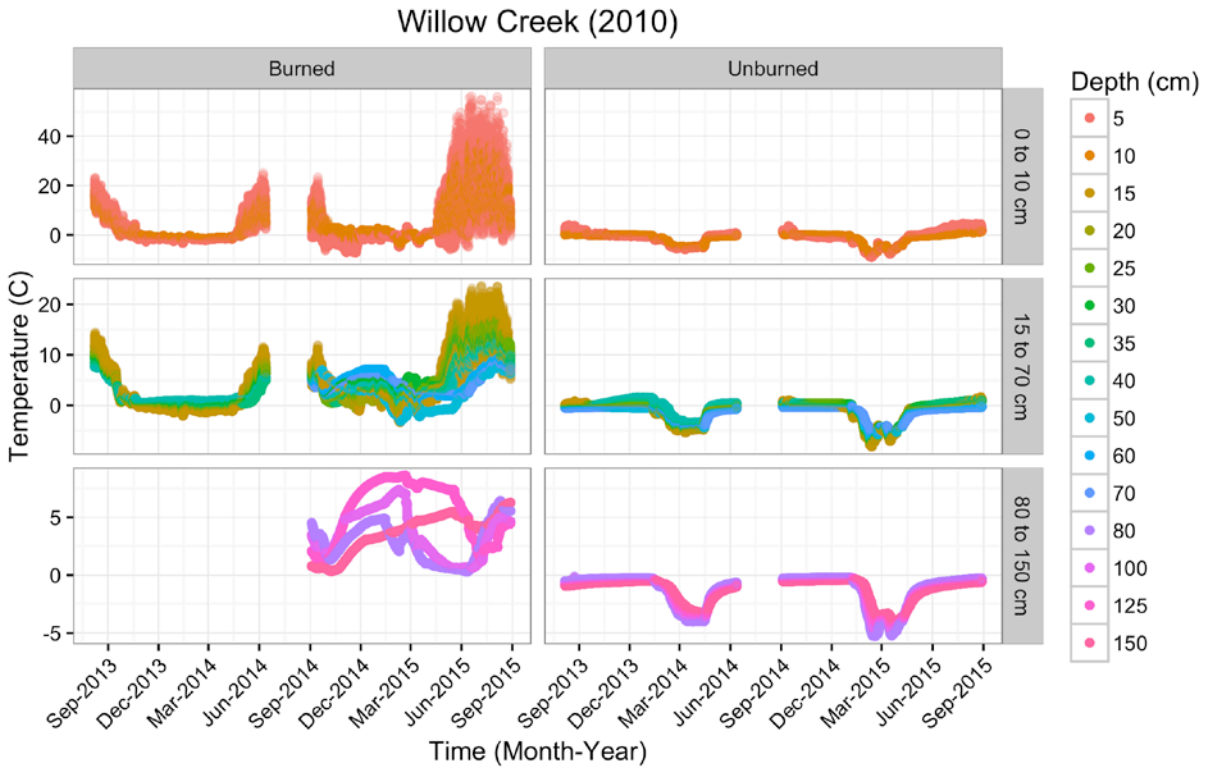

Figure 2.3 Continuous temperature record for burned-unburned paired sites instrumented for soil temperature measurements.

Task 3: Identification and sampling of fire management plots

T3: Materials and methods

Fire management in the boreal forest has become a common practice to reduce fire spread and lessen fire impacts on human and infrastructure safety. To investigate how these practices impact soils, permafrost, and vegetation, we sampled 12 shearbladed and 7 thinned sites located on military, state, and federally managed lands in Interior Alaska. Sites were sampled between 2011-2013 and included areas at Fort Wainwright, Fort Greeley, and Eielson Air Force Base. Adjacent, untreated stands dominated by black spruce were also sampled at each location for use as site controls. The year of fuel-reduction treatment varied across sites and ranged from approximately 2 to 12 years prior to our sampling. Harvested biomass was burned on site within a few years of treatment for most sites.

For most study sites, we established two, 20 m transects located approximately 20 m apart in each fuel reduction area and adjacent black spruce stands. When the location of burned windrows or piles were evident in treated stands, the transects were situated so that they crossed the burn area, to accurately capture the heterogeneity in SOL and woody debris. For three sites managed by the Bureau of Land Management, the treatment design was considerably different from all other locations and required a modification to the site sampling methods outlined above. These sites consisted of 9 m x 9 m plots control and thinned plots with multiple tree spacings (Ott and Jandt, 2005). We sampled two plots each that were thinned at 2.4 m x 2.4 m and 3.0 m x 3.0 m spacing where ladder fuels had also been removed. Harvested tree biomass had been removed from the plots and was not burned on site. We also sampled two control plots at each site. Because these plots were much smaller than all other sites we sampled, we modified our sampling protocol and sampled along two 7 m transects in each plot located at least 1 m from the plot edge and 2 m from the other transect within the plot, to avoid overlap in sampling area. In our seedling and SOL - thaw depth relationship analyses (detailed below), we also included data collected in 2011 in shearbladed and thinned stands at one site. This 2011 sampling consisted of measurements along three 30 m transects sampled at 5 m intervals.

Vegetation and woody debris

All live and standing dead trees and tall shrubs ≥ 1.4 m tall (diameter at breast height, DBH) rooted within 1 m of either side of the transect line were identified by species and DBH was recorded. Fallen dead trees standing at an angle of > 45 degrees were categorized as standing dead and DBH measurements were recorded. Dead trees lying at an angle < 45 degrees were considered part of the downed woody debris pool. Biomass was estimated using allometric equations reported by Alexander et al. (2012) for trees and Berner et al. (2015) for tall shrubs. For dead trees, biomass values were multiplied by 0.5 to account for the observation that many dead trees had lost crown and upper stemwood biomass, which we did not quantify in this study. We assumed the C concentration of all live and dead wood to be 50% for estimation of aboveground C stocks.

The density of seedlings and trees ≤ 1.4 m in height was estimated using five 1 m x 1 m quadrats placed at random locations (and 5 fixed locations for the 2011 Nenana Ridge sampling, using a

0.5 m x 0.5 m quadrat) along each sampling transect. Within each quadrat, all seedlings and small trees were counted and species was recorded. Additional vegetation classes were assessed using the point intercept method (Goodall, 1952). Every 1 m along the transect, a pin flag was dropped and the number of hits were recorded for each plant functional type identified, the composition of the ground layer at the point location, and the most abundant species of each plant functional type.

Downed woody debris was quantified using the line intercept method (Brown, 1974) along each 20 m sampling transect. Fine woody debris was categorized into 5 size classes and the number of intercepts of each of size class was recorded and converted to wood mass using black spruce multiplier values reported in Nalder et al. (1997). Coarse woody debris with a diameter ≥ 7 cm was converted to area using methods described in Ter-Mikaelian et al. (2008). Similar to aboveground biomass, we multiplied the resulting biomass values by 0.5 to estimate woody debris C pool sizes.

Soils

The SOL was characterized in the same five quadrats used to estimate seedling density. The depth of the SOL was estimated by removing an approximately 10 cm x 10 cm intact block of organic material using a knife, then recording the depth of each organic horizon using a ruler. At 2 of the 5 sampling locations along each transect, the removed 10 cm x 10 cm SOL block and the top 10 cm of mineral soil (6.9 cm diameter core) immediately below the SOL were collected for additional soil characterization. All samples were put on ice, then frozen until laboratory analysis. In some shearbladed locations no SOL was present and only mineral soils were collected. In contrast, at other locations frozen mineral soil was encountered in the 10 cm increment and collected cores were shallower than 10 cm. These differences were taken into consideration when estimating soil C pools. At some sites, SOL depth and thaw depth were measured at two locations along each transect and soils were collected at one location per transect. Thaw depth was estimated adjacent to each of the soil sampling locations using a 1.5 – 2 m steel probe that was inserted into the ground until ice was hit. Values reported here have been normalized to account for differences in SOL depth and represent the thaw depth of the mineral soil.

In the laboratory, soil samples were removed from the freezer and allowed to thaw prior to processing. Because of the large volume of many SOL samples, the blocks were split in half vertically using an electric turkey cutter and only one half the core was processed. Vascular plant material was removed from the surface of all SOL blocks and sample weight and dimensions were recorded. Green moss was then clipped off the SOL surface and roots > 2 mm in diameter and large pieces of non-decayed wood were removed from each block by hand. These components were weighed wet, dried at 60^{o}C, then re-weighed. The remaining SOL block was then thoroughly homogenized using pruners. A representative subsample was then weighed wet and dried at 60^{o}C to estimate moisture content and for C and nitrogen (N) analysis. Mineral soil cores were split into 0-5 cm and 5-10 cm increments for processing. Each 5 cm depth increment was pulled apart by hand and rocks and > 2 mm roots were removed. Roots were weighed wet, dried at 60^{o}C, then weighed dry. Rock volume was estimated by water displacement in a graduated cylinder. Mineral soil samples were then homogenized using pruners to chop any fine

roots, and a subsample was weighed and dried at 110°C to estimate moisture content. An additional subsample was dried at 60°C for C and N analysis.

Dried green moss and homogenized organic material were ground in a wiley mill (Thomas Scientific model 3383-L10) or coffee grinder and mineral soil was ground with a mortar and pestle. The ground samples were then analyzed for percent C and N using a Costech Analytical ECS 4010 Elemental Analyzer (Valencia, CA). Soil pH was measured on a field moist subsample of each SOL and mineral soil using a Thermo Scientific Orion 2 Star pH meter. For SOL samples, 5 g of material were mixed with 50 mL of deionized water in a cup and for mineral soils 20 mL of water were added. Each sample was thoroughly mixed, allowed to equilibrate for 30 minutes, then the pH was recorded once the value stabilized.

To estimate SOL C and N pools, we first summed the C and N pool sizes for each measured SOL horizon. We then used site-level %C, %N, and bulk density data from the laboratory samples to estimate C and N stocks of the field-only SOL measurements. This approach increased our sampling size and ability to capture soil heterogeneity. Ecosystem C stocks were then calculated by adding the estimated C values from all measured pools.

Statistics

Our statistical approach varied across analyses due observed skewed distributions resulting from our treatment types, which often contained many zeros. To account for these factors, tests that do not make assumptions about data distribution were used for most analyses. Additionally, to account for variability stemming from site location and sampling dates, we standardized many analyses by evaluating treatment differences based on the relative differences observed between unmanaged and managed stands for each site.

Aboveground stand characteristics (live tree biomass, dead tree biomass, basal area, and stem density) and downed woody debris, were evaluated using a Bayesian boostrapping approach applied in R (Baath, Rasmus. 2016. *Bayesboot: An Implementation of Rubin's (1981) Bayesian Bootstrap*. https://github.com/rasmusab/bayesboot.). This method included 4,000 draws each for the site-level difference between unmanaged and managed values for each variable, followed by calculation of the posterior difference. This method was also used to evaluate treatment effects on thaw depth, to limit any bias created by differences in sampling dates. Seedling density was analyzed using a generalized linear mixed model with a Poisson distribution that included site as a random effect, subsite nested within site (influences only the Nenana Ridge experimental blocks), and transect nested within subsite. Prior to analysis, data was standardized to reflect number of seedlings per m^2. Treatment differences in the SOL and mineral soils were evaluated using a linear mixed effects model with the same nesting described for seedlings. Analysis of understory plant composition and ground cover types was performed using the non-metric multidimensional scaling (NMDS) vegan function metaNMDS in R (Oksanen et al. 2015). This approach does not fit data to a distribution and is appropriate for datasets containing many zeros, as was common in this dataset. The collected data was standardized to the transect-level by dividing the total number of hits for each category by the number of sampling point along the transect prior to analysis. For many analyses, we also present absolute mean values for the unmanaged, thinned, and shearbladed sites without reporting statistical significance.

T3: Results and discussion

Aboveground stand characteristics

Across study sites, unmanaged black spruce forest stored an average of 3.1 kg C m^{-2} in aboveground biomass while thinned stands contained 1.2 kg C m^{-2} and close to zero biomass was found in shearbladed areas (Table 3.1). The difference between unmanaged and managed stands showed significantly larger relative reductions in aboveground biomass C in shearbladed areas, totaling nearly twice the C loss observed in thinned stands. Relative differences in standing dead tree biomass were not significant between treatments (Table 3.1). Live tree basal area differences between unmanaged and managed stands differed significantly, with shearbladed sites exhibiting more than twice the basal area reduction observed at thinned sites (Table 3.1). The relative reduction in stem density tended to be larger in shearbladed sites, however stem density was highly variable across sites and no significant relationship between treatment and stem density was observed (Table 3.1). The relative difference in downed woody debris between treatments reflected significantly larger pools in shearbladed areas relative to thinned stands. Mean downed woody debris pool sizes were 0.1 ± 0.02, 0.2 kg ± 0.05 C m^{-2} and 0.7 ± 0.04 kg C m^{-2} in unmanaged, thinned, and shearbladed areas, respectively.

Seedling density was highest in the shearbladed stands and similar in the unmanaged and thinned stands (Figure 3.1). Deciduous seedlings (primarily Alaska paper birch with a small portion of aspen) dominated the shearbladed sites while unmanaged areas were primarily black spruce seedlings and layering. Thinned stands showed comparable contribution of deciduous and conifer seedlings/layers. The mixture of understory plants (excluding seedlings) observed most frequently in the unmanaged and thinned stands were similar to one another and differed from those seen in the shearbladed areas (Figure 3.2). Evergreen plants showed a close association with the unmanaged and thinned stands while deciduous plants, forbs, and grasses were associated more commonly with the shearbladed stands. The ground cover also differed among treatments (Figure 3.3). Control stands were linked closely to non-sphagnum mosses and lichen while thinned stands were associated with lichen, leaf litter, and sphagnum mosses. Shearbladed stands were most different, with ground cover commonly including liverworts, mineral soil, and burned downed woody debris and SOL.

Soils

The SOL depth differed significantly among all stand types, with the deepest SOL observed in unmanaged forest and the shallowest in shearbladed areas (Table 3.2) Bulk density also differed among all stand types, with shearbladed stands exhibiting the highest bulk density, and unmanaged forest the lowest. Total C stocks were comparable in unmanaged and thinned stands, while SOL C stocks in shearbladed stands were approximately half that observed in unmanaged and thinned stands (Table 3.2). Mean N stocks were largest in thinned stands, but did not differ from unamanged forest. Shearbladed stands displayed smaller N stocks than unmanaged forest, but did not differ from thinned stands. Coarse root C in the SOL averaged 0.8 ± 0.2, 0.7 ± 0.1 and 0.3 ± 0.1 kg C m^{-2} in unmanaged, thinned, and shearbladed stands, respectively. These values resulted in significant differences between unmanaged and shearbladed ($p = 0.0004$) and thinned and shearbladed stands ($p = 0.0023$).

In the uppermost 5 cm of mineral soil, bulk density differed significantly between the unmanaged and shearbladed stands, while no difference in the 5-10 cm depth increment was

observed (Table 3.2). Significant differences in bulk density between the 0-5 cm and 5-10 cm depths were observed in the unmanaged and thinned stands, but not in the shearbladed ($p < 0.001$, $p = 0.0009$, $p=0.48$, respectively).

Thaw depth averaged 40 ± 7 cm in unmanaged stands, 53 ± 14 cm in thinned, and 86 ± 6 cm in shearbladed stands. The difference in thaw depth between unmanaged and thinned stands averaged 12.7 cm and difference between unmanaged and shearbladed was 45.8 cm. These differences resulted in a significantly larger effect of shearblading than thinning ($p = 0.03$). Looking across all sampling locations, the relationship between the SOL depth and the normalized thaw depth showed a trend for deeper thaw in shearbladed soils relative to unmanaged or thinned soils with a comparable SOL depth (Figure 3.4).

Total C stocks for all measured ecosystem C pools were 14.1 ± 0.7, 11.4 ± 1.5, and 8.3 ± 1.1 kg C m^{-2} for unmanaged, thinned, and shearbladed sites, respectively. These differences were driven primarily by changes in aboveground biomass, with additional influence of the SOL and dead wood pools (Figure 3.5).

Our results suggest that the use of thinning and shearblading treatments to reduce the likelihood of fire spread can alter ecosystem structure and function, with larger changes expected following shearblading than thinning. In addition to reductions in C storage, shearblading was associated with a greater increase in thaw depth, which may increase C losses for mineral soils over time. The high densities of deciduous seedlings observed also suggest that shearblading alters successional trajectories and is likely to result in deciduous stands in areas that were previously dominated by black spruce. While this transition may reduce the likelihood of fire return, this shift is likely to cause long-term changes in C and N cycling within the ecosystem.

Table 3.1. Aboveground stand characteristics and differences between adjacent unmanaged and managed study stands.

				Site-level differences	
	Unmanaged	Thinned	Shearbladed	Unmanaged - Thinned	Unmanaged - Shearbladed
Live tree biomass (C kg m^{-2})	3.1 (0.5)	1.2 (0.2)	0.0 (0.0)	1.7 (0.5)	3.3 (0.7)
Dead tree biomass (C kg m^{-2})	0.2 (0.1)	0.02 (0.02)	0.0 (0.0)	0.1 (0.1)	0.2 (0.1)
Basal area (m^2 ha^{-1})	21.2 (2.2)	9.6 (1.7)	0.0 (0.0)	10.0 (2.5)	21.9 (3.1)
Density (stems ha-^{1})	9370.0 (1301.0)	1700.0 (302.2)	20.8 (14.1)	7662.0 (2216.5)	10229.2 (1822.5)

Means (SE) across study sites (n = 18 unmanaged, 12 shearbladed, 7 thinned). The differences are based on site level differences.

Table 3.2. SOL characteristics estimated from field collections and laboratory processed samples.

	Unmanaged	Thinned	Shearbladed
Soil Organic Layer			
Depth (cm)	21.6 (0.8)[a]	16.2 (1.4)[b]	8.0 (1.4)[c]
Bulk Density (g cm^{-3})†	0.08 (0.00)[a]	0.10 (0.01)[b]	0.14 (0.01)[c]
C kg m^{-2}	5.9 (0.2)[a]	6.0 (0.7)[a]	3.2 (0.6)[b]
N g m^{-2}	178.3 (7.8)[a]	193.2 (29.8)[ac]	119.0 (22.4)[bc]
pH			
0-5 cm mineral soil†			
Bulk Density (g cm^{-3})	0.58 (0.04)[a]	0.52 (0.05)[ab]	0.60 (0.04)[b]
C kg m^{-2}	2.3 (0.2)	2.5 (0.3)	2.4 (0.1)
N g m^{-2}	120.6 (8.5)	129.7 (17.9)	122.6 (7.6)
pH	5.5 (0.1)	5.6 (0.2)	5.6 (0.1)
5-10 cm mineral soil†			
Bulk Density (g cm^{-3})	0.84 (0.04)	0.89 (0.11)	0.85 (0.07)
C kg m^{-2}	2.1 (0.1)	2.2 (0.3)	2.0 (0.2)
N g m^{-2}	109.1 (7.0)	112.9 (17.3)	109.2 (9.2)
pH	5.6 (0.1)	6.0 (0.2)	5.7 (0.1)

† Estimates calculated from laboratory processed samples only.
Values are mean (SE), n = 18 unmanaged, 12 shearbladed, 7 thinned sites.
Values exclude the green moss layer.

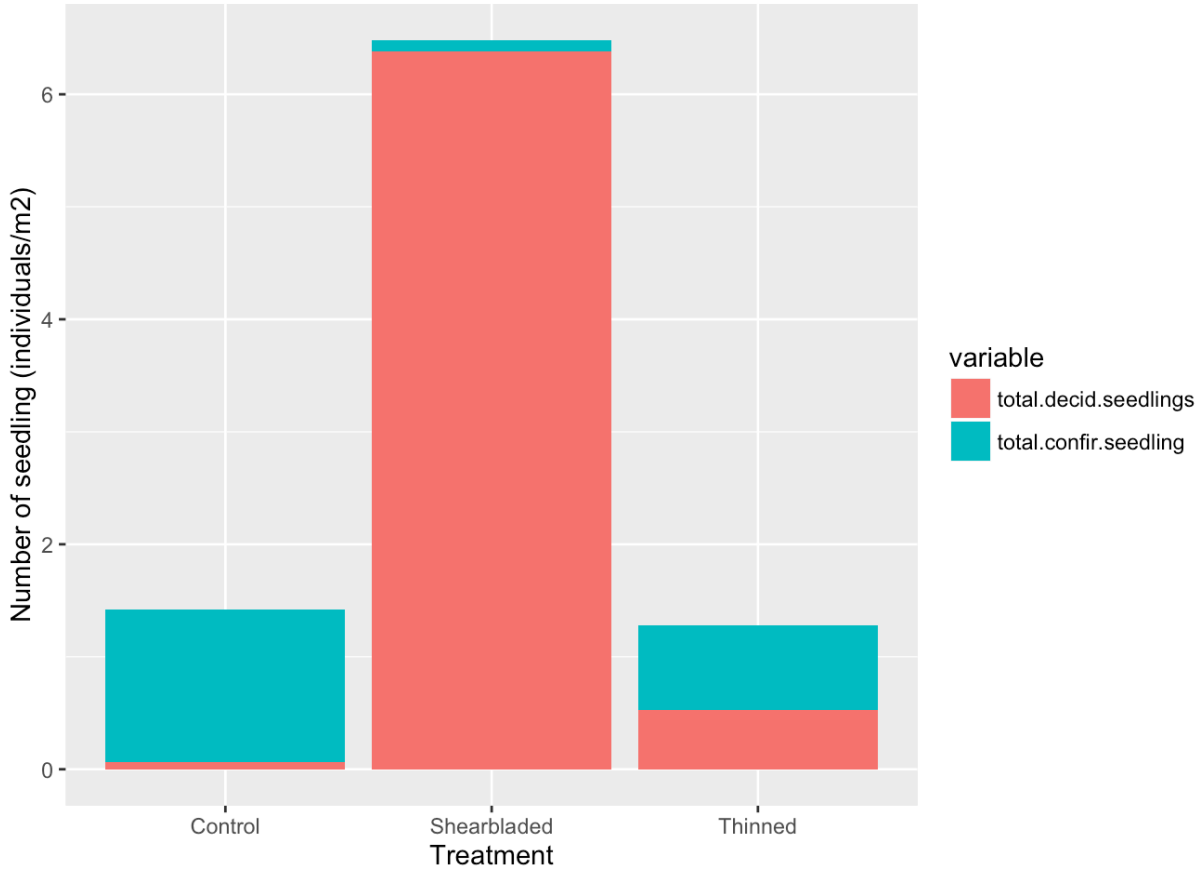

Figure 3.1. Mean deciduous and conifer seedling density (stems per m^{-2}) for unmanaged (control), shearbladed, and thinned study sites. Deciduous species include Alaska paper birch and aspen seedlings while conifer species include black spruce seedlings and layering.

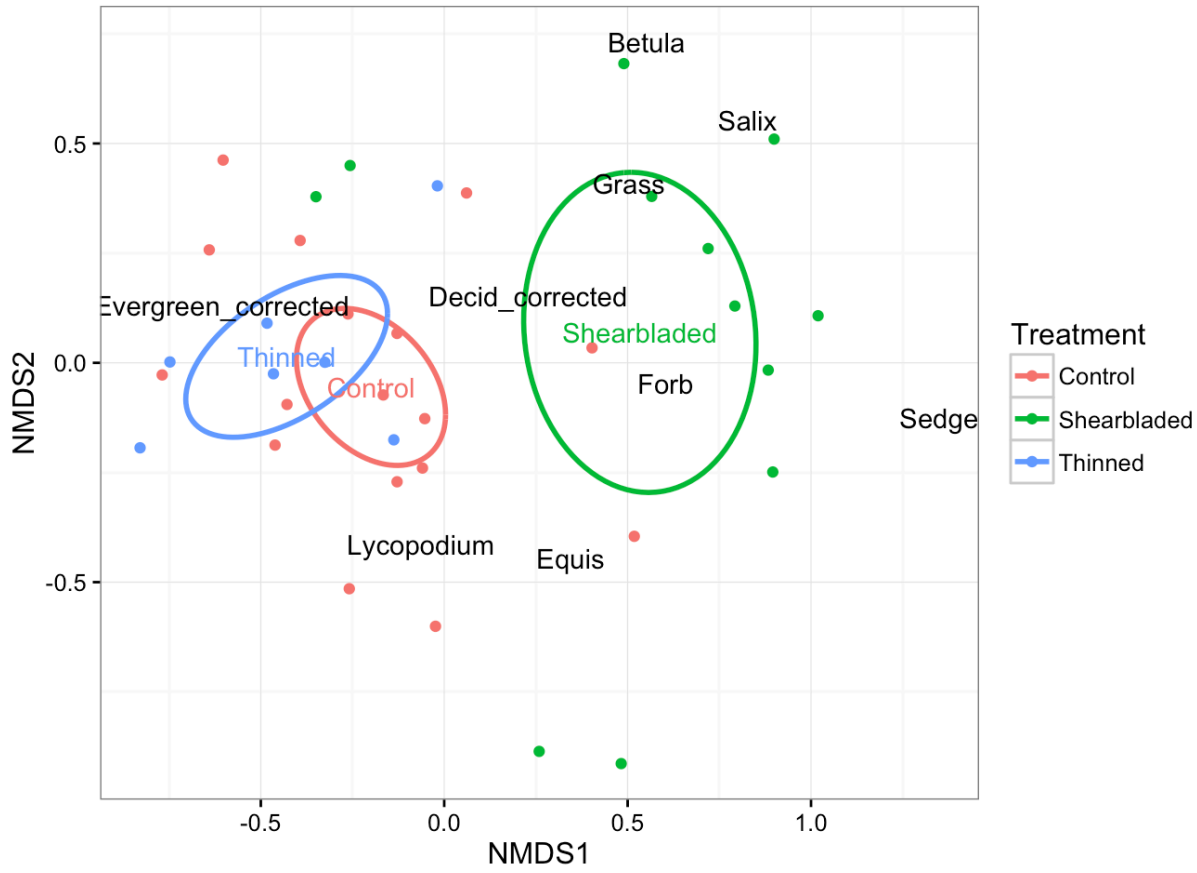

Figure 3.2. Vascular plant types (measured as number of hits per sampling location) using non-metric multidimensional scaling (NMDS). The location of the plant functional type name within the ordination illustrates the mean while the points represent unmanaged (control) and managed stands at each study site. The circles indicate 95% confidence intervals for each treatment type.

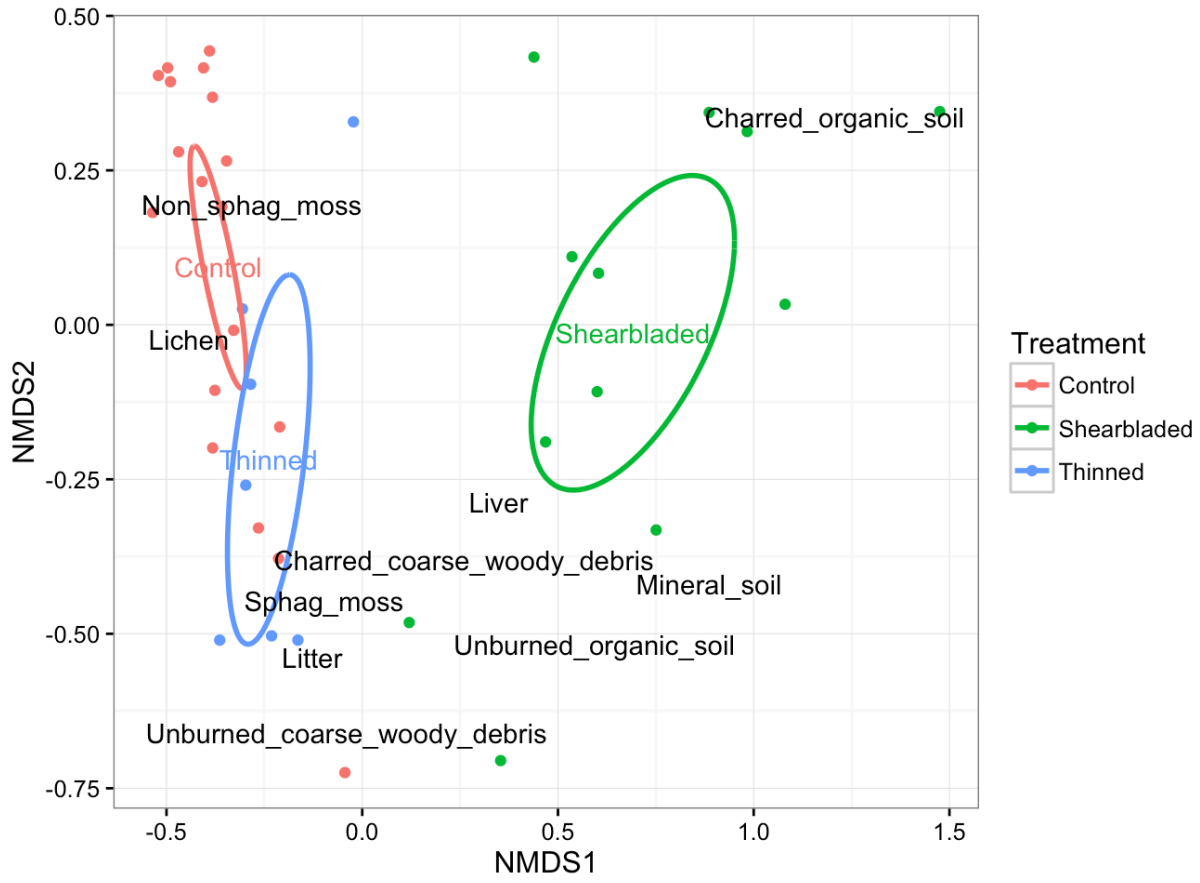

Figure 3.3. Ground cover (measured as number of hits per sampling location) using non-metric multidimensional scaling (NMDS). The location of the ground cover type name within the ordination illustrates the mean while the points represent unmanaged and managed stands at each study site. The circles indicate 95% confidence intervals for each treatment type. The SOL represents the soil organic layer and CWD is coarse woody debris.

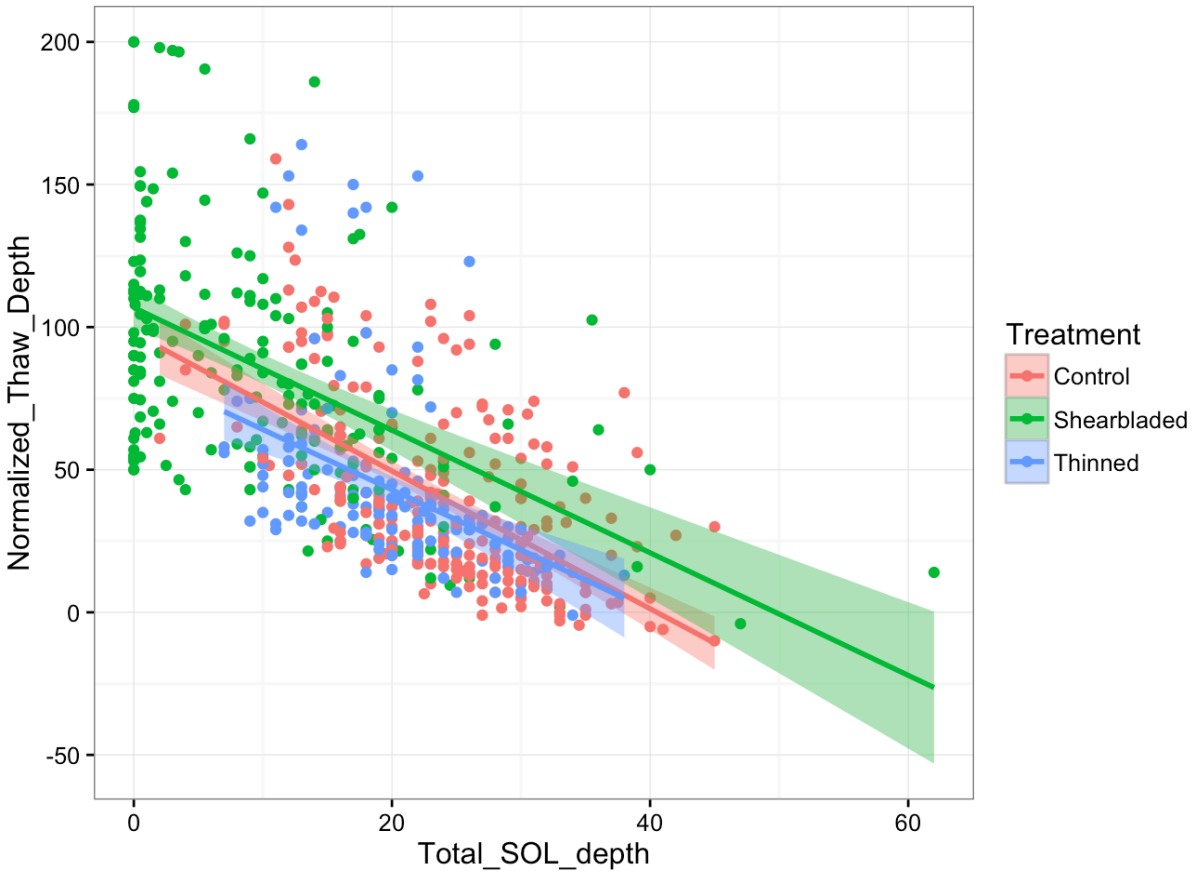

Figure 3.4. Relationship between SOL depth and normalized thaw depth for all sampling locations across all sites. The control label represents unmanaged stands.

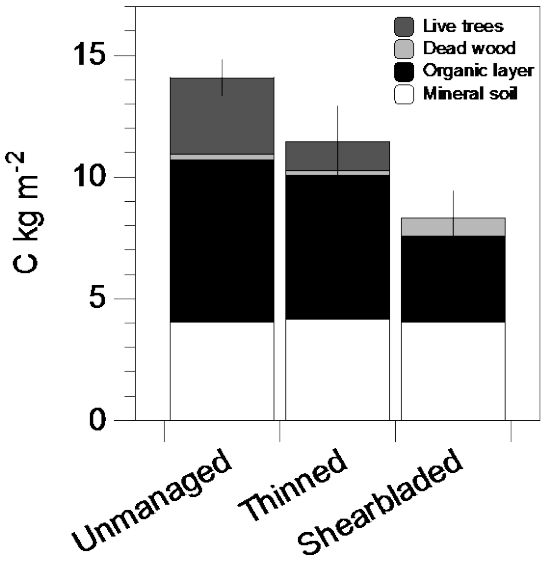

Figure 3.5. Total ecosystem C stocks for pools measured in this study. Values reported for each component and treatment type represent the mean of all sampled sites. Error bars indicated standard error of the summed C stocks.

Task 4: Moss and litter manipulation experiment

T4: Materials and methods

Site information

In summer 2012, we established 30 intensive study plots in the Tanana Valley State Forest, near Fairbanks Alaska (64° 53' N, 148° 23' W) to assess differences in plant-soil-microbial feedbacks between forests dominated by Alaska paper birch (*Betula neoalaskana*) and black spruce (*Picea mariana*). The forest in this area established following the Murphy Dome fire in 1958 and allowed us to quantify C and nutrient cycling in mid-successional forest stands and to investigate the impacts of deciduous foliar litter on moss growth and survival. Three spatially explicit blocks containing adjacent stands dominated by Alaska paper birch and black spruce were identified and 5 plots (10 m x 10 m) were established for each species in each block, for a total of 15 plots dominated by each species.

Environmental measurements

In June 2012, we installed 1 meteorological station (Onset, Bourne MA) in each stand type within each block (n = 6). At each station air temperature, relative humidity, photosynthetically active radiation, soil temperature (10 cm from the SOL surface) and soil moisture (10 cm from the mineral soil surface) were measured every hour. Two additional soil temperature sensors (iButton®) were installed at 10 cm below the SOL surface in each plot to provide additional records of soil temperature every 4 hours. Data were downloaded 2 times per year. To estimate depth of the snow pack, iButton® temperature sensors were installed on 1 wooden stake located near the meteorological station in each stand in September 2012 (Lewkowicz 2008). Sensors were placed on the stake at heights 2, 16, 29, 42, 55, 68, 81, 94, 107, and 120 cm and record the temperature every 4 hours. Data were downloaded in June 2013 and sensors were re-deployed in August 2013.

Aboveground and understory

To quantify aboveground biomass and C pools, we recorded diameter and species of all live trees and standing dead trees within each plot. Trees taller than 1.4m were measured at DBH height and basal diameter measurements were taken on trees < 1.4 m in height. Dead trees that had fallen at an angle of < 45 degrees were considered part of the downed woody debris pool while those fallen at an angle > 45 degrees were categorized as a standing dead tree, with DBH or basal diameter measurements recorded. Downed woody debris was quantified using the line intercept method (Brown, 1974). Three 10 m transects were placed at random locations across each plot and the number of intercepts of each of 5 size classes were recorded. The forest floor was characterized using the point frame method (Schuur et al., 2007). At 10 random locations within each plot, a 0.5 m x 0.5 m point frame was placed on the SOL surface. Fishing line was strung at 10 cm intervals across the frame, creating sixteen intersections within the grid. At each intersection, a pin flag was used to quantify hits on moss, herbs, lichen, shrubs, and “other” plants.

Fresh foliage from the upper canopy was collected from each plot in July 2012. In black spruce stands, tall pruners were used to retrieve samples and in birch stands a slingshot was used. For the birch, ten intact leaves that were representative of the collection were selected for specific leaf area (SLA) analysis. For the spruce, ~100 needles from the current year’s growth were removed from the branches using scissors or a razor. Samples were shipped on ice to Florida for

SLA analysis. Black spruce needles on the tree that that had been produced in previous years were also retained and used for chemical analyses (details below).

Annual litter production was assessed using litter collection baskets within each plot. In July 2012, three litter baskets (62.2 cm x 45.4 cm) lined with fiberglass window screen were installed at random locations within each birch plot. In the spruce stands, 50 cm x 50 cm wooden frames with fiberglass lining the bottom were installed. These wooden baskets sit close to the ground and are able to capture needles falling from low limbs on the spruce trees. Litter was collected from birch baskets following leaf fall in September 2012 and October 2013 and from all baskets in June and July 2013.

Moss transplant and deciduous litter manipulation

To assess the impact of deciduous leaf litter on moss growth, we installed a moss transplant and litter addition experiment across our study plots. *Hylocomium splendens* was selected as the target moss species because, as its common name "stair-step moss" suggests, it forms a new 'step' (hereafter called shoot) every year (Figure 4.1). This modular growth and strong apical dominance facilitates monitoring and measurement of growth (Tamm 1953, Busby et al. 1978). Moreover, *H. splendens* is very abundant in the circumpolar boreal forest, as well as in interior Alaska (Økland 1995, (Turetsky, 2003). The production of new shoots occurs by branching, i.e. the new shoot grows on the shoot of the previous year. It takes about 1.5 years for a shoot to be considered mature and to have reached its full growth. After about 3-4 years, the shoots become buried in the SOL, photosynthesis stops, and decomposition begins (Økland 1995).

Within each of the 15 black spruce plots, we identified 6 areas with a high abundance of *H. splendens*. Next, we excavated plugs of live moss measuring 30.48 cm in diameter down to the fibric horizon of the SOL in each of the 6 areas. Once the 30 moss plugs from one black spruce stand were collected, they were randomly reassigned to either birch or spruce stands in the same block. In the spruce stands, we randomly chose 3 out of the 6 harvested locations to be replaced with randomly selected transplanted plugs. In the birch stands, we removed the forest floor to the mineral soil using the 30.48 cm frame and inserted the moss transplant into the hole. We delineated moss transplants using bamboo sticks. All mosses were randomly assigned to one of 3 treatments: litter exclusion, litter addition, and ambient litter (Figure 4.2). In August of 2012, 2013, and 2014, we installed plastic mesh tents over the litter addition and exclusion transplants to prevent deciduous leaf litter from falling on them. The mesh contained holes that were large enough to allow precipitation and light to reach the transplant, but prevented the deciduous litter from accumulating. In October 2012, 2013, and 2014, we added birch litter manually to the litter addition transplants at the ambient input rate (estimated from the litter collection baskets outlined above). The added birch foliar litter was a well-homogenized sample comprised of litter collected from all the birch litter baskets across the site. In the ambient litter treatment, the transplants received the natural litter input from the stand they are located in. We identified control areas with a high abundance of *H. splendens* in each plot. In some of the birch stands, these areas were small or found on decomposing logs. In 2013, we installed iButtons® under each transplant to record the soil temperature.

Moss growth measurements and species composition

We marked five *H. splendens* shoots in each of the 120 transplants in June 2013, and an additional 5 shoots in September 2013. We used PVC rings (HAMA plastic beads, Malte Haaning Plastics Co., Nykøbing Mors, Denmark; outer diameter 2.5 mm and inner diameter 1 mm) with a slit that allowed the rings to be placed as markers on the shoots using pincers (Figure 4.1). The marked *H. splendens* shoots were chosen systematically using a grid system. We measured width and length of all the shoots, as well as mortality or growth anomalies on the marked individuals in June and September 2013, 2014, and 2015 (Figure 4.1).
To see if the moss species composition in the transplants changed following the litter treatments, we used point-intercept sampling (Goodall, 1952) with a 100 point grid of which ~76 points fell on the transplant. The grid was positioned in the same place over the transplant for assessments in September 2012 and July 2015. We recorded every moss species that touched a metal pin flag pushed down at every point. *H. splendens* records were visually categorized as green or brown to make a qualitative assessment of their condition. Every fall, pictures were taken with a Normalized Difference Vegetation Index (NDVI) camera and the pictures were analyzed using the software PixelWrench (Tetracam inc., Chatsworth, California, 2015) to support the visual qualification of the greenness of the transplants. Leaf litter cover on the transplants was calculated using perpendicular pictures of the transplants taken in June and October 2012 to 2015. Pictures were processed to obtain the percentage of leaf cover on the transplants using Adobe Photoshop. In 2014, we noticed that leaf litter seemed to induce a higher cover of fungal infection of the moss, so we estimated the percent cover of fungal hyphae on all the transplants in August 2015.

In October 2013, and June and October 2014, we collected one 10 cm diameter core of *H. splendens* in the proximity of each plot. These samples were dried and brought back to the laboratory at the University of Saskatchewan. Measurement of the shoot density, as well as length, width and weight of individual shoots were assessed in the laboratory during 2014-2015. We will use those results to build allometric equations for biomass accumulation of *H. splendens* in each stand as defined by Økland (1995) and by Benscoter and Vitt (2007). The development of these equations is a work in progress and here we use an estimate of shoot area (width*length/2, cm^2) as an approximation for biomass.

Soil
The SOL and top 10 cm of mineral soil were collected from 3 random locations within each study plot in August 2012. A ~10 cm x 10 cm intact block of the SOL was first removed using a knife and pruners. The total OL depth and depths of green moss, brown moss, and fibric horizons was recorded. The mineral soil immediately below the OL was removed using a 6.8 m diameter soil corer. Samples were wrapped, put on ice, then frozen until analysis.

To estimate N and phosphorus (P) pools in the field, 1 anion and 1 cation resin bag were deployed in the SOL and mineral soil within each plot in August 2012. The SOL bags were placed halfway between the SOL surface and top of the mineral soil. This was accomplished by cutting 3 sides of a 10 cm x 10 cm square with a knife, gently flipping up the OL, and then cutting a horizontal insert into the side of the hole. Mineral soil resins were installed ~ 5 cm below the surface of the mineral soil. A SOL square near (but not obstructing) the SOL resin bags was removed, then a trowel was inserted into the mineral soil at one of the edges of the hole, so that the resin bag was located under undisturbed SOL. The removed SOL square was

then placed back into the hole. All birch resins and the SOL spruce resins were removed and replaced with new bags in June 2013. In August 2013, all bags were removed and a new set was installed. All resins were rinsed with deionized water after returning to the lab and refrigerated until analysis (see below).

A 5-year mass-loss foliar litter and wood decomposition experiment was installed in August 2012. Senesced black spruce needles, senesced birch leaves, and brown moss had been placed into mesh bags prior to being taken to the field (details below). Birch craft sticks were also deployed as a uniform wood sample. Bags were grouped into sets that contained 1 bag of each litter type and 1 craft stick. Bags within a set were tied together with fishing line, leaving at least 10 cm between bags. 5 sets of bags were then deployed in each study plot around a central stake and fanned out in a star pattern. An additional craft stick was also deployed for removal after the litter portion of the experiment.

Foliage and litter

Specific leaf area was estimated on a subsample of fresh foliage produced in 2012. All remaining foliage was dried at 60ºC following field collection. Leaf litter obtained from birch plots in fall 2012 was sorted immediately into birch foliar litter and other components. A subsample from each plot (composite of the 3 baskets) was then dried at 60ºC to estimate moisture and for chemical analyses. Non-foliar litter components and foliar litter collected in summer 2013 from all plots was dried at 60ºC following each field collection, then sorted into foliar litter (by species), wood, seeds, cones, and other miscellaneous components. After sorting, all samples were re-dried and weighed. Spruce foliar litter collected in July 2013 from the 3 baskets in each spruce plot were composited into one plot sample for chemical analysis. For both species, a subsample of dried live foliage (both current and past year's needles for spruce) and foliar litter were ground using a wiley mill (Thomas Scientific model 3383-L10). A portion of this material was analyzed for percent C and N using a Costech Analytical ECS 4010 Elemental Analyzer (Valencia, CA) and an additional subsample was shipped to the Louisiana State University AgCenter for total P, calcium (Ca), magnesium (Mg), and potassium (K) analysis. Briefly, 5 mL of concentrated nitric acid was added to 0.5 g of ground sample. After 50 minutes, 3 mL of hydrogen peroxide was added and the sample was left to digest for 2.75 hours on a heat block. Sample was then cooled and diluted, then run on a Spectro ARCOS iCAP inductively coupled plasma spectrometer (Germany).

Soil

Samples were removed from the freezer and allowed to thaw prior to processing. Vascular plants and green moss were removed from the top of the SOL samples and dimensions of each organic horizon were recorded. Green moss was weighed, then dried at 60ºC. For spruce samples, the remaining SOL was cut horizontally at the interface between the brown moss and fibric horizons, when a brown moss layer was present. Birch organic samples consisted of a partially decomposed litter layer and fibric material and were processed as a single horizon. For all organic samples, a ~3 cm x 3 cm intact piece of each horizon was removed so as to include the entire vertical length of the horizon. These subsamples were then placed in a 32 oz mason jar with glass beads and perforated aluminum foil lining the bottom of the jar. For each horizon, the subsamples originating from the 3 field sampling locations within a given plot were put into a single jar, creating 1 composite sample per plot, per horizon. For each 10 cm mineral soil core, a

small portion of soil was removed using a spatula, incorporating soil from the entire vertical length of the core. Once in jars, deionized water was added to each sample to approximate field capacity and samples were placed in the dark at 15ºC. Soil carbon dioxide (CO_2) respiration was measured using an automated CO_2 flux system (Bracho et al., 2016) for 90 days. The remaining portion of each core was re-frozen immediately after removal of the incubation subsample. These samples were later thawed and a second subsample was removed and placed in a jar using the same method described above. These samples were incubated in the dark at 15ºC for 30 days to estimate net N mineralization and nitrification. Within the last 20 days of the experiment, a subset of each sample type was analyzed for $^{14}CO_2$ to determine the age of the C being respired by the different species and soil horizons (Schuur et al., 2009).

The remaining material for each organic horizon and mineral core were homogenized and a composite subsample was made for each plot. This composite sample was then analyzed for moisture content, percent C and N, and pH using the same methods described for Task 3 (above). Exchangeable base cations were measured as outlined in Robertson et al. (1999), using 50 mL of 1 M ammonium chloride (NH_4Cl) mixed with 5 g of field moist organic horizon sample and 10 g of mineral soil, respectively. After shaking for 1 hr on a shaker table, samples were filtered through a GF/A filter via vacuum filtration and frozen until analysis at the Louisiana State University AgCenter (Baton Rouge, LA) on a Spectro CIROS inductively coupled plasma spectrometer (Germany). A 5 g subsample of the composite soil was air-dried and used for analysis of Mehlich P following Kuo et al. 1996. Initial pool sizes of ammonium (NH_4) and nitrate (NO_3) were measured as outlined in Robertson et al. (1999), using the same method used for exchangeable cations, but using 2 M potassium chloride (KCl) instead of NH_4Cl. Samples were analyzed on an Astoria-Pacific International Autoanalzyer (Clackamas, OR) at the University of Florida. At the completion of both 30- and 90-day incubations the entire incubated sample was homogenized and analyzed for NH_4 and NO_3 as described.

In the laboratory, anion and cation resin bags retrieved in June 2013 were rinsed for 20 seconds with running nano-pure water to remove soil particles. Each bag was placed in a tube with 30 mL of a mixture of 0.1 M hydrochloric acid and 2.0 M sodium chloride and shaken for 1 hour on a shaker table. Extractant was then drip-filtered through a Whatman GF/A filter and frozen until further analysis. This extraction process was repeated two additional times for each resin bag. Ammonium and nitrate concentrations were measured colorimetrically using a segmented flow autoanalyzer (Astoria-Pacific, Inc., Clackamas, Oregon, USA). Phosphate (PO_4^{2-}) was measured colorimetrically within 1 week of extraction using a spectrophotometer microplate reader (PowerWave XS Microplate Reader, Bio-Tek Instruments, Inc., Winooski, VT) using the ascorbic acid molybdenum-blue method (Murphy and Riley 1962). Resins retrieved in August 2013 were extracted using the same method, but with a single extraction and additional N concentration estimated using relationships developed from the June dataset.

Litter decomposition experiment preparation

Mesh bags were constructed and later filled with leaf material for the mass-loss foliar litter decomposition experiment. Senesced foliar litter for both birch and spruce was collected in the Murphy Dome area in fall 2011 and additional spruce litter was collected in spring 2012. Brown moss was collected in early summer 2012. Foliar litter was thoroughly homogenized, then dried at 30ºC in the laboratory. Approximately 0.8 g of birch litter was added to 12 cm x 12 cm gray

fiberglass window screen mesh bags. For black spruce, 1 g of needles were added to 8 cm x 8 cm mesh bags constructed with no-see-um mesh. Additional samples of birch litter were added to no-see-um mesh to act as a mesh control. Brown moss was placed field moist for 1 minute in a conventional microwave to inhibit further growth. Moss was then thoroughly homogenized and dried at 30^{o}C. Subsamples weighting 0.5 g were then inserted into 8 cm x 8 cm no-see-um mesh bags. Birch craft sticks (Loew Cornell Woodsies brand) were purchased and a small hole was drilled in one end of the stick. Sticks were then dried at 30^{o}C and weighed.

Statistical analyses

To identify significant differences between species and assess variance among blocks, we conducted analysis of variance tests using two model designs. First, we used a nested model with species as the main effect and block nested within species (JMP Pro 9.0, SAS Institute, Cary NC) to test how within-species variability across blocks might affect our ability to detect overall species differences. For most analyses, differences between species were present and no significant differences were observed between blocks of the same species, suggesting low variability across the blocks. In the instances where there was a significant block effect, a post-hoc Tukey test was used to confirm that overall species effects were not driven by any one block acting as a large outlier. Therefore, we simplified our model to include only the species main effect and report the overall species effect here (Underwood, 1997). Prior to the analysis of variance testing, datasets were transformed when needed to meet normality and homoscedasticity assumptions prior to analysis. For datasets that could not be transformed to comply with normality assumptions, a nonparametric Wilcoxon test with a 2-sample normal approximation was used.

To analyze moss growth, biomass production, and greenness cover of the transplants according to litter manipulation treatments, we performed mixed-model analyses of variance (ANOVAs) including blocking (3 areas), and 2 levels of nesting (stand type and plot) in R (R Development Core Team 2012). Response variables were transformed using a square root transformation where required to meet ANOVA assumptions. Analyzes are currently in progress to include a repeated measure factor in the model to take in account the 3 years of measurement (2013, 2014 and 2015). We therefore here present results from the September 2013 and September 2014 data. We conducted a Spearman correlation to examine the relationship between leaf litter cover and fungus infection. We will assess the similarity of initial and final species composition according to treatment types using a mixed-model multivariate analysis of variance by permutations (PerMANOVA) using the same design as the univariate analyses (Legendre and Legendre 1998). As those analyses are in progress, we present averages and general trends.

T4: Results and discussion

Aboveground

The mean age of trees across the study site was 45 years (Table 4.1), indicating forest establishment following the 1958 fire. Within birch plots, birch trees accounted for 97% of live tree aboveground biomass while black spruce comprised 79% of the aboveground biomass in spruce plots. Stem density was over seven times higher in spruce stands compared to birch. However, spruce tree diameters were relatively small, resulting in significantly smaller basal area and less than half the total tree biomass found in birch stands (Table 4.1). Birch aboveground net primary productivity was also more than double that found in spruce plots.

Fresh birch foliage exhibited concentrations of N, P, Ca, and Mg, that were at least double that found in current year black spruce needles (Table 4.2). A higher concentration of K was also observed in birch foliage while black spruce showed a higher C concentration and larger C:N ratio (Table 4.2). Foliar litter N, P, Mg, and K concentrations were also higher in birch while black spruce contained a higher Ca concentration, as well as a larger C:N ratio. Specific leaf area of birch foliage was 3.5-fold that of spruce ($P < 0.0001$). Total litter inputs in birch stands were more than double that in spruce (242.8 ± 14.9 vs. 93.8 ± 10.8 g m^{-2} yr^{-1}, Figure 4.3A). This pattern was driven by larger inputs of foliar litter and wood in birch plots. Total foliar inputs of C, N, Mg, and K were all four to six times larger in birch plots relative to spruce, and Ca inputs were also statistically larger (Figure 4.3B).

Moss transplant and deciduous litter manipulation

Preliminary results suggest that the average area of the marked moss shoots increased over the two first years of the experiments (Figure 4.4). It also seemed like most of the growth occurs during the summer and that only a negligible amount of growth occurred in the shoulder seasons (Figure 4.4). The larger growth associated with the summer of 2014 could be due in part to wetter environmental conditions, but also to the fact that the data is not corrected yet for the increase in the number of steps that were being measured.

Leaf litter cover was about 88% ± 1.2 in all addition transplants, while it was of only 1% ± 0.2 in all exclusion transplants. Leaf litter cover on ambient transplants differed according to forest types, averaging 71% ± 5.0 in birch stand vs. 12% ± 2.7 in spruce stands. Leaf litter cover on control areas was 37% ± 3.6 in birch stands and 14% ± 2.7 in spruce stands. There was a strong positive correlation between the cover of leaf litter and the cover of fungal hyphae on the mosses measured ($\rho = 0.87$, $p < 0.001$).

In the control moss patches, we found that, both in September 2013 and September 2014, marked shoots in spruce stands were larger than in birch stands ($F_{1,271} = 66.86$, $p < 0.001$ and $F_{1,299} = 65.57$, $p < 0.001$, respectively, data not shown). Control mosses were in general always larger than the ones from the transplants, although this gap seemed to be closing up in the transplants without leaf litter cover (exclusion in birch, exclusion and ambient in spruce, data not shown), which suggests that the transplants have adapted to their new location and are getting closer to grow in a similar fashion to natural occurrences of moss.

In September 2013, a year after the leaf litter manipulation was initiated, we found that the average area of the marked moss shoots was significantly higher in spruce than in birch stands ($F_{1,26} = 14.96$, $p = 0.001$). There was no significant difference between the different treatments ($F_{2,56} = 0.09$, $p = 0.916$) or interaction between forest type and treatments ($F_{2,56} = 0.991$, $p=0.378$, Figure 4.4). In September 2014, there was a significant interaction between forest type and treatments ($F_{2,56} = 5.55$, $p = 0.006$, Figure 4.4). Following a Tukey Honest Significance post-hoc test, we found that, while mosses were still on average larger in spruce stands than in birch stands, within each forest type, mosses associated with treatments leading to a high leaf litter cover were smaller (Figure 4.4, addition and ambient in birch, addition in spruce). In summary, after one year the marked mosses had adapted their growth form to the environmental conditions

associated with their new stand, and after two years of treatments we were able to detect impacts of the leaf litter treatments in both forest types.

Initial moss species composition among the different treatments was very similar. Overall, *H. splendens* covered about 85% of the transplants and *Pleurozium schreberi* was the second most common species, covering about 38% of the transplants. Note that these species can occur together at the same grid point, and thus total cover is higher than 100%. Preliminary results suggest that the major differences observed in species composition were an increase in healthy looking *H. splendens* cover in transplants with leaf litter excluded in both spruce and birch stands (increase of about 14% and 32%, respectively), and a decrease in the addition treatment in spruce stands (-30%). Changes in *P. schreberi* mostly occurred in excusion transplants in birch stands (19% increase) and in addition transplants in spruce stands (-9%). So far, it seems like most changes in moss species composition in the transplants were driven by the complete exclusion or addition of leaf litter in both forest types.

Soils

The soil temperature 10 cm below the SOL surface was higher in birch soils relative to black spruce in September - October 2012, and June - July 2013. However, once soils dipped below freezing, species differences were no longer detectable. The SOL in black spruce soils was deeper (Table 4.2), exhibited a larger mass (9.7 ± 0.3 vs. 5.2 ± 0.9 kg organic material (OM) m^{-2}, $P < 0.0001$), and contained larger C and N stocks than paper birch soils (Figure 4.5B,D). Radiocarbon analysis of the SOL indicated that the uppermost ~9-12 cm of the SOL in black spruce stands was composed of C that accumulated in the years since the 1958 fire and accounted for ~3.6 ± 0.6 kg C m^{-2} of the observed SOL C stocks. Soil organic layer C stocks measured across all black spruce plots averaged 4.8 kg C m^{-2}, suggesting that approximately 75% of the observed SOL C accumulated in the years since the fire and 25% of the C survived the 1958 fire and is a legacy of the previous forest. In the birch SOL, bulk soil $\Delta^{14}C$ values indicated that the bulk C pool was ≤ 26 years old, indicating all SOL C has accumulated post-fire and that the SOL turns over relatively rapidly in the deciduous stands.

Birch SOL samples contained higher concentrations of N, Mehlich P, exchangeable Ca and Mg, and showed higher pH, while a larger C:N ratio was observed in the black spruce SOL (Table 4.3). Despite higher concentrations of exchangeable Ca and Mg in paper birch, the larger SOL mass in black spruce offset this, resulting in no difference in the total pool size of either base cation in the SOL (data not shown). Within the uppermost 10 cm of mineral soil, black spruce contained higher concentrations of C and N, a larger C:N ratio, and higher pH than birch, while birch soils showed greater concentrations of Mehlich P and exchangeable K (Table 4.3). There was a trend for higher total elemental P in black spruce soils, but the small sample size prevented statistical analysis.

Accumulation of resin bound NH_4^+ was higher in both SOL and mineral soils of birch stands relative to spruce (Figure 4.6A). A similar pattern was observed for resin bound PO_4^{2-} (Figure 4.6E). Nitrate accumulation was also higher in the SOL in birch soils, while no difference was observed in mineral soil (Figure 4.6C). For the 90-day incubation, there was a trend for higher potential net N mineralization and nitrification in organic and mineral birch soils (Figure 4.6B, 4D), however these differences were only significant for N mineralization in mineral soil and

nitrification in the SOL. A similar pattern was observed for the 30-day incubation (data not shown). No difference in cumulative CO_2-C released or the $\Delta^{14}C$ value of the CO_2-C was observed between species for either soil layer.

Our results illustrate large interspecific differences in plant-soil-microbial feedbacks in boreal forest that strongly influence C and nutrient turnover and distribution. In general, these findings supported our hypotheses: differences in C and nutrient pool sizes and potential N mineralization were consistent with relatively slow biogeochemical cycling in black spruce forest and more rapid C and nutrient turnover in birch stands. Small fluxes and low nutrient availability were coupled with slow tree growth and large soil OM pools in spruce while large fluxes, small nutrient pool sizes, and more rapid growth characterized stands of the same age that were dominated by birch. Our findings indicate that shifting from black spruce to Alaska paper birch-dominated regeneration following severe fire events could result in dramatic changes to the structure and function of boreal ecosystems. The legacy of fire and the development of contrasting, species-specific linkages between forest productivity, C and nutrient pools, and the soil environment, may cause landscape-scale shifts in the distribution of ecosystem C pools and nutrient cycling rates.

Table 4.1. Mean stand characteristics for black spruce and Alaska paper birch forest across the study site, reported in Melvin et al. (2015).

	Black spruce	Paper birch	*F*	*P*
Tree age (years)	42.6 (1.1)	48.2 (0.6)		
Density (stems m^{-2})				
All stems	7.31 (0.65)	0.93 (0.10)	242.21	< 0.0001
Plot species				
BD	3.70 (0.65)	0.03 (0.01)		
DBH	3.05 (0.21)	0.72 (0.06)		
Other species				
BD	0.02 (0.01)	0.12 (0.05)		
DBH	0.18 (0.04)	0.02 (0.004)		
Tall shrubs	0.37 (0.05)	0.04 (0.02)		
Basal area (m^2 ha^{-1})				
All stems	21.80 (1.48)	28.63 (1.60)	9.80	< 0.0001
Plot species				
BD	3.19 (0.57)	0.02 (0.01)		
DBH	13.95 (1.48)	27.50 (1.58)		
Other species				
BD	0.10 (0.04)	0.12 (0.04)		
DBH	2.06 (0.46)	0.08 (0.03)		
Tall shrubs	2.49 (0.41)	0.91 (0.30)		
Live aboveground tree biomass (kg m^{-2})				
All stems	5.30 (0.51)	11.33 (0.70)	48.28	< 0.0001
Plot species				
BD	0.17 (0.03)	0.001 (0.001)		
DBH	3.96 (0.39)	10.99 (0.70)		
Other species				
BD	0.01 (0.002)	0.01 (0.004)		
DBH	0.68 (0.16)	0.02 (0.01)		
Tall shrubs	0.49 (0.10)	0.30 (0.11)		
Proportion biomass				
Plot species	0.79 (0.02)	0.97 (0.01)		
Other species	0.12 (0.02)	0.003 (0.0001)		
Tall shrubs	0.09 (0.02)	0.03 (0.01)		
$ANPP_{tree}$ (g m^{-2} yr^{-1})	192.5 (17.2)	463.9 (28.5)	69.64	< 0.0001

Values are mean (SE), n = 15 study plots for each species. *P* values indicate significant differences between the two forest types for the given row variable (df = 1, 28 for all analyses). Trees ≥ 1.4 m in height are included in the rows labeled DBH (diameter at breast height) and trees < 1.4 m tall are included in the BD (basal diameter) category.
Other species category includes all measure trees that were not the focus species studied within the given plot.

Table 4.2. Live foliage and foliar litter chemistry for studied stands of black spruce and Alaska paper birch forest near Fairbanks, Alaska. Table is published in Melvin et al. (2015).

	Live foliage				Foliar litter			
	Black spruce	Paper birch	*F*	*P*	Black spruce	Paper birch	*F*	*P*
C %	49.93 (0.09)	47.16 (0.81)	11.57	<0.0001	49.27 (0.13)	49.39 (0.06)	0.69	0.4136
N %	1.08 (0.03)	2.52 (0.05)	584.81	<0.0001	0.73 (0.04)	0.92 (0.02)	18.63	0.0002
C:N	46.45 (1.09)	18.73 (0.26)	616.98	<0.0001	70.10 (3.79)	54.46 (1.38)	15.07	0.0006
P %	0.12 (0.004)	0.24 (0.01)	345.94	<0.0001	0.03 (0.002)	0.21 (0.01)	475.38	<0.0001
Ca %	0.30 (0.01)	0.70 (0.02)	240.57	<0.0001	1.74 (0.02)	0.96 (0.02)	555.69	<0.0001
Mg %	0.09 (0.002)	0.38 (0.01)	863.53	<0.0001	0.04 (0.001)	0.44 (0.01)	2211.41	<0.0001
K %	0.49 (0.01)	0.87 (0.02)	278.90	<0.0001	0.10 (0.003)	0.41 (0.02)	708.52	<0.0001

Values are mean (SE) for 15 plots per study species. For all statistical analyses df = 1,28 and *P* values indicate differences between the two tree species for the given row variable.
*** indicates $P < 0.0001$.
The foliar litter concentrations of P, Ca, Mg, and K for black spruce were obtained from samples collected only in study block A and statistical analyses for these variables were comparisons between only block A samples for both species, however presented values for birch include all study blocks.

Table 4.3. Soil organic layer and mineral soil (0-10 cm) characteristics in adjacent stands of black spruce and Alaska paper birch in interior Alaska, published in Melvin et al. 2015.

	Black spruce	Paper birch	*F*	*P*
Organic layer				
Depth (cm)	16.4 (0.9)	7.6 (0.4)	87.01	< 0.0001
Bulk density (g cm^{-3})	0.06 (0.01)	0.07 (0.003)	0.73	0.40
C %	43.01 (0.55)	41.07 (0.83)	3.64	0.07
N %	1.33 (0.04)	1.75 (0.04)	54.54	< 0.0001
C:N	32.62 (0.93)	23.58 (0.47)	75.58	< 0.0001
Mehlich P (mg g^{-1})	0.11 (0.01)	0.17 (0.01)	19.75	< 0.0001
Exchangeable Ca ($cmol_c$ kg^{-1})	14.72 (1.37)	23.65 (1.45)	20.10	0.0001
Exchangeable K ($cmol_c$ kg^{-1})	2.92 (0.12)	2.87 (0.13)	0.10	0.75
Exchangeable Mg ($cmol_c$ kg^{-1})	5.78 (0.90)	12.54 (0.86)	29.25	< 0.0001
pH	4.33 (0.09)	4.98 (0.10)	22.99	< 0.0001
Mineral				
Bulk density (g cm^{-3})	0.65 (0.03)	0.71 (0.04)	2.21	0.15
C %	6.41 (0.65)	3.65 (0.28)	18.59	0.0002
N %	0.31 (0.03)	0.20 (0.02)	12.45	0.002
C:N	20.61 (0.48)	18.60 (0.61)	6.72	0.02
Mehlich P (mg g^{-1})	0.006 (0.003)	0.03 (0.004)	19.14	0.0002
Exchangeable Ca ($cmol_c$ kg^{-1})	6.10 (1.35)	3.79 (0.45)	2.31	0.14
Exchangeable Mg ($cmol_c$ kg^{-1})	2.39 (0.72)	1.30 (0.17)	2.26	0.14
Exchangeable K ($cmol_c$ kg^{-1})	0.23 (0.02)	0.29 (0.02)	4.90	0.04
pH	5.21 (0.11)	4.95 (0.06)	4.31	0.05
Total element concentrations				
P %	0.0773 (0.0042)	0.0637 (0.0081)		
Ca %	1.22 (0.29)	1.26 (0.32)		
Mg %	0.86 (0.09)	0.94 (0.15)		
K %	1.26 (0.05)	1.26 (0.12)		

Mean (SE), n = 15 plots of each tree species. *P* values indicate differences between species for the row soil characteristic (df = 1,28). For total element concentrations in the mineral soil, n = 3 samples per species (1 plot composite per species, per block) and no statistical analyses were performed.

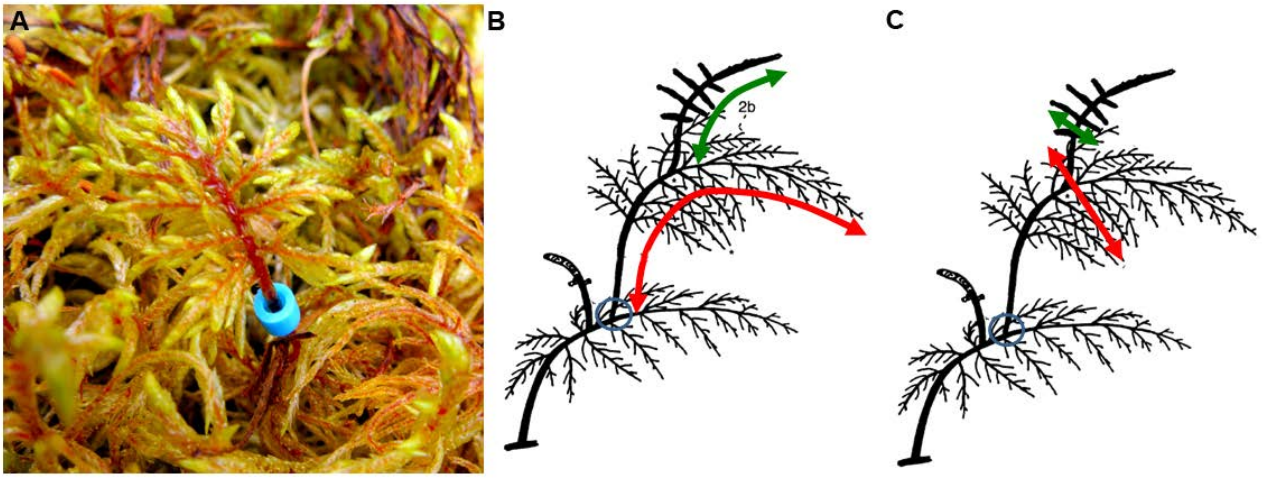

Figure 4.1 Measurements method for the growth of *H. splendens.* The red arrows represent the measurements on mature previous year shoots, and green arrows represent measurements on current year growth shoots A) PVC markers on a shoot. B) Length measurements. C) Width measurements (modified from Økland (1995).

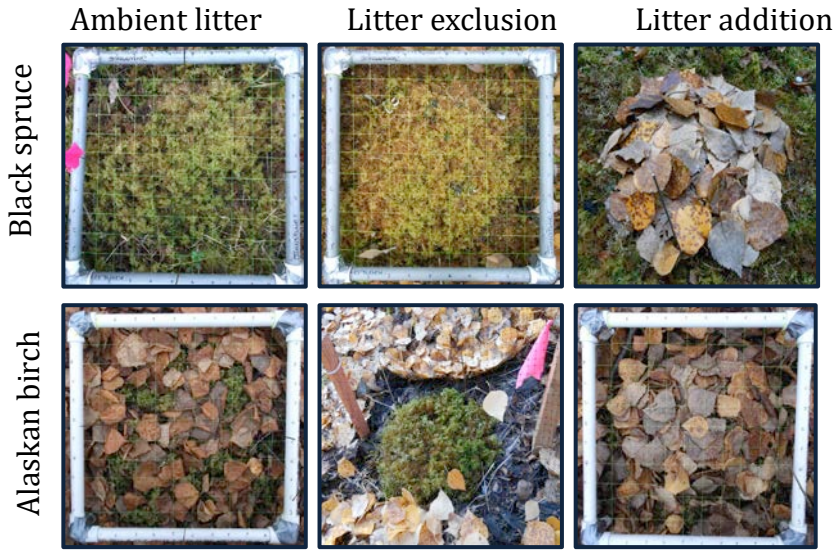

Figure 4.2 Leaf litter treatments on moss transplants. Transplants in black spruce stands are shown in the first row, and those in Alaskan paper birch stands are shown in the second row. Treatments are shown in the columns (1- ambient litter, 2- litter exclusion, 3- litter addition).

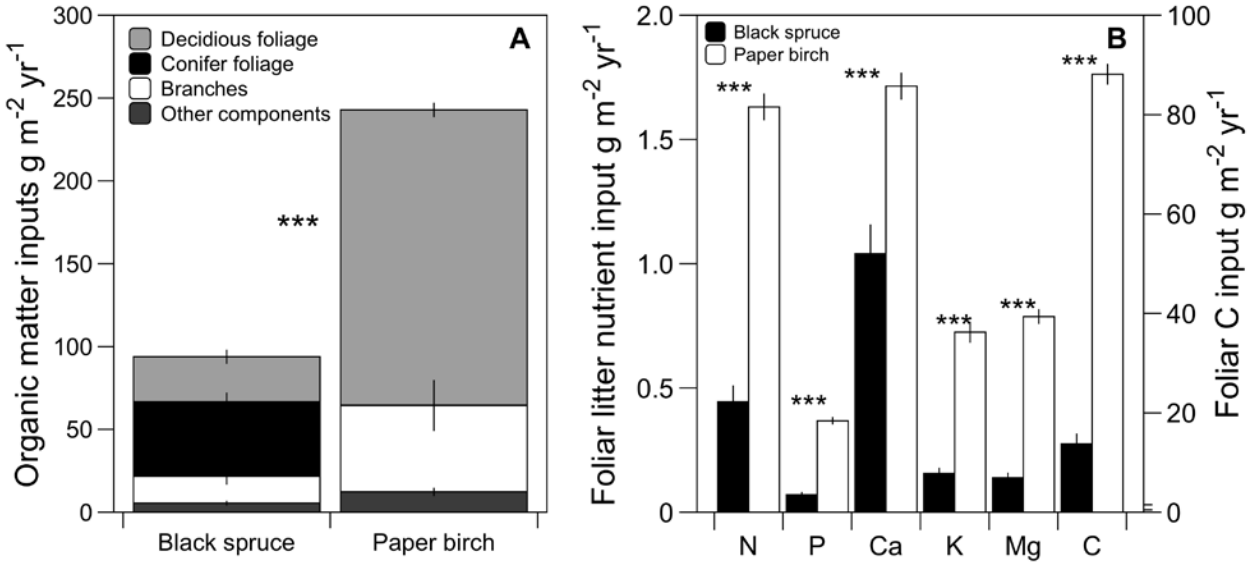

Figure 4.3. Annual litter input and composition in black spruce and Alaska paper birch stands (A), and input rates of nutrients in foliar litter in each stand type (B). Carbon input values correspond to the axis on the right side of panel B. Values are presented as mean (SE) for each indicated component, (n = 15 plots per species). Significant differences between tree species for each variable are indicated with *** ($P < 0.0001$), determined using a nonparametric Wilcoxon test. Figure published in Melvin et al. (2015).

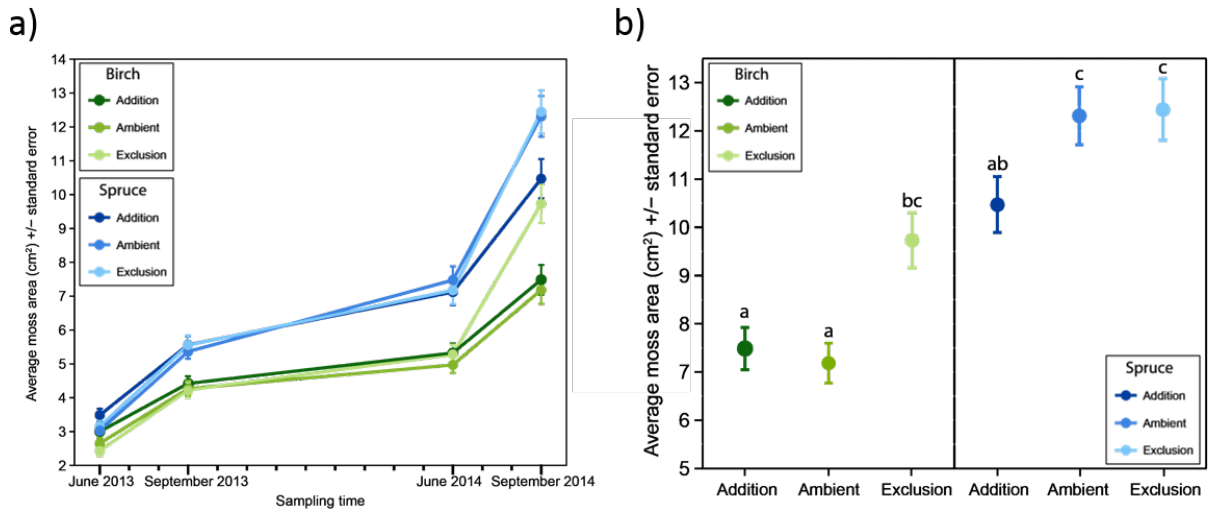

Figure 4.4. a) Average moss area (cm^2) according to time. The four sampling points are represented as dots with standard error. The treatment and forest types associated with the measurements are identified by colors. b) Average moss area in September 2014 and standard error. The letters indicate a significant difference following a Tukey Honest Significant Difference (HSD) post hoc test.

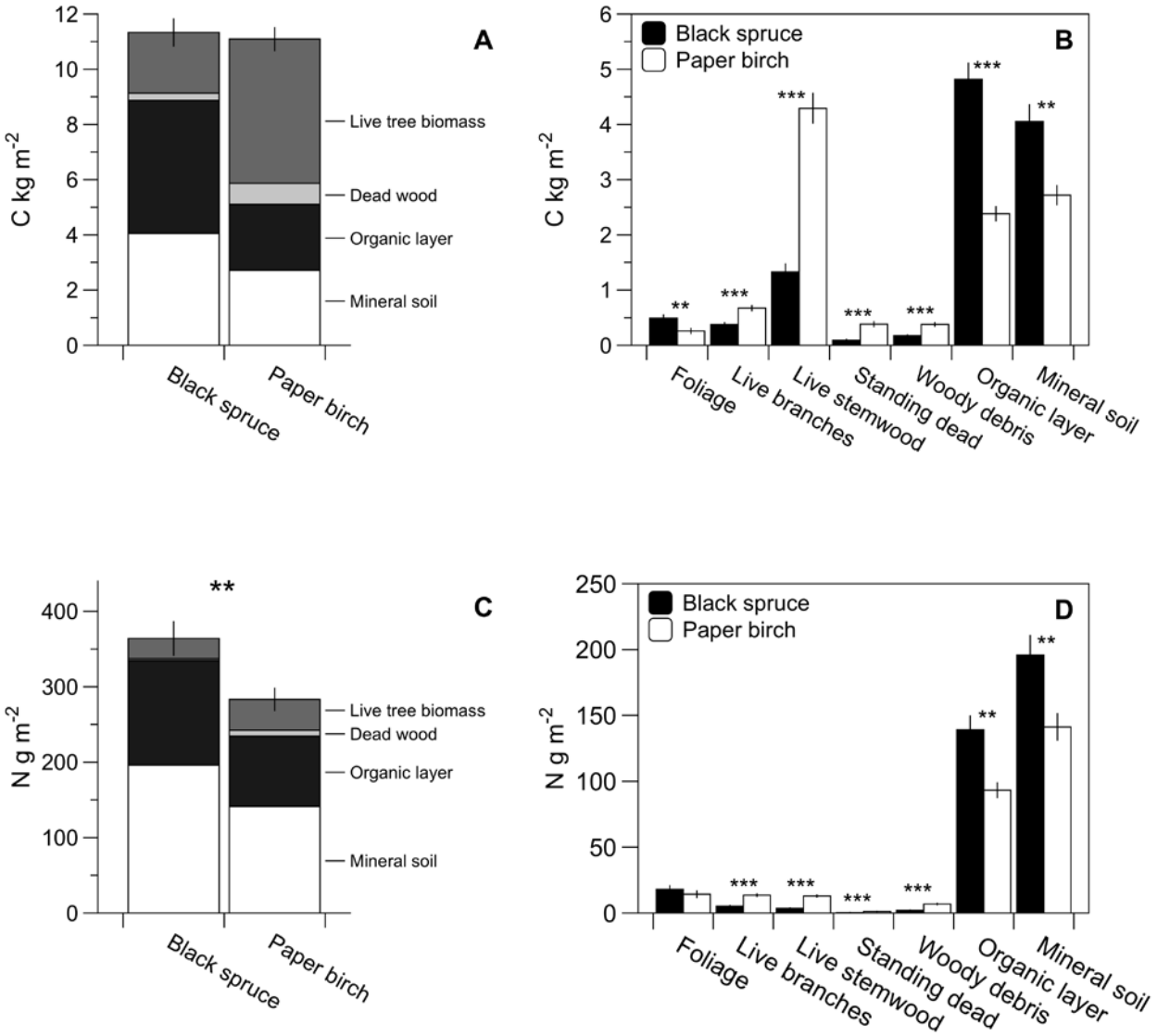

Figure 4.5. Measured forest stand C and N stocks (A and C) and the distribution of stocks among the measured forest stand pools (B and D). Mineral soil includes the uppermost 10 cm. Values are reported mean (SE), n = 15 plots per species. For A and C, error bars and statistical analyses are for the total summed ecosystem stocks. Significant differences between species for each stock and pool are indicated by ** $P < 0.001$ and *** $P < 0.0001$. Figure published in Melvin et al. (2015).

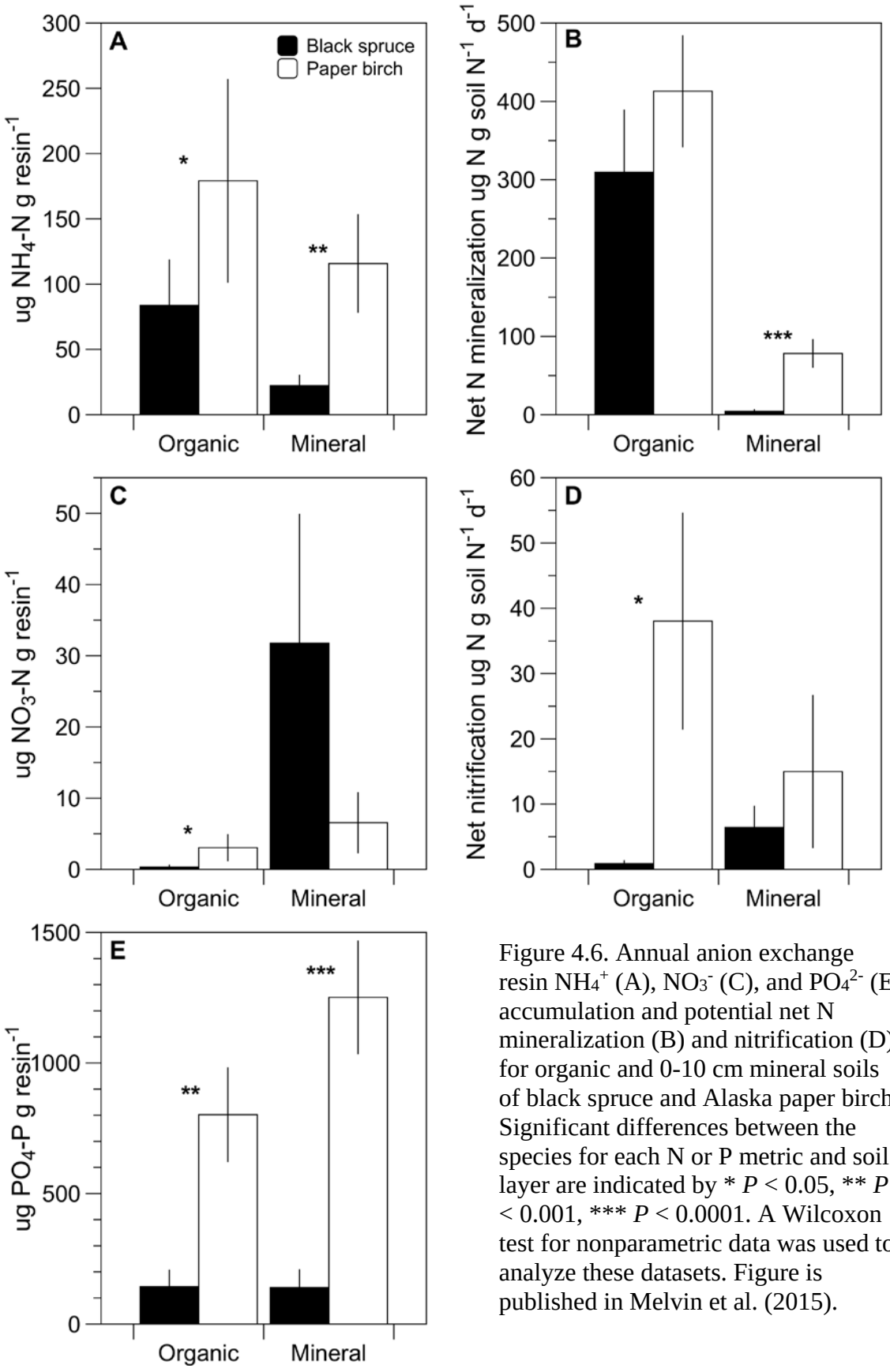

Figure 4.6. Annual anion exchange resin NH_4^+ (A), NO_3^- (C), and PO_4^{2-} (E) accumulation and potential net N mineralization (B) and nitrification (D) for organic and 0-10 cm mineral soils of black spruce and Alaska paper birch. Significant differences between the species for each N or P metric and soil layer are indicated by * $P < 0.05$, ** $P < 0.001$, *** $P < 0.0001$. A Wilcoxon test for nonparametric data was used to analyze these datasets. Figure is published in Melvin et al. (2015).

Task 5: Monitor mid-successional wildfire network

T5: Materials and methods

To improve our understanding of the impacts of tree species composition shifts on C cycling and storage in Alaska's boreal forest, we identified mid-successional sites across the interior that fell along a deciduous to conifer gradient. These sites were used to develop allometric equations to estimate biomass of all tree and shrub species common to the interior. Methods are detailed in Alexander et al. (2012).

We revisited these sites to include a more intensive investigation of the linkages between mosses, plant litter, and stand structure that complement our litter manipulation experiment (Task 4). We focused on the understory species composition in 51 mid-successional stands (20-62 years since fire) in 17 burn scars in interior Alaska that were sampled by Alexander et al. (2012), as well as an additional 9 mature stands (> 62 years since fire). We added a total of 29 new, early succession (8-20 years since fire) stands in 8 fire scars to include a wider range of ages in our dataset. A subset of five sites sampled by Alexander et al. (2012) were resurveyed in 2015 to ensure that data collected by both observers was comparable.

Understory species and ground cover were obtained using a 50 cm x 50 cm grid and point-intercept sampling with five replicates per stand. A pin was inserted in the ground at each of the 25 sampling points. All vascular and non-vascular plant species and other ground cover types (e.g. leaf litter, bare ground, coarse woody debris) that touched the pin were recorded. We also collected stand structure information (DBH, tree density, deciduous importance value, forest type) and some environmental variables (slope, exposition, pH, SOL depth) that were published in Alexander et al. 2012, or collected in 2014-2015. Forest types (black spruce, Alaskan paper birch, and trembling aspen) were determined based on the species that contributed to the larger amount of biomass to the canopy. Bryophyte species were grouped into functional types according to Turetsky et al. (2012).

Univariate and multivariate statistical analyses were used to assess 1) how moss abundance and species composition vary among mid-successional deciduous, mixed, and coniferous stands, and 2) evaluate how moss abundance, diversity and species composition can be explained using the environmental variables. We compared moss and lichen cover and species composition among three forest types (black spruce, Alaskan paper birch, and trembling aspen) using analyses of variance, indicator species analyses, and a non-metric multidimensional scaling (NMDS) ordination. We used multivariate regression trees, and variation partitioning to assess the relationship between moss and environmental variables. Analyses and development of a manuscript for this task are still in progress and we herein present preliminary results.

T5: Results and discussion

Bryophyte cover varied according to forest types and the three post-fire successional stages ($F_{4,74}$=9.098, p<0.0001; Figure 5.1). Bryophyte cover was high in all early successional forest types ($\bar{x}$ = 69%, Figure 5.1). While overall bryophyte cover was reduced to an average of 32% during the mid-successional stage, the bryophyte cover was higher in spruce ($\bar{x}$ = 53%) compared to birch and aspen ($\bar{x}$ = 32% and $\bar{x}$ = 24%, respectively; Figure 5.1). Bryophyte cover divergence continued in the late succession where bryophyte cover increased to an average of

94% and 31% in spruce and aspen, respectively. We observed the lowest bryophyte cover ($\bar{x}$ = 5%) in birch during the late succession (Figure 5.1). In terms of total bryophyte cover, a divergence between the coniferous (spruce) and deciduous (birch and aspen) successional trajectories occurred between 20 and 40 years since fire. This divergence seemed to coincide with major changes in leaf litter cover associated with the canopy type (Figure 5.1). Indeed, this was supported by the multivariate regression tree analysis conducted on total bryophyte cover, which identified a threshold of 70% leaf litter cover as a major driver of bryophyte cover.

Colonizer species declined quickly from 8 to 40 years, following a very similar trend in all forest types (Figure 5.2). In all forest types, colonizer species cover was dominated mostly by *C. purpureus* and *M. polymorpha* from 10-20 years after fire, and from 20-40 years after fire the declining cover of colonizers was dominated by larger acrocarpous species such as *P. commune* and *P. juniperinum*. Feather mosses remained low in deciduous stands throughout succession, but increased in spruce stands until about an average of 63% cover in late succession (Figure 5.2). The increase in feather mosses in late succession aspen stands was mostly driven by a single site (Figure 5.2). In all stands *P. schreberi* and *H. splendens* share the dominance of the feather moss cover. *P. schreberi* seemed to be slightly more abundant than *H. splendens* until about 65 years and 110 years since fire in spruce stands. The cover of other true mosses was higher in spruce stands (about 18%) than in deciduous stands (< 7%), and remained relatively low in all forest types throughout succession (Figure 5.2). *Sphagnum* cover increased steadily in older spruce stands and was absent from deciduous stands, while liverworts were rare in all forest types at every stage of succession.

An indicator species analysis was run to determine bryophyte and lichen species that are characteristic of the different forest types at different successional stages. During early succession, indicator species were found for spruce stands (*Aulacomnium turgidum* and *Peltigera. Canina* (lichen)) and aspen stands (*Polytrichum juniperinum* and *Ceratodon purpureus*), but not for birch stands (Table 5.1). During mid-succession, *Peltigera neopolydactyla* (lichen) was identified as the only indicator species of aspen stands, and birch stands did not have indicator species (Table 5.1). Because of the overlap in species composition in the earliest years of the mid-succession stage among all forest types, the only indicator species found in spruce stands at this stage was *Peltigera aphtosa* (lichen) (Table 5.1). Indicator species of late succession spruce stands were *H. splendens*, *P. schreberi*, *Sphagnum* spp., and *Dicranum* spp. (Table 5.1). No indicator species were found for either deciduous forest types.

Table 5.1. Bryophyte indicator species. Results from three analyses using 4999 randomizations on non-vascular understory species percent cover according to forest type (black spruce, Alaskan paper birch and trembling aspen) and successional stage (early, mid-, and late succession).

	IV	*p*
Early succession (<20 years)		
Black spruce stands:		
Aulacomium turgidum	0.58	0.048
Peltigera canina	0.44	0.078
Aspen stands:		
Polytrichum juniperinum	0.54	0.001
Ceratodon purpureus	0.37	0.003
Mid-succession (20-60 years)		
Black spruce stands:		
Peltigera aphtosa	0.34	0.016
Trembling aspen stands:		
Peltigera neopolydactyla	0.47	0.044
Late succession (>60 years)		
Black spruce stands:		
Sphagnum spp.	0.71	0.005
Hylocomium splendens	0.50	0.004
Dicranum spp.	0.47	0.050
Pleurozium schreberi	0.38	0.018

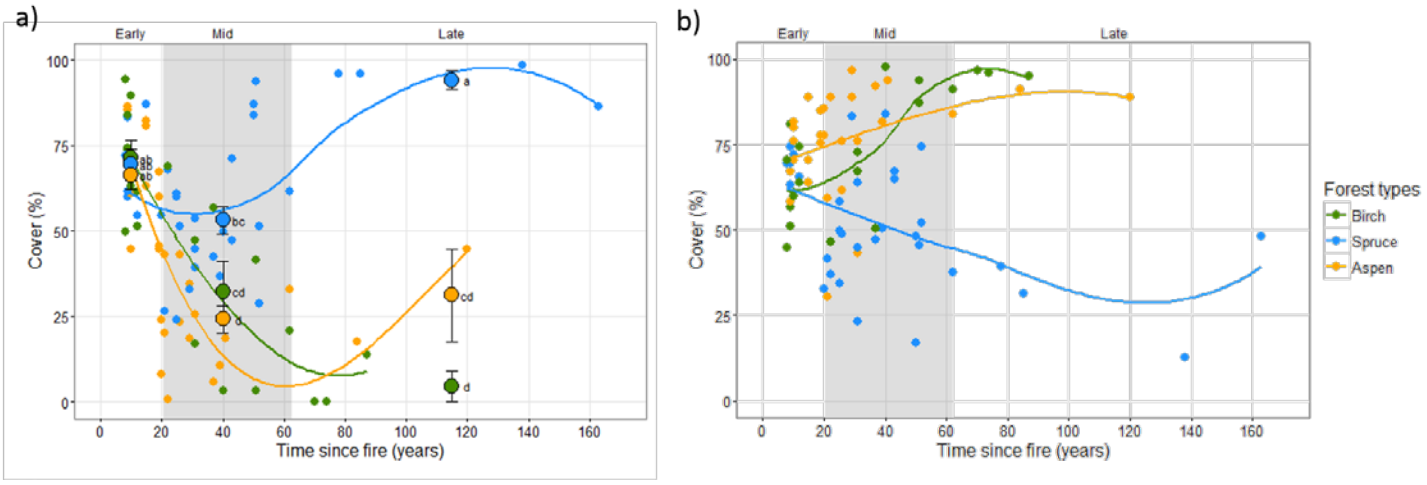

Figure 5.1. a) Variations in total bryophyte cover (%) in spruce (blue), birch (green) and aspen (yellow) stands over time since fire (years). b) Variations in leaf litter cover (%) over time since fire (years).The dots represent percent cover according to time since fire (years) for each of the 83 sampled stands and the curves are fitted using LOESS (locally weighted scatterplot smoothing) with a smoothing parameter of 1 for each series of points. The three post-fire successional stages are indicated by boxes above the plot and consist of: early succession (8-20 years since fire), mid-succession (20-62 years since fire), and late succession (>62 years since fire). The larger points and error bars represent the average bryophyte cover and standard error for each forest type in each time period. Lower case letters indicate significant differences among forest types and successional stages following a Tukey Honest Significance Difference post-hoc test ($p<0.05$).

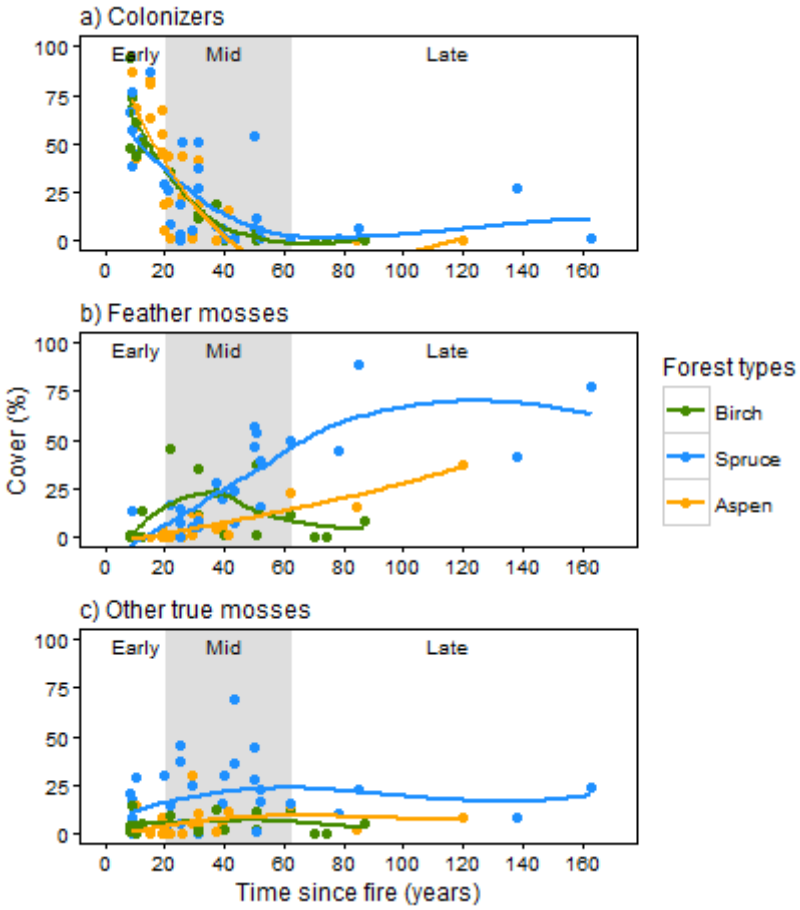

Figure 5.2. Variations in bryophyte cover from the major functional types (colonizers, feather mosses and other true mosses) over time since fire (years) in spruce (blue), birch (green), and aspen (yellow) stands. The dots represent bryophyte percent cover according to time since fire (years) for each of the 83 sampled stands. The curves are fitted using LOESS (locally weighted scatterplot smoothing) with a smoothing parameter of 1 for each series of points.

Task 6: Tree ring sampling and analysis

T6: Materials and methods

In the summer of 2012 and 2013, we established 72 sites within three large burned areas in interior Alaska that arose from multiple fire ignitions in 2004 (Figure 6.1). Within each burn complex, we established 24 sites dominated by black spruce prior to burning. We established 12 pure black spruce sites that were stratified by landscape position, with three sites each of moist lowland (M), north facing midslope (Nf), south facing midslope (S), and dry upland (D) positions within each burn complex. In addition, we established six sites each in mixed trembling aspen/black spruce stands (TA) and mixed paper birch/black spruce stands (PB), which were generally located in drier and warmer landscape positions within each burn. To randomize site selection, we identified every possible road accessible site within a burn complex that fit the broad-scale landscape positions, or presence in the case of mixed stands, and then randomly selected a subset. Although tree mortality from fire was close to 100%, fires rarely consumed all the branches or bark on a tree; pre-fire tree species were easily identifiable with well-preserved stems when sites were sampled in the summers of 2012 or 2013. Sites in the Steese and Taylor regions have coarse soils and are relatively well drained, whereas a thick cap of loess characterizes soils in the Dalton and Dempster regions. The majority (75-80%) of the boreal forest throughout these regions is underlain by permafrost (Osterkamp and Romanovsky 1999), with the exception of south-facing slopes and floodplains near major rivers (Viereck et al., 1983).

Site characteristics were sampled along two parallel 30 m transects separated by 20 m. We recorded latitude, longitude, and elevation in the center of the 30 m x 20 m area with a handheld GPS, and the slope and aspect with a clinometer and compass. Using these measurements, we calculated a unitless index of heatload that takes into account topographic and latitudinal effects on incoming solar radiation (McCune and Keon 2002). Soil texture class was assessed in the field by hand texturing the uppermost mineral horizon, following the Canadian System of Soil Classification (Branch et al. 1987). Understory composition was noted, in particular the presence of indicator species outlined by Hollingsworth and others (2006). Based on understory composition, topography, and drainage conditions adjusted for soil texture, site moisture classes were estimated on a six-point scale, ranging from xeric to subhygric (Johnstone et al. 2008).

At each site, we collected 10 stem disks at the standard height of 1.4 m from pre-fire black spruce trees randomly selected along the two transects. Stem disks were sanded with increasingly finer sandpaper up to 400 grit to produce visible rings (Cook and Kairiukstis 1990). Annual ring widths were measured on two radii per stem disk (WINDENDRO version 2012c, resolution 0.001 mm). We visually cross-dated each tree-ring series against master chronologies developed for each site and region. We quality-checked our cross-dating using COFECHA version 6.06 (Grissino-Mayer 2001), which uses statitical measures of similarity or dissimilarity to assess the quality of the cross-dating and measurement accuracy (Grissino-Mayer 2001).

Environmental conditions are known to influence the relative amount of ^{13}C to ^{12}C in individual tree rings. Specifically, stomatal closure due to drought stress increases the relative proportion of ^{13}C to ^{12}C. To determine the extent of annual variation in $\Delta^{13}C$ we randomly selected six trees, three from each the south and north-facing slopes in the Poker Flats Research Range (PFRR)

within the Boundary Fire (Figure 6.1) for stable isotope analysis on annual rings. Ring samples were manually separated from the outer thirty years (1974-2003) on two perpendicular radii (2.5 cm x 2.5 cm) per tree using a dissecting scope, razor, and chisel. Wood from the two radii were homogenized into one sample using scissors to pass through ~20 mesh. This method ensured minimal sample loss. The samples were then oven-dried at 60°C for 48 hrs. We encased approximately 2.5 mg of each sample in a tin cup for isotopic analysis. We chose to use wholewood for this analysis based on previous results obtained from analyzing $\Delta^{13}C$ of various wood components. All samples were measured for $\delta^{13}C$ using a continuous flow, stable-isotope mass spectrometer at the Light Stable Isotope Mass Spec Lab in the Department of Geological Science at the University of Florida. The $\delta^{13}C$ values are expressed relative to the Vienna PeeDee belemnite (VPDB) standard (Coplen 1995).

We estimated pre-fire and post-fire stem density and forest composition by measuring pre-fire (burned) trees and newly established seedlings. We counted all standing or fallen pre-fire trees and measured diameter at breast height (dbh) on all individuals taller than 1.4 m that were originally rooted in two parallel 2 m x 30 m belt-transects. We used these data to estimate total density (stems ha^{-1}) and basal area (m^2 tree area ha^{-1}) of each tree species prior to the fire. Similarly, we estimated post-fire density by counting post-fire seedlings within ten randomly positioned 1 m x 1 m quadrats along the same two transects. We identified each seedling to species and calculated the proportion of spruce stems relative to total stems in both the pre-fire and post-fire stand.

Data analysis

Climate data for each of our study regions was characterized based on spatially interpolated mean monthly temperature and total monthly precipitation for the period 1975 to 2003. Climate data were obtained from SNAP (Scenarios Network for Alaska and Arctic Planning 2013), which uses GCMs (Global Climate Models) (GCMs) and a PRISM (Parameter-elevation Regressions on Independent Slopes Model) approach (Daly et al. 1997) to downscale climate data to a 1 km resolution. We used averaged downscaled climate data corresponding to each of the burn scars examined in this study. We calculated a monthly climatic moisture index (CMI) from total monthly precipitation minus monthly potential evapotranspiration (PET), a function of temperature (Hogg 1997). High CMI values signify high moisture availability.

All remaining data analyses were conducted in R version 3.0.2 (R Development Core Team 2011). To remove the non-climatic trends in ring growth, raw ring width measurements were detrended using a smoothing spline, with a frequency response of 0.5 at a wavelength of 0.67*n years in the package 'dplR, version 1.5.7' (Bunn 2010). A dimensionless ring width index for each series was produced by dividing the actual ring-width measurement by the curve-fitted value in each year (Cook and Briffa 1990, Bunn 2010). We calculated bootstrapped correlations of detrended, individual ring-width chronologies with monthly temperature and precipitation over a 17 month climatic window, extending from April of the year preceding growth to August of the current year of growth (1975 to 2003). The significance of each climate correlation was tested using the 95 percentile range (Zang 2010). From these correlations, we categorized the growth response of each individual tree to temperature and precipitation as positive, negative, mixed, or no response and then calculated the proportion of trees in each temperature and precipitation category for each site. We used the proportion of trees responding negatively to

temperature and the proportion responding positively to precipitation as two indicators of stand-level drought stress.

We estimated the sensitivity of tree growth to climate at each site using bootstrapped correlations of mean ring-width chronologies for each site and mean monthly temperatures, total monthly precipitation, or monthly CMI. This resulted in 51 radial growth correlations to monthly climate parameters at each site. For subsequent analyses we used only those growth-climate correlations that elicited a significant response in at least 20% of the sites and that were not highly collinear (Spearman's rank correlation $\rho>0.6$). Our selection process resulted in five variables associated with CMI that represented the strongest and most widespread relationships between site-level patterns of tree growth and monthly climate.

To assess how site types varied in their growth responses to climate, we created mean chronologies based on site type (dry flat, wet flat, north facing slope, and south facing slope) in the package 'dplR, version 1.5.7' (Bunn 2010). General chronology statistics of mean correlation between trees (R), mean sensitivity (MS), signal to noise ratio (SNR), and autocorrelation (AR) for each of the standard chronologies developed per site type and region were calculated to ensure that all the chronologies were suitable for growth-climate analyses (Speer 2010). We then determined the growth-climate responses of each site type using the package 'bootRes, version 1.2.3' (Zang 2010), by calcualting bootstrapped correlations between ring widths and mean monthly temperatures and total monthly precipitation for the period 1975 to 2003. Growth-climate correlations were calculated using a 17-month climate window, extending from April of the year preceding growth to August of the current year of growth (Fritts 1976)(, over the priod 1975 to 2003. The significance of each of the 34 climate correlations was tested using the 95 percentile range (Zang 2010).

To confirm our growth-climate responses using stable isotope analysis, we created mean $\delta^{13}C$ chronologies based on site type (north facing slope and south facing slope) in the package 'dplR, version 1.5.7' (Bunn 2010). To assess how climate influenced these chronologies we correlated $\delta^{13}C$ discrimination over the 30-year period with mean monthly temperature using the same methods as for growth-climate correlations (see above).

As a proxy for ecosystem resilience we estimated the change in tree composition (black spruce dominance) after fire as the difference in the proportion of total trees that were black spruce in the pre-fire vs. post-fire stand at the same site. Negative values represent a decrease in the proportion of black spruce trees in the post-fire stand. We assessed three sets of explanatory variables as potential predictors of the change in black spruce dominance: measures of a) pre-fire stand composition (pre-fire; 7 variables), b) site environmental conditions (site; 9 variables), and c) dendroclimatic variables (dendro; 8 variables) (Table 6.1). In addition to the two climate-growth responder categories and the five climate-growth correlations (see above) we included average radial growth from 1975-2003 for each of the site chronologies in the dendro explanatory matrix (Table 6.1).

To evaluate potential thresholds in the effects of explanatory variables and examine functional responses we used boosted regression tree (BRT) analysis in the packages 'gbm' (Ridgeway et al. 2013) and 'dismo' (Hijmans et al. 2013) with the proportional change in black spruce as the

response variable. To avoid over-fitting, we used a stepwise selection process, using model adjusted R^2 and variable retention at a permutation value of p=0.05 (Blanchet et al. 2008) to identify individual variables that were significantly associated with variation in the proportional change of black spruce and removed an additional four variables that were correlated to other explanatory variables (Spearman's ρ>0.4; Table 6.1). We fit BRT models using five-fold cross-validation to identify the optimum number of trees (Elith et al. 2008) and the following parameters: Gaussian error distribution, a learning rate of 0.001, a bag fraction of 0.5, and tree complexity of three. Next, we used a stepwise selection process that began with the set of candidate predictor variables (Table 6.1) and tested if the model could be simplified based on changes in the cross validation (cv) deviance (Elith et al. 2008). The lowest cv deviance was obtained by dropping five of the nine predictor variables. We subsequently found no substantial change in cv deviance when tree complexity was reduced to model only main effects, and partial dependencies between response variables and covariates were constrained to monotonic relationships. We used this simplest model form for the final model. We examined the relative influence of the predictor variables by creating partial dependency plots, which represent the effects of each variable on the change in proportion of black spruce after accounting for the average effects of the other variables included in the BRT model (Elith et al. 2008).

To determine how ecosystem resilience may vary among landscape units, we assessed how our site type categories related to the proportional change in black spruce and the most important variables explaining this change (identified with the BRT model). We tested the statistical significance of differences between means using a mixed model approach in the 'lme4' package (Bates et al. 2009) with the change in black spruce proportions and the top three most important variables (Table 6.1) identified in the BRT analysis as response variables. Variability due to individual sites within site categories was set as a random effect. To visualize the differences between sites we created boxplots of each of the variables stratified by site type.

T6: Results and discussion

The three study regions differed in terms of annual (data not shown) and monthly (Figure 6.2) climate conditions over the thirty-year period examined. Annual climate summaries indicate that the Dalton region was relatively cool and dry, the Steese region warm and moist, and the Taylor region warm and dry. On a monthly basis, the Dalton Highway region experienced a greater change in temperature throughout the year than the other three regions, such that it was relatively warm and dry during the growing season (JJA) compared to the other two regions (Figure 6.2). Regional differences in monthly precipitation were greatest during the growing season, while differences in temperature were greatest during winter.

Standard, averaged chronologies based on site types within regions produced chronology statistics indicating they were suitable for climate analysis. These chronologies demonstrated a negative growth response to previous growing season temperature (July) and current spring temperatures (April and May) at most site types (Figure 6.3). Radial growth responses of trees to precipitation were more variable; trees along the Taylor Highway responded negatively to previous and current May precipitation regardless of site type (Figure 6.4).

The correlation between $\delta^{13}C$ chronologies and mean monthly temperatures for a subsmaple of trees in the PFRR indicate that drought stress is likely the mechanism for the observed negative

radial growth responses to previous growing season and current spring temperatures. Radial growth responses to temperature were similar on both aspects; negatively correlated to previous and current July and positively correlated to November (Figure 6.5). $\delta^{13}C$ was more strongly negatively correlated with precipitation and CMI on the north compared to the south aspect, specifically throughout the winter months (Figure 6.5). Additionally, $\delta^{13}C$ on the south aspect was positively correlated to CMI in the current growing season (Figure 6.5).

The chronologies we developed in this study demonstrate a widespread sensitivity of black spruce radial growth to temperatures in the previous growing season and current spring. These results are in direct contrast to our expectation that black spruce, which are frequently found in the coldest and wettest positions of the boreal forest landscape (Viereck et al. 1983), would respond positively to warm summer temperatures. The most widely accepted explanation for reduced tree growth in response to warmer spring and summer conditions is temperature-induced moisture stress (Barber et al. 2000, Lloyd and Bunn 2007). Warmer temperatures during the previous growing season can result in a reduction in photosynthetic tissue, which limits radial growth the following year (Fritts 1976). Increased spring (April and May) temperatures also restrict radial growth of trees through stimulation of photosynthesis and transpiration of evergreen foliage prior to soil thaw. This can result in severe water stress, as trees are unable to obtain sufficient moisture to sustain their evaporative demands (Berg and Chapin III 1994). In interior Alaska, reduced growth in response to warm spring temperatures has also been observed for white spruce growing at treeline (Ohse et al. 2012) and black spruce trees growing in lowland forests (Wilmking and Myers-Smith 2008). Our dendroisotopic results indicate that the negative radial growth responses are likely due to temperature-induced moisture stress.

To assess the change in proportional representation of black spruce pre- to post-fire, the final model of the BRT analysis explained 25% of the variation. This model consisted of four of the possible nine predictor variables, modelled with only the main effects, and was constrained to monotonicity. Of the four explanatory variables included in the final BRT model, post-fire ROL depth had the strongest relative influence (Figure 6.6). Growth response to CMI in May, pre-fire black spruce basal area, and elevation also contributed to explaining the proportional change in black spruce composition (Figure 6). Partial dependency plots indicate that the greatest change in black spruce occurred at sites with thin post-fire organic layers, a positive response to CMI in May, and a relatively large black spruce basal area (Figure 6.6).

In exploring how our predetermined site type classification corresponded to the change in black spruce proportions, we found that the south (S) and mixed spruce-deciduous (TA and PB) stands experienced the greatest amount of composition change (Table 6.2 and Figure 6.7). Organic layer depth varied among site types, with the lowest depth in mixed (TA and PB) stands, and greatest depth in moist (M) stands. Pre-fire stands also differed in black spruce basal area among site types, with the lowest in moist sites. Although site types were specifically selected to capture a topographic gradient in moisture availability, stand level correlations between tree rings and May CMI were similar and largely positive among all site types (Table 6.2 and Figure 6.7).

Patterns of black spruce recovery after fire across our study landscape were related to environmental gradients and tree ring indicators of climatic stress. We observed a decrease in the proportion of spruce relative to total trees from the pre-fire to the post-fire stand in nearly all

examined stands, indicating shifts from black spruce dominated stands to mixed or deciduous dominated stands. However, these shifts were not uniform across the landscape. Forest stands most likely to show the largest change in black spruce dominance, and therefore the lowest resilience to disturbance, were those that had relatively thin post-fire organic layer depths and showed dendroclimatic indications of recent drought stress. These sites were generally located at warmer and drier landscape positions, suggesting a landscape pattern of lower resilience to disturbance compared to sites in cool and moist locations. Our results suggest that changes in ecological resilience and post-disturbance successional trajectories have a deterministic component that is likely to vary in a predictable way at the landscape scale.

Table 6.1. Variables included in each explanatory matrix for black spruce dominance.

Matrix	Variable	Units	Mean ± SD	Range
Pre-fire compo-sition	Black spruce density	stems/m^2	0.40 ± 0.26	0.002 – 1.18
	Black spruce basal area + #	m^2/ha	8.88 ± 6.70	0.02 – 34.55
	Trembling aspen density	stems/m^2	0.04 ± 0.07	0 – 0.25
	Trembling aspen basal area	m^2/ha	4.04 ± 13.40	0 – 84.31
	Paper birch density	stems/m^2	0.03 ± 0.05	0 – 0.23
	Paper birch basal area	m^2/ha	1.48 ± 3.07	0 – 14.82
	Total deciduous density	stems/m^2	0.06 ± 0.08	0 – 0.28
Site variables	Latitude +	radians	1.14 ± 0.02	1.11 – 1.17
	Moisture class (1-6)	unitless	2.56 ± 1.40	1– 6
	Elevation (m.a.s.l) +	m.a.s.l	457.3 ± 225.9	111 – 898
	Slope (radians)	radians	0.13 ± 0.13	0 – 0.47
	Aspect (radians)	radians	1.39 ± 0.82	0.21 – 3.12
	Heatload +	unitless	-1.54 ± 0.98	-2.79 – 0.29
	pH +	unitless	5.69 ± 0.66	4.45 – 7.60
	Organic layer depth + #	cm	9.63 ± 7.55	1.00 – 41.80
	Mean stand age (ring count at DBH)	years	56.95 ± 19.81	31.10 – 131.30
Dendro-climatic variables	CMI previous July	correlation	0.29 ± 0.17	-0.13 – 0.68
	CMI previous August	correlation	0.26 ± 0.19	-0.18 – 0.62
	CMI current April	correlation	0.30 ± 0.18	-0.13 – 0.60
	CMI current May + #	correlation	0.31 ± 0.16	-0.24 – 0.60
	CMI current August +	correlation	0.25 ± 0.14	-0.05 – 0.49
	Proportion of trees responding negatively to temperature (prop temp neg) +	proportion	0.56 ± 0.21	0 – 1
	Proportion of trees responding positively to precipitation (prop precip pos)	proportion	0.35 ± 0.19	0 – 0.86
	Average radial growth (1970-2003)	mm	0.44 ± 0.22	0.12 – 0.95

+Variables included in the boosted regression tree analysis.
Variables tested in the mixed effect models.

Table 6.2 Mixed effect models to test for differences among site types in observed changes in black spruce proportion after fire, as well as measures of post-fire organic layer depth, pre-fire black spruce basal area, and pre-fire stand response to May CMI (current year).

Model coefficients (Site Types)	Black spruce proportion (1 to -1)	Organic layer depth (cm)	Black spruce basal area (m^2/ha)	Correlation to May CMI
Intercept (Dry)	**-0.237±0.079**	**12.290±1.961**	**12.026±1.969**	**0.305±0.049**
North	-0.042±0.112	3.690±2.772	**-5.442±2.783**	-0.102±0.069
South	-0.156±0.096	-3.367±2.772	1.893±2.783	0.055±0.069
Moist	0.161±0.096	**-5.967±2.772**	**-9.224±2.783**	-0.102±0.069
Trembling aspen	**-0.230 ±0.097**	**-7.533±2.401**	**-5.390±2.410**	0.065±0.060
Paper birch	**-0.182±0.097**	**-6.252±2.401**	-0.787±2.410	0.035±0.060

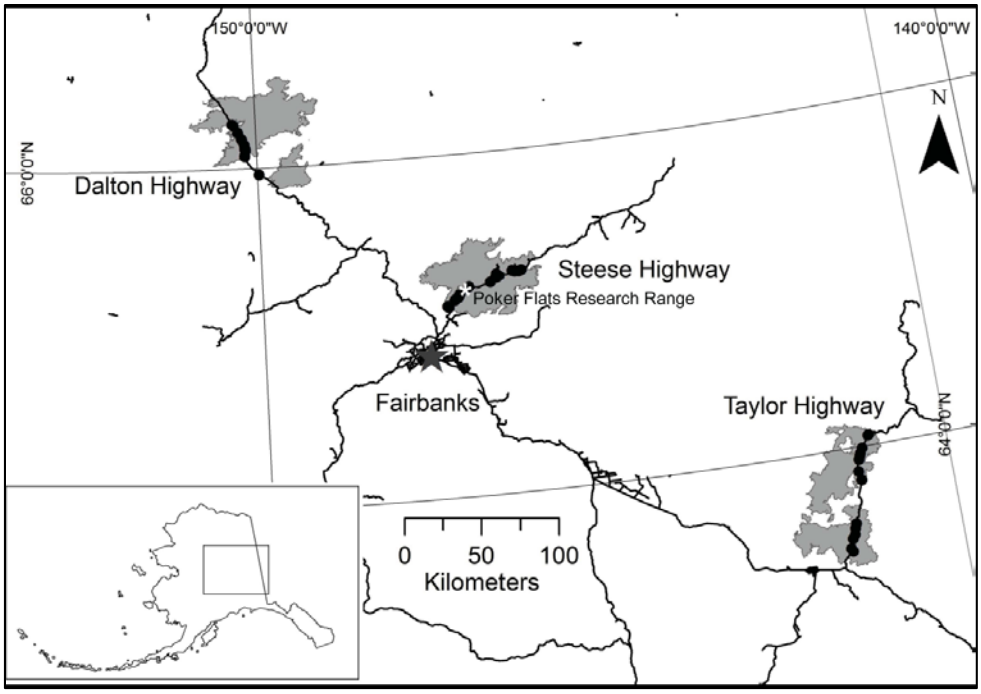

Figure 6.1. Location of study sites (black dots), located in three separate 2004 burn complexes (grey), along the Dalton, Steese, and Taylor Highways in interior Alaska. Note: additional sites were sampled within the Poker Flats Research Range along the Steese Highway.

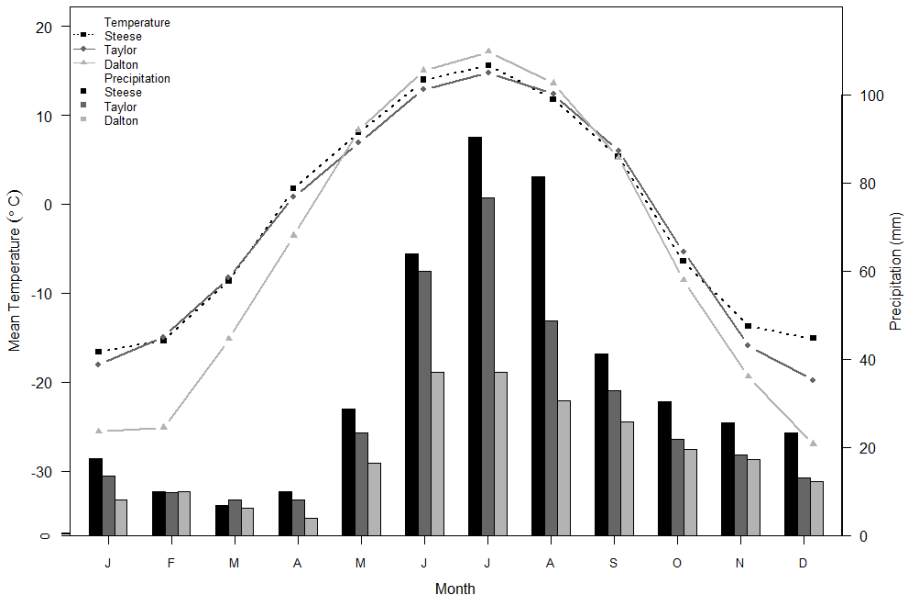

Figure 6.2. Mean monthly temperature (points) and total monthly precipitation (bars; averaged over the period 1974-2003) for each of the four regions examined in this study. Climate data were obtained from the Scenarios Network for Alaska and Arctic Planning (2013).

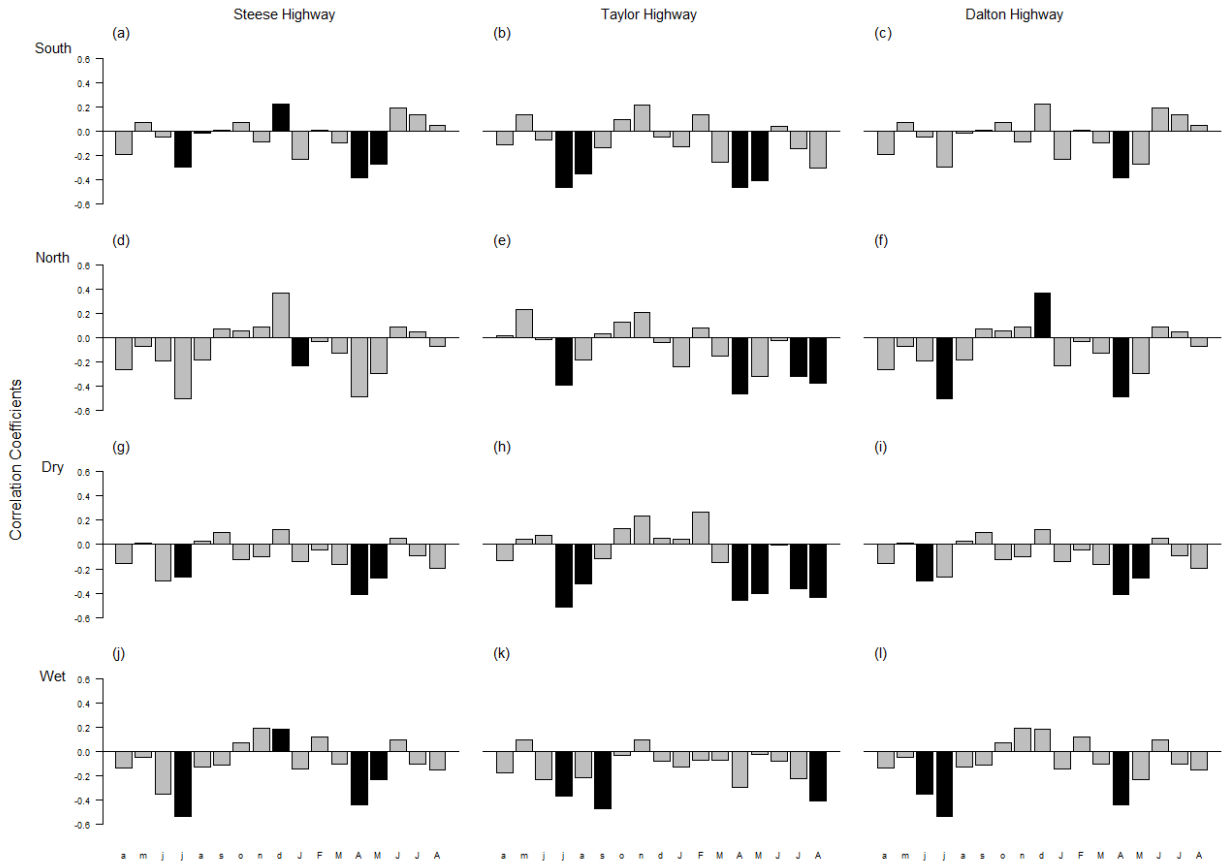

Figure 6.3. Correlations between ring width chronologies and mean monthly temperatures. Temperatures were obtained from SNAP climate data over a 17 month climatic window for the Steese (a,d,g,j),Taylor (b,e,h,k), and Dalton (c,f,i,l) Highways. Standard ring width chronologies were developed for south facing (a,b,c), north facing (d,e,f), dry flat (g,h,i) and wet flat (j,k,l) sites. The Y-axis in each figure represents correlation coefficients (black bars indicate=significant correlations at $p<0.05$), and the X-axis represents months of the year (lower case = year prior to ring formation, uppercase = year of ring formation).

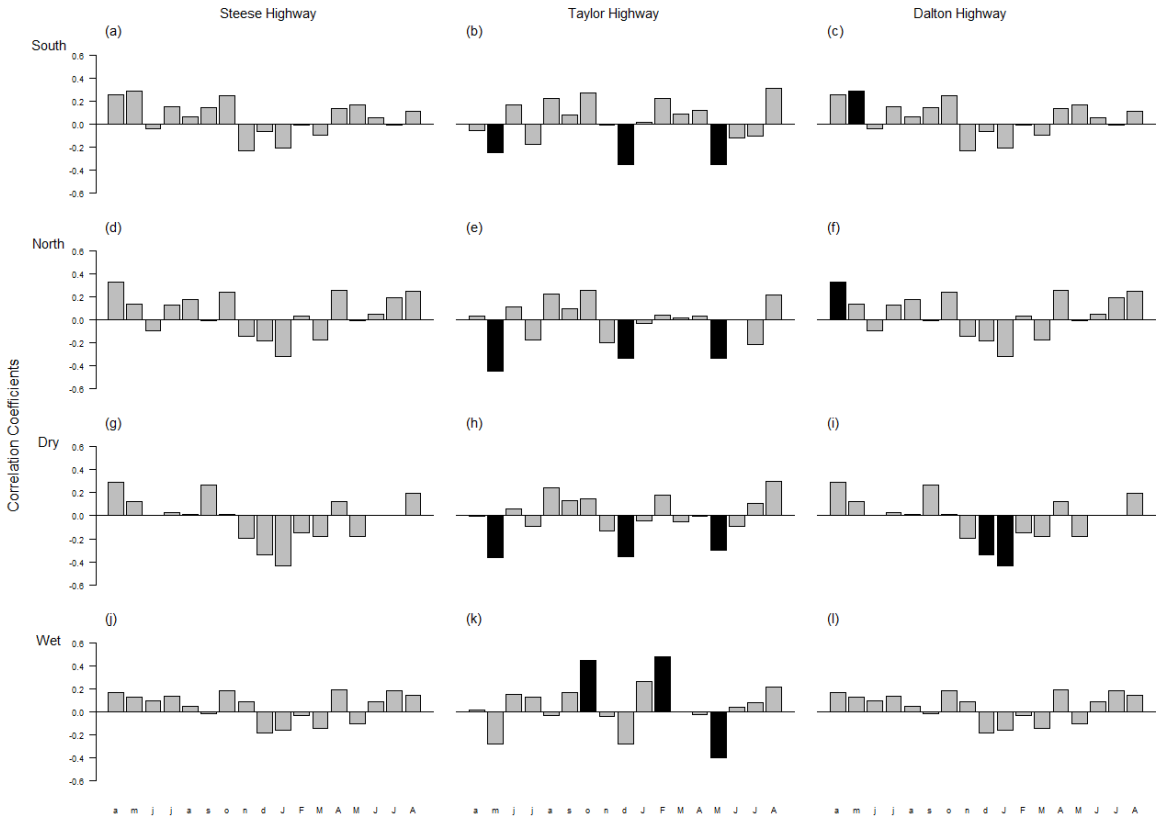

Figure 6.4. Correlations between ring width chronologies and total monthly precipitation. Precipitations were obtained from SNAP climate data over a 17 month climatic window for the Steese (a,d,g,j),Taylor (b,e,h,k), and Dalton (c,f,i,l) Highways. Standard ring width chronologies were developed for south facing (a,b,c), north facing (d,e,f), dry flat (g,h,i) and wet flat (j,k,l) sites. The Y-axis in each figure represents correlation coefficients (black bars indicate=significant correlations at $p<0.05$), and the X-axis represents months of the year (lower case = year prior to ring formation, uppercase = year of ring formation).

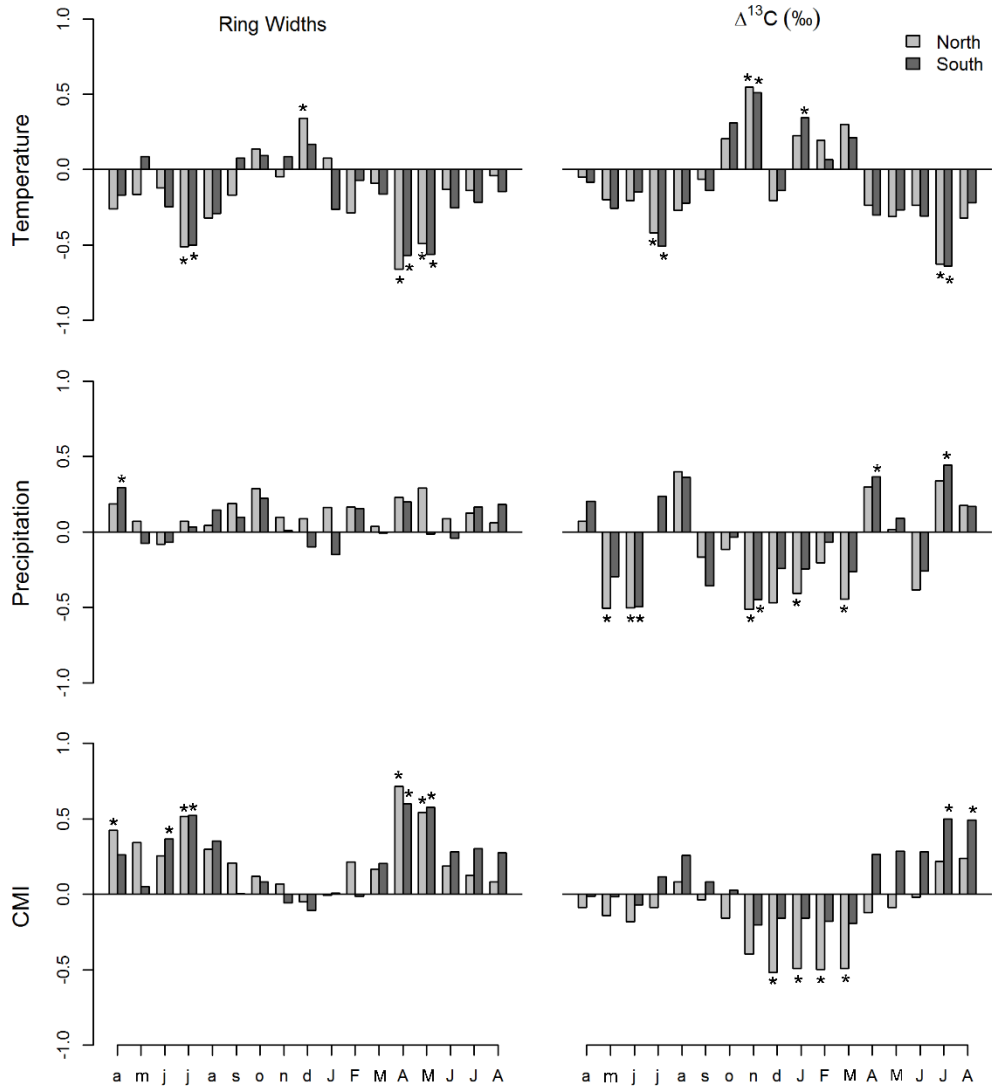

Figure 6.5. Averaged chronologies of ring widths and $\delta^{13}C$ correlated with 17-month climatic window of temperature, precipitation, and climate moisture index (CMI) from 1979 to 2003. Each of the north and south facing chronologies are composed of 9 trees each. y-axes represent correlation coefficients (* = significant) and x-axes represent months of year (lower case = year prior to ring formation, uppercase = year of ring formation).

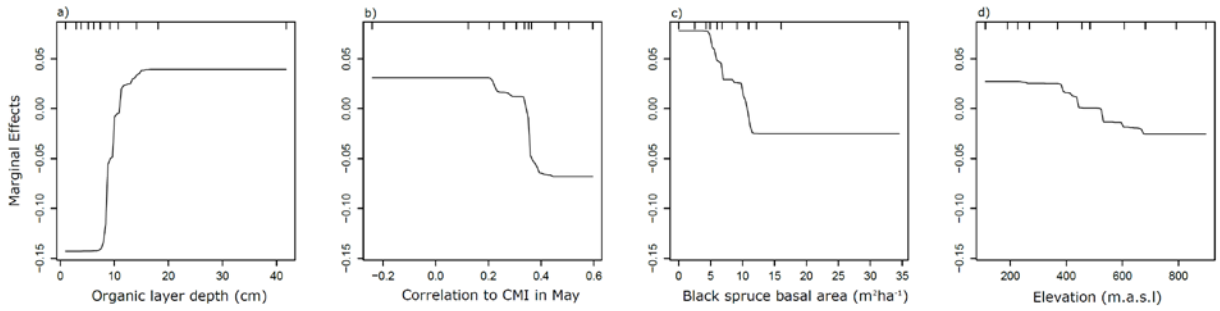

Figure 6.6. Partial dependency plots based on output from a boosted regression tree (BRT) model that explained 25% of the variation in the change in proportion of black spruce after fire. Plots represent the marginal effects of a) organic layer depth (relative influence: 42.3%), b) radial growth correlation to climate moisture index in May of the current growing season (relative influence: 22.9%), c) black spruce pre-fire basal area (relative influence: 22.5%), and d) elevation (relative influence: 12.3%), when all other variables are held constant. The BRT included only main effects and was constrained to monotonicity. Tick marks at the top of each plot represent the 10% quantiles of the explanatory variable distributions.

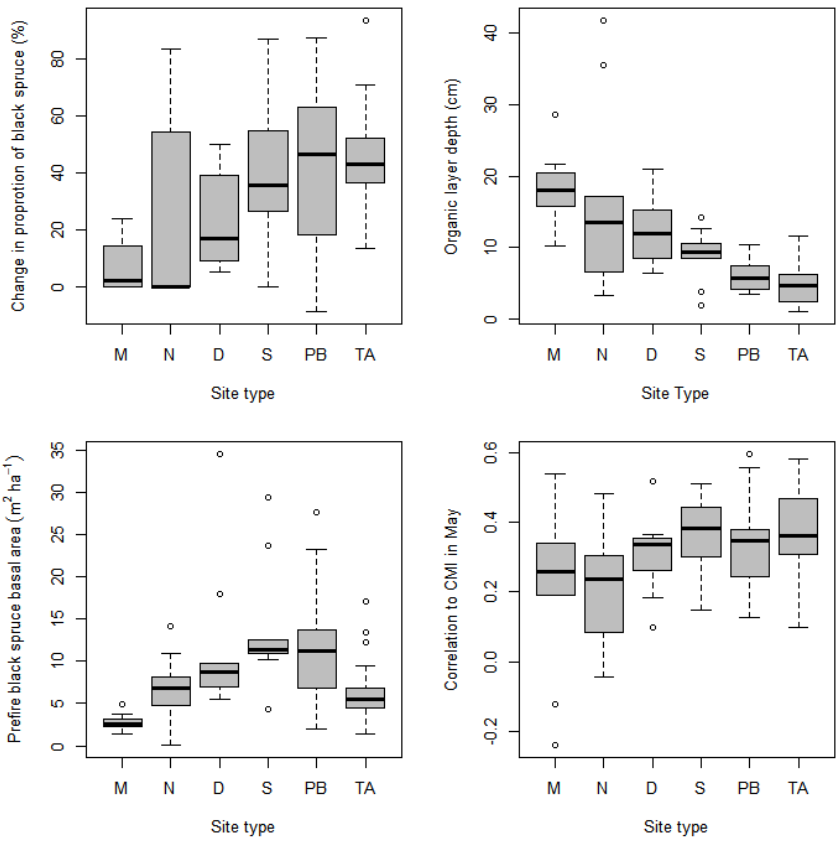

Figure 6.7. Boxplots showing the variability between site types (M=moist, N=north, D=dry, S=south, PB=paper birch, TA= trembling aspen) for each of: a) change in black spruce proportion (%), b) organic layer depth (cm), c) black spruce pre-fire basal area (m^2 ha^{-1}), and d) the stand response to CMI in current may (correlation coefficient).

Task 7: Monitor invasive species in wildfire and management plots

T7: Materials and methods

Fires may create windows of opportunity for the colonization and spread of non-native species. However, fire conditions are heterogeneous and this heterogeneity plays an important role in driving post-fire community assembly (Turner et al. 1997). We conducted observational and empirical studies aimed at determining the effects of fire on current distributions and potential recruitment of non-native plants in Alaskan black spruce forests. Specifically, we surveyed an equal number of burned (n = 33) and mature (n = 33) black spruce stands along major roadways in interior Alaska to test the effect of fire on non-native plant occurrence and assess whether there are stand characteristics that predict the observed distribution of non-native plants. We also conducted seeding experiments with three non-native species in burned and mature forest to test how variations in substrate types affect seedling germination.

Surveys of non-native plants focused on forests dominated by black spruce and located along two major roadways in interior Alaska (Figure 7.1). Initial surveys were conducted in 2011 and detailed surveys were performed in July 2012. Sites were divided equally between recently burned and mature (estimated > 60 years old) forest stands. Roadside samples were selected within areas that had frequent occurrences of non-native plant species along the road verge to provide a potential seed source for colonization. Fifty sites (25 burned, 25 mature) were surveyed adjacent to the Dalton highway north of the Yukon River (burn year 2004), and 16 (8 burned, 8 mature) sites were surveyed adjacent to the Parks highway south of Nenana (burn year 2006). Sampling at each site was based on a 100 m x 2 m belt transect running into the forest from the road verge edge, perpendicular to the road. We recorded the presence of non-native plants along the road edge, the density of individual non-native plants found within the belt transect, and the presence of any non-native plants encountered at the site but outside the sample transect. We also recorded seedling densities of black spruce, Alaska paper birch, and trembling aspen (*Populus tremuloides*) in five randomly located, 1 m x 1 m plots along the transect. Soil measurements of organic layer depth, thaw depth, and mineral soil pH were made at three randomly selected points along the transect.

Seeding trials with non-native plants were conducted in the Caribou Poker Creeks Research Watershed (CPCRW), located approximately 50 kilometers north of Fairbanks, Alaska along the Steese highway (Figure 7.1). Experimental plots were located in a recently burned (2004) and mature black spruce forest. The seeding trials used seed from three non-native plants common in interior Alaska that differed greatly in average seed mass (estimated in the lab from the weight of 100 seeds): *Vicia cracca* L. (bird vetch, 0.012 $g \cdot seed^{-1}$), *Melilotus officinalis* (whites sweet clover, 0.0018 $g \cdot seed^{-1}$), and *Taraxacum officinale* G.H. Weber ex Wiggers (common dandelion, 0.00081 $g \cdot seed^{-1}$). Seeds for the experiment were collected in September 2011 from established populations in Fairbanks, Alaska. Seeding plots were laid out in a stratified random design in adjacent areas of mature and recently burned black spruce forest. Plots were 15 cm x 15 cm in size and clustered in blocks at 10 m intervals along a 100 m transect in each forest type (n = 10 per treatment). Seeds were sown in plots representing five substrate types characteristic of recently burned forests: broadleaf litter, grass litter, regenerating moss (largely *Ceratodon purpureus* and *Polytrichum juniperinum*), charred organic layer, and exposed mineral soil. There was no exposed mineral soil in the burned forest at the time of the experiment, so mineral soil

plots were created by hand removal of surface organic soil and plant litter. Each seeded plot was covered with a mesh cage of galvanized metal (mesh size = 0.5 cm) to prevent small animals from removing seeds or seedlings. Ten seeds of each species were sprinkled on the surface of each plot on 4 June 2012. Total germination counts were made on 30 July 2012, and then all seedlings and visible seeds were removed, and the substrate was dug out and removed from the site to prevent any non-native propagules remaining at the site.

Twelve sites were sampled for invasive plant presence in shearbladed (n = 11) and thinned (n = 1) forests and adjacent unmanaged forest within 150 km of Fairbanks, Alaska in Summer 2012. This sampling was done concurrent with Task 3. Within each site, two 20 m X 2 m transects were placed parallel to each other within the treatments (or mature forests) in a position meant to capture the dominant features of the disturbance. These transects were surveyed for invasive plant presence, and native plant community was measured by recording the presence of all genera that occurred along the transects. The presence of invasive plants that were not along transects was noted, but density estimates were not made. The two transects were also used to visually estimate dominant ground cover types (for a description of ground cover types see sampling protocol for invasive plant surveys above) at ten points on each transect (n = 20).

We used information on the presence and absence of non-native plants in burned and mature stands to evaluate the effects of fire on non-native plant occurrence. As *T. officinale* was present at every site with non-native plants, and *C. tectorum* and *M. officinalis* were only encountered in one site each, these analyses are largely predicting the presence of *T. officinale.* We first used a chi-squared test to determine whether the presence of non-native plants was affected by forest type (mature or burned). We then developed models to predict non-native plant presence within burned stands using an information theoretic approach to model selection and inference (Burnham and Anderson 2003). All models were run as binomial linear regression models in the statistical package R 2.14.1. with non-native plant presence as the response variable. We used Fisher's exact test to compare germination counts among substrate types in the seeding experiment.

T7: Results and discussion

Fire had a strong influence on non-native plant presence. Non-native plants were never observed in unburned stands, whereas 11 of the 33 surveyed burned stands (eight in the Dalton highway study region, three in the parks highway study region) had non-native plants present ($\chi^2 = 12.32$, df = 1, $p < 0.001$). Within burned stands, stand variables were able to correctly classify non-native plant presence in at least 70% of instances. Four of five top models contained ROL depth and/or regenerating paper birch seedlings as model covariates, indicating that they were closely associated with non-native plant presence. Residual organic layer depth was generally lower in sites where non-native plants were present. High densities of regenerating paper birch seedlings were more frequently observed in sites where non-native plants were present.

Seed germination success in the experimental seeding trial in burned forest was affected by substrate type for all species ($p < 0.001$), Germination of the three species was consistently highest on the mineral soil substrate, and no species had successful germination on charred organic soil (Figure 7.2). Germination on plant litter and regenerating moss was generally lower than observed on mineral soil, although *V. cracca* had higher rates of germination on the litter

and moss substrates compared to *M. officinalis* and *T. officinale.* Overall *V. cracca* had the highest total germination (15%) across all substrate types within the burned forest relative to *M officinalis* (7%) and *T. officinale* (4%).

Four of the twelve managed sites had invasive plants present, and none of the undisturbed controls had invasive plants present. Ground cover in the undisturbed control sites was predominantly moss, leaf litter, and lichen, whereas managed sites had a variety of substrates present. *Crepis tectorum* was present in four sites and *Taraxacum official* was also present at one of those sites. All of the sites with invasive plants present had been treated by shear blading. Some of the shearbladed sites had exposed mineral soil present, whereas the thinned site did not have mineral soil present. In the thinned site the ground cover was predominantly moss.

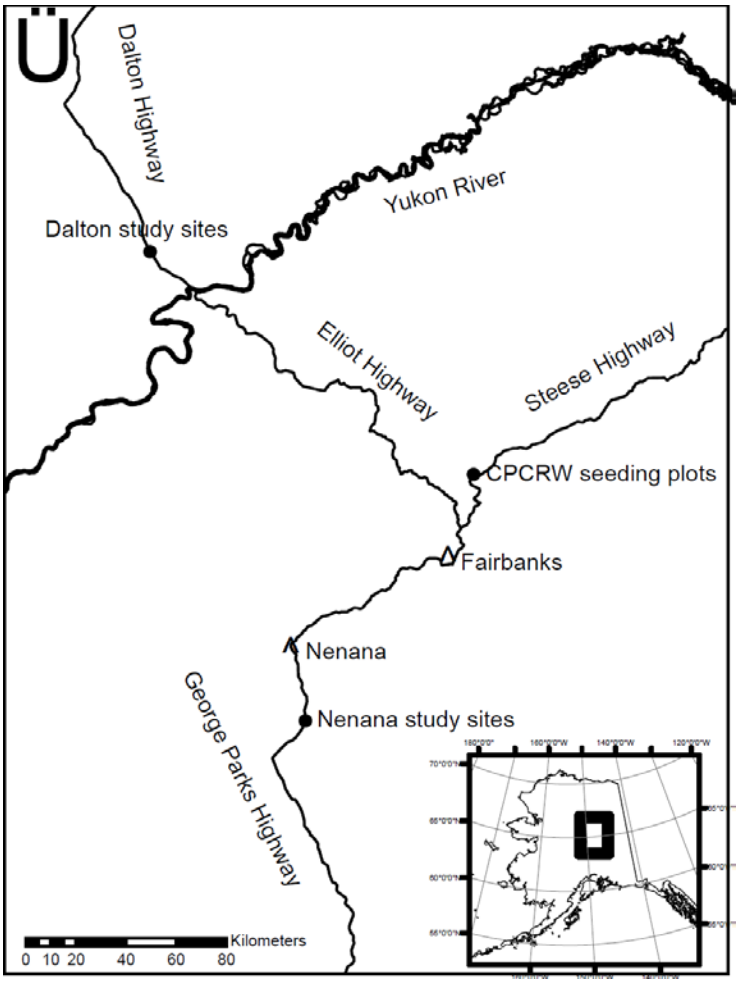

Figure 7.1 Map showing the general location of the Dalton survey sites, Nenana survey sites, and Caribou Poker Creeks Research Watershed (CPCRW) seeding trials in interior Alaska. The inset box shows the position of the study area map within Alaska (USA).

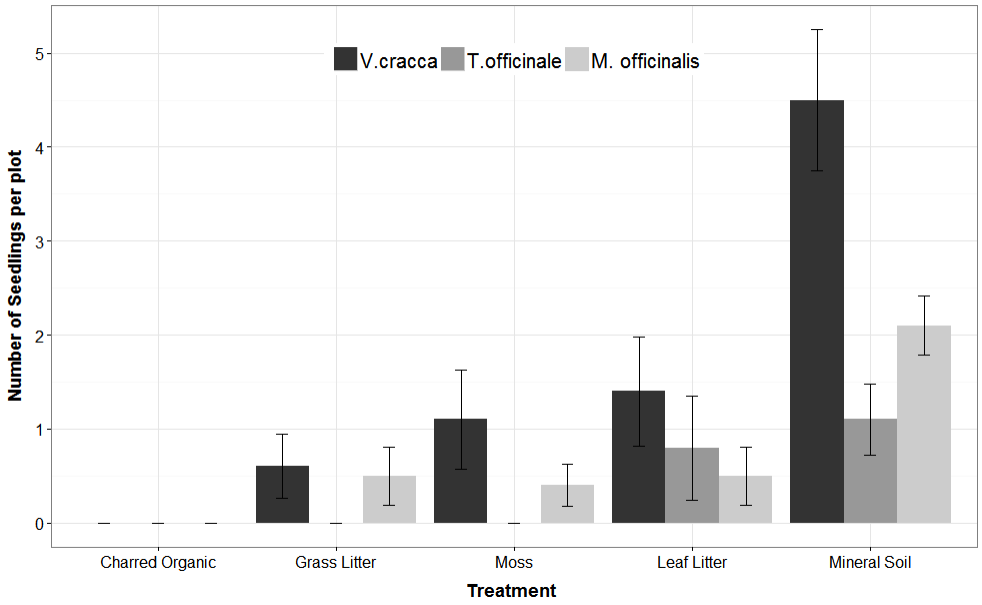

Figure 7.2. Seedling counts (means ± 1 SE) from germination trials on substrates within a burned forest (n=10).

Task 8: Provision of data for model development, parameterization, and testing

T8: Materials and methods

Field observations collected during the project were used to improve the representation of the linkages among climate, fire, and ecosystem structure and function in the models of this study. Specifically, model developments were focused on (1) the combustion of the SOL and permafrost degradation following fire and (2) the vegetation succession following fire.

Our approach for incorporating information about the combustion of the SOL and effects on permafrost degradation involved the development of a predictive model of post-fire reduction of SOL thickness. This model was then incorporated into the Dynamic Organic Soil version of the Terrestrial Ecosystem Model (DOS-TEM; Genet et al., 2016, 2013) to assess the impact of fire combustion of the SOL on ecosystem C dynamic (results presented in Task 9). The impact of SOL combustion and post-fire SOL recovery on permafrost was then estimated with the Geophysical Institute Permafrost Laboratory model (GIPL) using information of fire severity and post-fire SOL recovery from DOS-TEM. The predictive model of SOL combustion was developed using existing observations pre- and post-fire SOL thickness in recently burned black spruce forests of interior Alaska (Turetsky et al., 2011 and data collected in Task 1, Figure 8.1), along with information about topography, weather and fire history (see Genet et al. 2013).

The predictive model of post-fire vegetation trajectory was developed based on a synthesis of field observations from empirical tasks undertaken in this study, and data from the literature. The synthesis was focused on representing the main drivers of vegetation succession after a fire, such as drainage conditions, fire severity and biological legacies including pre-fire vegetation composition and maturity. The model considers self-replacement, relay floristics, and recruitment failure.

T8: Results and discussion

Modeling the impact of fire severity on the SOL

The predictive model of SOL combustion identified landscape drainage as the primary driver of the relative amount of SOL burned during fire (i.e. the ratio between the difference of pre- and post-fire SOL thickness and the pre-fire SOL thickness). Drainage conditions accounted for 24.8% of the variability of observations. Relative SOL combustion was lower in flat lowlands (0.467 ± 0.177 cm cm^{-1}, mean ± standard deviation) and higher on slopes (0.712 ± 0.174 cm cm^{-1}) and flat uplands (0.605 ± 0.140 cm cm^{-1}). Secondarily, relative SOL combustion also increased with the slope, ET/PET ratio, date of the burn and area burned. Relative SOL combustion was negatively related to northern aspects, flow accumulation, the compound topographic index, and the volumetric water content of the OL. The predictive model of relative SOL combustion explained 49.6% of the variability of the observations used for this analysis (Figure 8.2).

The parent version of DOS-TEM, which used a look-up table approach, significantly underestimated SOL combustion (paired t-test: $t = 7.67$, $p < 0.001$) and the effect of landform drainage categories on SOL combustion was not significant ($F = 0.13$, $p = 0.878$; Figure 8.2).

The introduction of the new model in DOS-TEM improved the representation of the main drivers of relative SOL combustion and the spatial heterogeneity of fire severity.

Impact of fire and post-fire SOL regrowth on permafrost

Fire disturbance and no SOL regrowth had a substantial impact on permafrost thermal stability. In the upland black spruce site permafrost started to thaw progressively when 12 cm (30%) of the pre-fire organic layer thickness was removed (Figure 8.3A). In contrast, permafrost did not progressively thaw at the lowland site until 24 cm (30%) of the pre-fire organic layer thickness was removed (Figure 8.3B). Fire disturbance at the lowland site did not immediately degrade permafrost after 24 cm of the pre-fire organic layer was burned until approximately 100 years had passed. It is notable that for the highest burn severity (48 cm, 60% removal) at the lowland site the rate of permafrost degradation was less pronounced than for 15 cm (50%) removal at the upland site. When the organic soil layers were allowed to re-accumulate after fire (outputs from DOS-TEM) at the upland site, the permafrost did not totally degrade down to 5 m for 15 cm (50%) removal of pre-fire organic layer thickness (Figure 8.4A). In contrast, permafrost at the lowland site was able to fully recover its thermal state and active layer thickness (ALT) within 40 years after fire for all of the levels or organic layer removal we considered (Figure 8.4B).

Conceptual modeling post-fire vegetation succession

We developed a conceptual model of post-fire vegetation succession based on field observations and literature review (Figure 8.5). Under subhygric conditions, the degradation of permafrost from fire will lead to shallower water table and seasonal flooding with a high probability for post-fire recruitment failure and transition to wetland vegetation (Jorgenson et al. 2001). In mesic environments, post-fire vegetation succession is primarily driven by pre-fire biological legacy and fire severity. Burned deciduous forests will likely lead to post-fire self-replacement succession as the composition of the seedbank and post-fire environment will favor deciduous species (Johnstone et al. 2010a). Post-fire succession of evergreen stand fire will depend on fire severity and pre-fire stand age. Severe fires will burn most of the organic layer, providing environmental conditions favorable to deciduous species that will out-compete conifers (Johnstone and Kasischke 2005). In this case, a relay-floristic succession may take place and result in the development of mixed stands. After low severity fires, the ROL is usually too thick, providing a micro-environment too dry and hot to allow deciduous species to recruit (Johnstone et al. 2010b). If pre-fire stands are mature enough (older than 50 years old) to provide a significant seedbank, a self-replacement succession will take place, resulting in the development of a conifer stand (Viglas et al. 2013). If there is not a seedbank for conifer recruitment, then grassland will develop. Finally, under xeric conditions, post-fire vegetation succession will favor deciduous species over evergreen species. Therefore, deciduous stands will develop after a severe fire or if pre-fire stands were deciduous. After low-severity fire in a conifer stand, a mixed stand will establish if a seedbank is present.

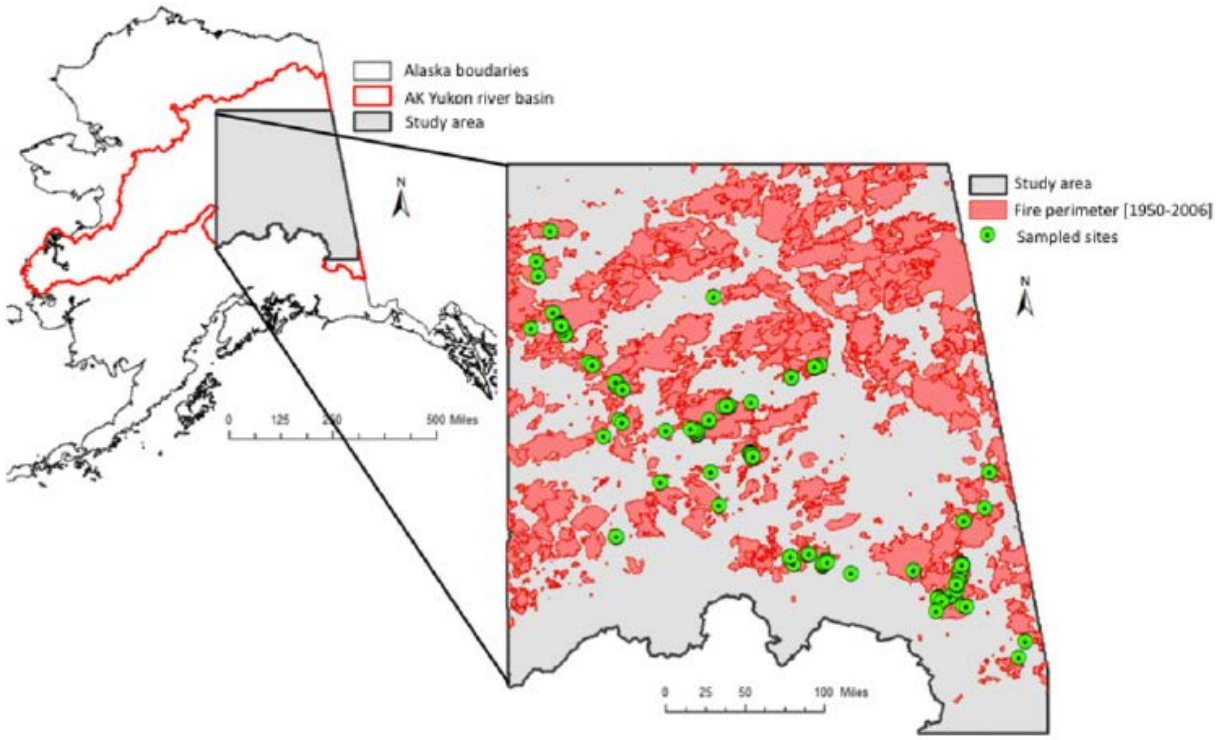

Figure 8.1: Location of the sampled sites and the area of simulation in interior Alaska for the development, testing, and application of the model of soil organic layer fire severity presented in Genet et al. (2013).

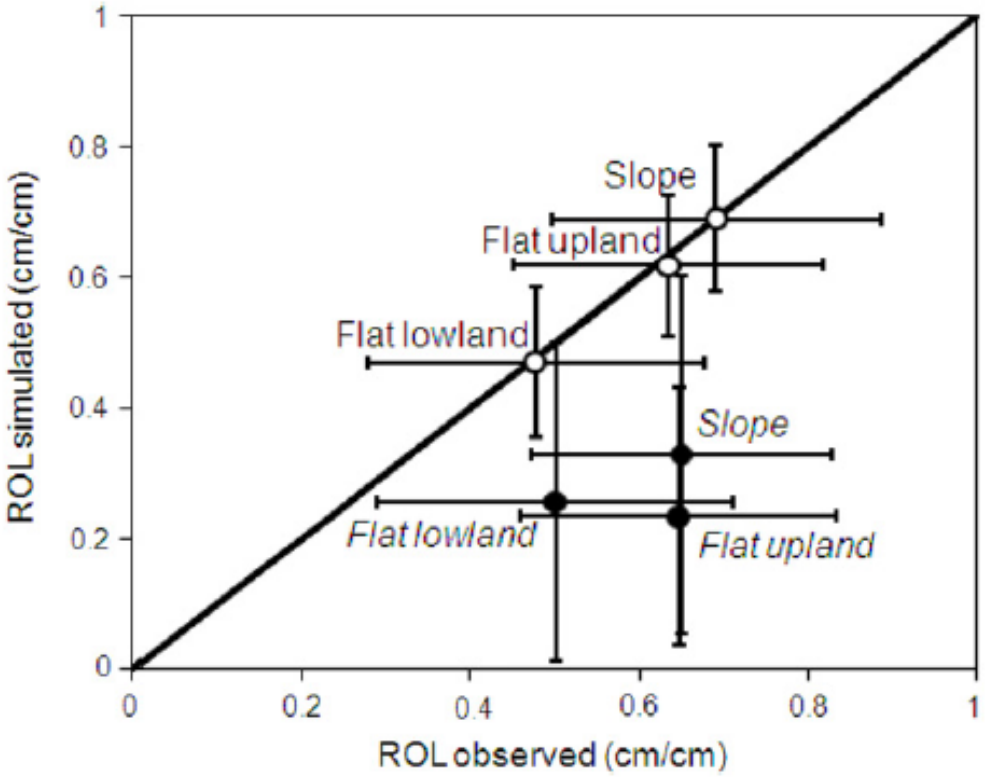

Figure 8.2: Comparison of the ROL computed from observations and from simulated by DOS-TEM with the original version of the model (closed circle) and with the modified fire module (open circle) (see Genet et al., 2013 for more details). The vertical lines represent standard deviation of the simulated ROL, the horizontal line represent standard deviation of the observed ROL for each landscape categories. The oblique line represents the [1:1] slope.

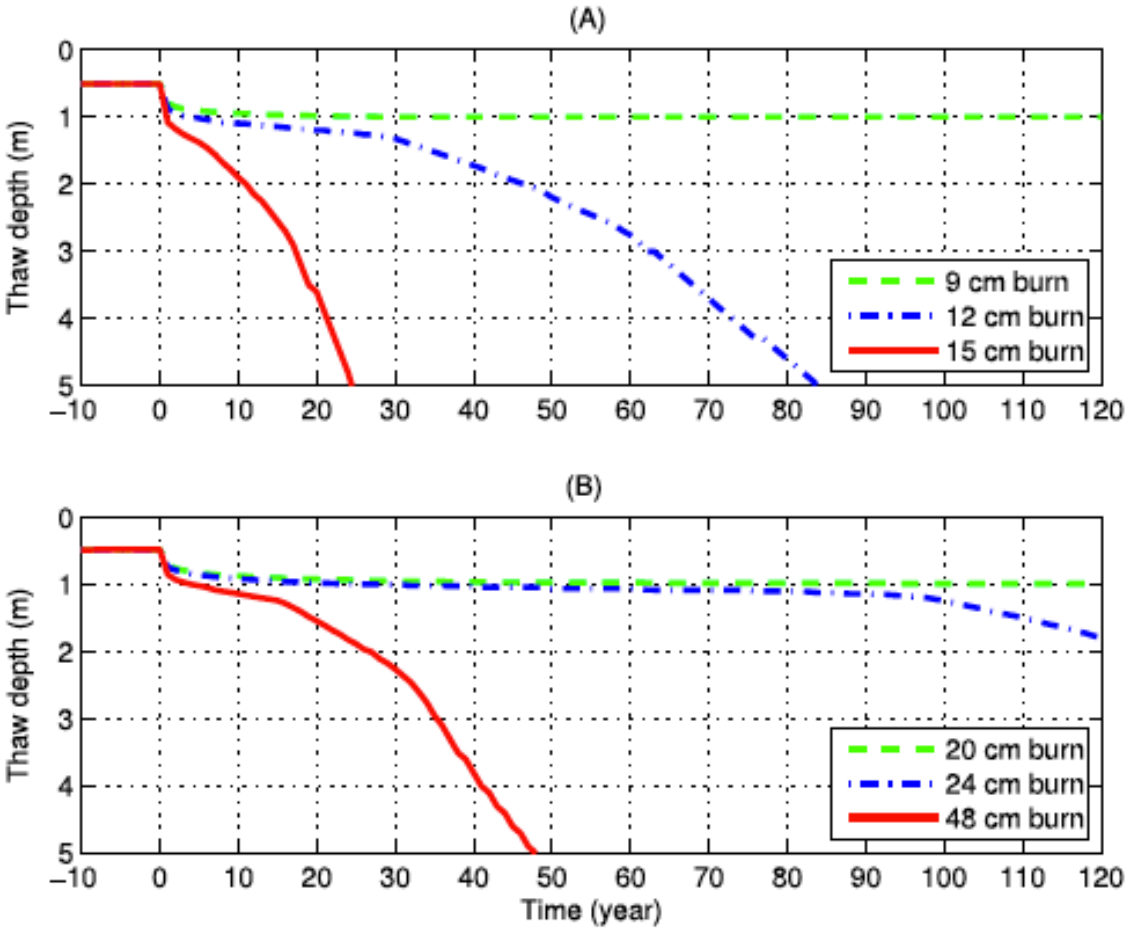

Figure 8.3: Simulations of the permafrost table depth for (A) upland and (B) lowland boreal spruce forest sites for different fire severities under baseline climate scenario (mean annual air temperatures -2 ^{o}C), for no organic layer regrowth (from Jafarov et al., 2013). Time interval [-10, 0] corresponds to the equilibrium run, and [0, 120] corresponds to the transient run, where 0 is a year corresponding to the upper organic layer removal.

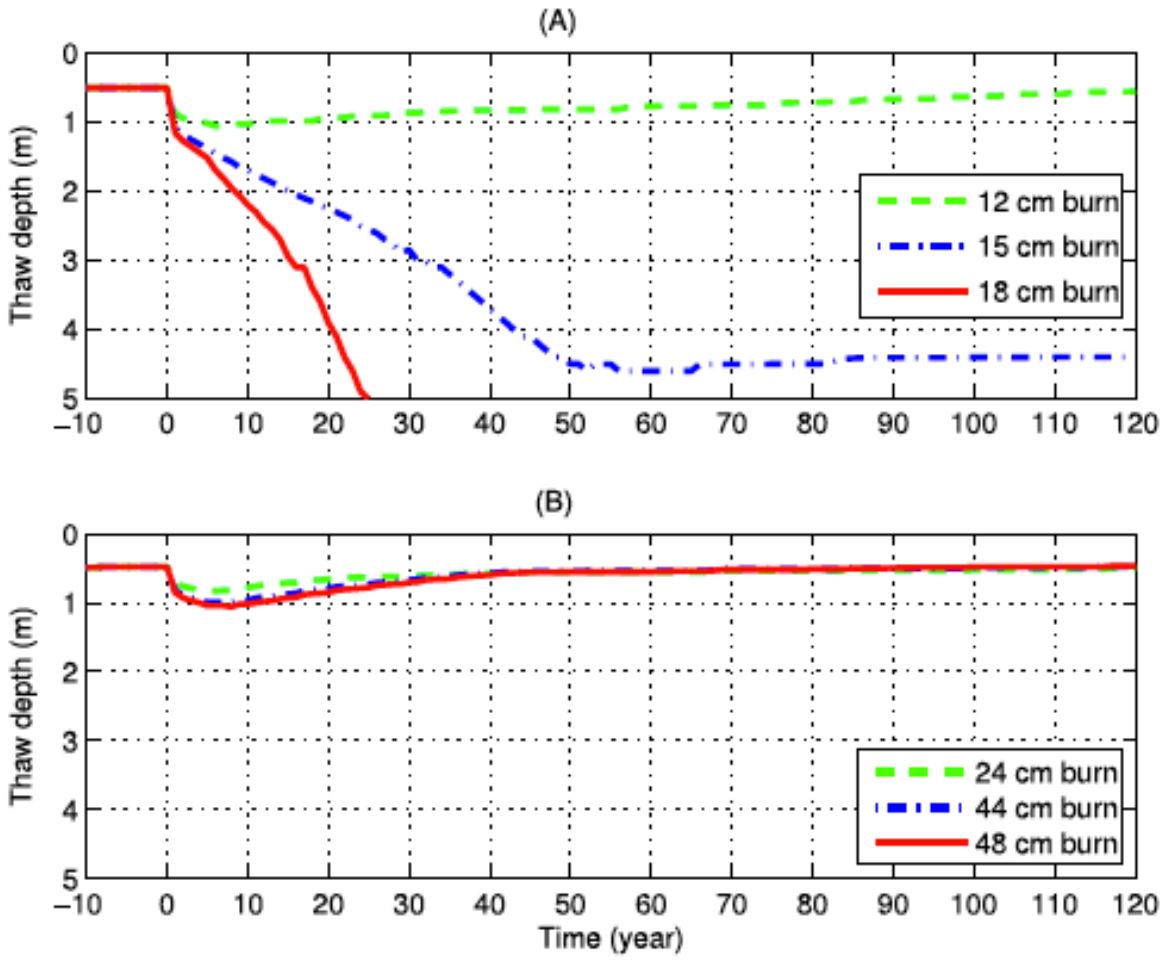

Figure 8.4: Simulations of the permafrost table depth for (A) upland and (B) lowland boreal forest sites for different fire severities under the baseline climate scenario (mean annual air temperatures -2^{o}C) using dynamic organic soils recovery rates (from Jafarov et al., 2013). Time interval [-10, 0] corresponds to the equilibrium run, and [0, 120] corresponds to the transient run, where 0 is a year corresponding to the upper organic layer removal.

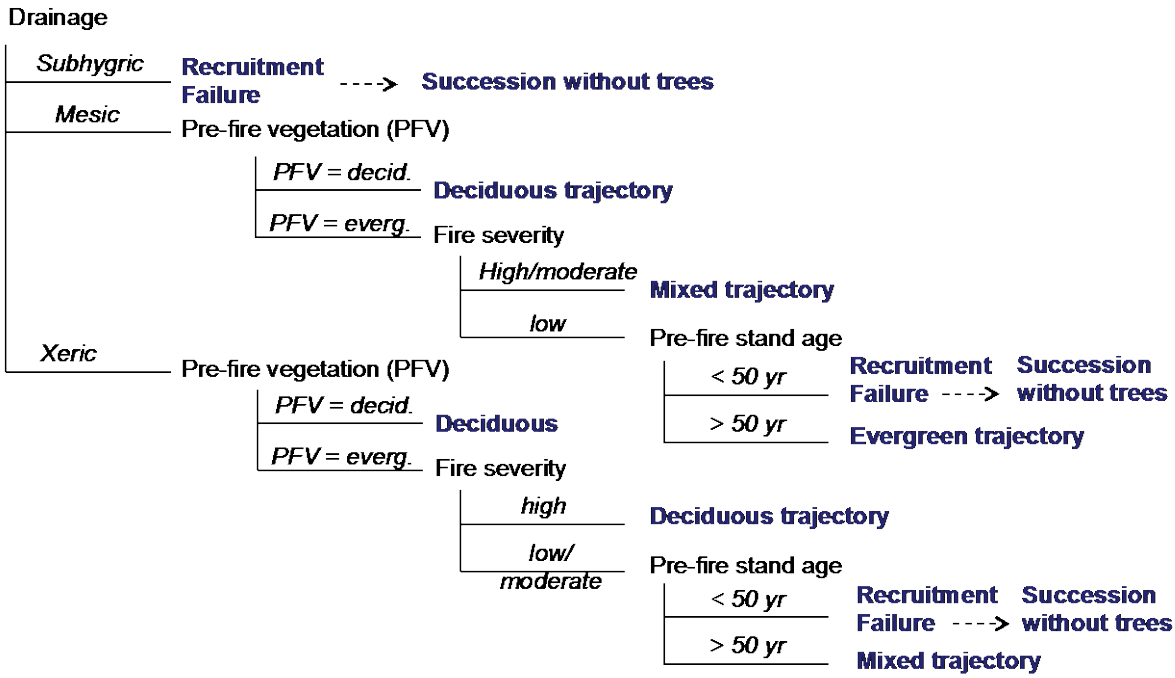

Figure 8.5: Post-fire vegetation conceptual successional model representing the effects of drainage conditions, pre-fire stand legacies, and fire severity.

Task 9: Forecasts of future landscape distribution, permafrost distribution, and carbon dynamics for interior Alaska with coupled models

T9: Materials and methods

The application of the model framework in this study was conducted for a historical period (1950–2009) and a future projection period (2010–2099) for the northern boreal region of Alaska (i.e., the boreal forest region between the Alaska and Brooks Ranges, also known as interior Alaska). The future projections of the model framework were driven by data from three Special Report on Emissions Scenarios (SRES A1B, A2, and B1) that were used to force two of the best performing Coupled Model Intercomparison Project Phase 3CMIP3 GCMs: the Canadian Centre for Climate Modeling and Analysis (CCCMA; Flato, 2005; McFarlane et al., 1992) and the European Centre Hamburg Model (ECHAM; Roeckner et al., 2004). The selection of the GCMs represented a range of projected climate change and to which the fire regime simulations were considered sensitive.

The model framework consisted of a coupling of the Alaska Frame-Based Ecosystem Code (ALFRESCO; Rupp et al. 2016) with DOS-TEM (Genet et al., 2016, 2013). ALFRESCO was used to simulate changes in fire regime and vegetation distribution at 1 km resolution from 2010 through 2099. DOS-TEM was used simulate changes in permafrost distribution and carbon dynamics for uplands and lowlands at 1 km resolution during both the historical period and the future projection period. DOS-TEM used input data on soil texture, land cover, historical climate, historical fire, historical forest harvest, and model projections of future climate and fire disturbance (from ALFRESCO) to estimate changes in ecosystem pools and fluxes for the two time periods for upland and wetland ecosystems. ALFRESCO was calibrated on the basis of historical data about fire occurrence for Alaska from 1950 through 2009. DOS-TEM was parameterized with information from this study and from the Bonanza Creek Long-Term Ecological Research (LTER) Program. Empirical estimates of permafrost distribution were used to validate the permafrost simulation of DOS-TEM for the historical period (1950–2009) (Wylie et al., 2016). The carbon dynamics simulated by DOS-TEM were evaluated separately for upland (Genet et al., 2016) and lowlands (He et al., 2016).

T9: Results and discussion

ALFRESCO Simulation of Future Fire Dynamics

The northern boreal forest region of Alaska is notable because 85 percent of the statewide historical fire activity occurs in this region and the future projections of wildfire by ALFRESCO for the state of Alaska are dominated by wildfires in this region as well. The CCCMA model simulations resulted in an increase in the 50^{th} and 95^{th} percentiles for the distribution of the number of ignitions for all scenarios (Table 9.1 and Figure. 9.1A). The distributions of area burned exhibited mixed magnitudes and direction of change across scenarios. The 50^{th} percentile resulted in increases for all scenarios (ranged from 0.9 percent to 47.6 percent). In contrast, the 95^{th} percentile increased for the A1B and A2 SRESs whereas the B1 SRES decreased. The ECHAM model resulted in decreases in both the 50^{th} and 95^{th} percentile for the distribution of the number of ignitions (Table 9.1 and Figure. 9.1B). This result was consistent across all scenarios. The distribution of area burned for the A1B and A2 SRESs showed general increases. The B1 SRES showed a decrease in both the 50^{th} and 95^{th} percentiles. The distribution of area

burned for the A1B scenario exhibited the largest change with 44 percent and 17 percent increases in both the 50th and 95th percentiles of area burned, respectively.

ALFRESCO Simulation of Future Vegetation Dynamics

Projected changes in white and black spruce in the northern boreal forest region of Alaska decreased substantially (ranged from 7.9 percent to 43.9 percent) under both the CCCMA and ECHAM scenarios, except for the B1 SRES which resulted in minimal increases of approximately 3 percent (Table 9.2). Graminoid tundra also decreased (ranged from 44.0 percent to 49.7 percent) under both the CCCMA and ECHAM scenarios. In contrast, shrub tundra increased (ranged from 1.0 percent to 5.0 percent) under both the CCCMA and ECHAM scenarios. The northern boreal forest region of Alaska exhibited moderate to large changes in forest distribution across GCMs and SRESs (Figure 9.2). The CCCMA simulations varied from moderate decreases in white and black spruce forest extent in the A2 SRES to small increases under the B1 SRES. In contrast the ECHAM simulations resulted in large decreases in white and black spruce forest across all SRESs, with a concomitant increase in early successional deciduous vegetation. Graminoid tundra decreased in both GCMs and across all SRESs. Shrub tundra responded oppositely, exhibiting decreases under the CCCMA simulations but increases under the ECHAM simulations.

DOS-TEM Simulation of Historical and Future Permafrost Distribution

By the end of the historical period [2000-2009], near-surface permafrost (NSP) was estimated to underlay 17% and 36% of mainland Interior Alaska at 1m and 3m depth respectively (Table 9.3). The active layer depth (ALD, annual maximum thaw depth) in the region was 1.35m (s.d. 1.00). Compared to other estimates of NSP and ALD developed from field observations, remote sensing analyses, and process-based modeling (Table 9.4), DOS-TEM estimates of NSP were generally lower and estimates of ALD were generally higher than estimates from the other products (Figure 9.3). The differences between DOS-TEM and the other estimates of NSP and ALD in Interior Alaska are partially related to the lack or incomplete representation of the effect of fire on permafrost stability, mainly through the partial or complete removal of the insulating organic layer. In response to projections of climate and wildland fire, DOS-TEM estimates of NSP extent at 1m and 3m were 6.64% and 10.97% respectively by the end of the 21st Century. Compared to the end of the historical period, NSP extent at 1m and 3m decreased by 60% and 70% respectively (Table 9.3). The largest decrease in permafrost extent was observed for the CCCMA – A2 scenario, one of the warmest scenario with high fire frequency. The projected ALD of the remaining permafrost was not necessarily increased compare to the historical period, except for the scenarios with the lowest warming trends (CCCMA – B1 and ECHAM5 – B1). . The relative increase of ALD for the other 4 scenarios, despite the decreasing extent of NSP, was reflecting the characteristics of the remaining permafrost, often shallow and concentrated in colder areas less likely to thaw. The reducing extent of NSP extent during the projections resulted from increasing air and soil temperatures and the reduced soil insulation due to fire burning the organic layer, allowing deeper penetration of warm temperature in the soil.

DOS-TEM Simulation of Historical and Future Carbon Dynamics

Interior Alaska is composed of about 75% of uplands well to moderately well drained ecosystems and 25% of lowlands, generally poorly drained ecosystems (Table 9.5). Boreal ecosystems in Interior Alaska store 10.3 PgC, which represent about 18 % of the total C stocks in

Alaska. During the historical period, boreal ecosystems lost -7.33 TgC/yr from both uplands and lowlands. While heterotrophic respiration is the main source of C loss in uplands and lowlands, the second main important pathway of carbon loss differ between the two types of ecosystems. The second main causes for net ecosystem carbon loss in uplands is fire emissions. During large fire years (where total area burn exceeds 20,000 km^2), the carbon loss from fire emissions can be equivalent to about three decades of carbon sequestration in boreal forest (Figure 9.4). In lowlands, the second source of carbon loss after heterotrophic respiration, is biogenic methane emissions. Because of the large warming potential of methane, the impact of small methane emissions on the greenhouse gas warming potential can be substantial. After taking methane emission into account, our analyses indicate that interior Alaska represented a carbon source of 47.6 $TgCO_2$-eq/yr from 1950 to 2009, 43% emitted from uplands and 57% emitted from lowlands. During the projections, interior Alaska shifted from being a net source of CO_2 to a net sink of CO_2 ranging from 4.8 to 11.3 TgC/yr among climate scenarios (Table 9.6). Compare to the historical period, both vegetation and soil C stocks increased of 22 and 5% in average respectively. The increase in C loss from fire and biogenic methane emissions (Figure 9.5C,D) were offset by a large increase in vegetation net primary productivity (Figure 9.5A) during the 21^{st} century (9% in average compare to the end of the historical period).

Table 9.1. Simulated fire activity for interior Alaska. [Historical period represents simulated data for the period 2000-2009. Projected results are for the period 2090-2099. Percentiles are computed across 200 simulations.]

Scenario	Percentile	Historical period Ignitions	Historical period Area burned	Projected Ignitions	Projected Area burned	Percent change Ignitions	Percent change Area burned
CCCMA							
B1	50th	42	2,216	48	2,622	15.5	18.3
B1	95th	62	10,511	67	7,855	7.3	-25.3
A1B	50th	42	2,274	45	2,295	5.9	0.9
A1B	95th	62	10,342	64	10,199	3.5	-1.4
A2	50th	42	2,194	44	3,239	7.2	47.6
A2	95th	63	10,459	66	16,626	5.3	59
ECHAM							
B1	50th	42	2,230	38	1,798	-7.2	-19.4
B1	95th	63	10,264	57	8,090	-9.2	-21.2
A1B	50th	42	2,200	40	3,174	-3.6	44.3
A1B	95th	63	10,426	62	12,217	-0.6	17.2
A2	50th	42	2,186	37	2,176	-10.8	-0.5
A2	95th	63	10,422	61	12,642	-3.1	21.3

Table 9.2. Projected change (%) in land cover type by the end of the century (2100) for interior Alaska. [Change was calculated as difference between the end of the baseline period (2009) and the end of the simulation period (2100).

	Interior Alaska		
CCCMA	B1	A1B	A2
Black Spruce Forest	3.0%	-8.0%	-25.9%
White Spruce Forest	3.7%	-7.9%	-24.3%
Deciduous Forest	-5.1%	24.5%	69.2%
Graminoid Tundra	-46.1%	-49.7%	-46.3%
Shrub Tundra	1.0%	1.8%	1.5%
ECHAM	B1	A1B	A2
Black Spruce Forest	-13.6%	-43.9%	-34.1%
White Spruce Forest	-12.2%	-41.9%	-33.8%
Deciduous Forest	34.8%	113.0%	91.4%
Graminoid Tundra	-44.0%	-45.6%	-44.3%
Shrub Tundra	4.7%	4.5%	5.0%

Table 9.3. Mean and standard deviation (s.d.) of the decadal active layer depth (annual maximum thaw depth) and extent of permafrost at 1m and 3m depth in the soil, for the historical period and the end of the six projections.

Scenario	Period	Active layer depth (m)		Permafrost extent to 1m deep		Permafrost extent to 3m deep	
		Mean	s.d.	km^2	%	km^2	%
Historical	[2000-2009]	1.345	0.998	185,248	17.23	382,404	35.57
CCCMA – B1	[2090-2099]	1.627	1.205	84,546	7.87	186,558	17.35
CCCMA – A1B	[2090-2099]	0.619	0.346	99,313	9.24	111,293	10.35
CCCMA – A2	[2090-2099]	1.071	0.563	37,952	3.53	66,404	6.18
ECHAM5 – B1	[2090-2099]	1.533	1.050	54,677	5.09	120,589	11.22
ECHAM5 – A1B	[2090-2099]	0.978	0.673	54,855	5.10	78,223	7.28
ECHAM5 – A2	[2090-2099]	0.669	0.461	96,704	8.99	144,211	13.42

Table 9.4. Summary of spatial and process model near-surface (within 1m) permafrost and active-layer thickness data products evaluated.

Source	Resolution	Method	Reference
LandCarbon	30 m	Data mining	*Pastick* et al. 2015
STATSGO	1 km	Means Extrapolated to Polygons	*Wylie* et al. 2016
GIPL[1.3]	2 km	Numerical model	*Marchenko* et al. 2008

Table 9.5. Average vegetation and soil carbon stocks and fluxes from last decade (2000–2009) of the historical period in upland and lowlands of Interior Alaska. HR = heterotrophic respiration, NECB = Net ecosystem carbon balance, GWP = Global warming potential.

Drainage conditions	Extent	Veg C stock	Soil C stock	NPP	HR	Fire emission	Biogenic Methane flux	NECB	GWP
	km^2	TgC	TgC	TgC/yr	TgC/yr	TgC/yr	$TgCO_2$ eq/yr	TgC/yr	$TgCO_2$ eq/yr
Uplands	335,491	1,272	6,686	71.57	-54.4	-24.23	2.89E-03	-5.12	20.57
Lowlands	112,077	427	1,965	24.95	-18.29	-8.97	-20.45	-2.21	27.01
Total	447,568	1,699	8,651	96.52	-72.69	-33.20	-20.45	-7.33	47.58

Table 9.6. Average vegetation and soil carbon stocks and fluxes from last decade (2090–2099) of the six climate projections in upland and wetlands of Interior Alaska. NPP = Net primary productivity, HR = heterotrophic respiration, NECB = Net ecosystem carbon balance, GWP = Global warming potential.

Drainage conditions	Vegetation C stock	Soil C stock	NECB	GWP
	TgC	TgC	TgC/yr	$TgCO_2$-eq/yr
CCCMA – B1	1935	8798	4.79	5.58
CCCMA – A1B	1965	8982	7.19	-3.70
CCCMA – A2	2051	9318	11.32	-0.04
ECHAM5 – B1	2128	8991	8.01	-3.50
ECHAM5 – A1B	2163	9097	10.15	18.98
ECHAM5 – A2	2180	9172	10.98	-7.53

(a)

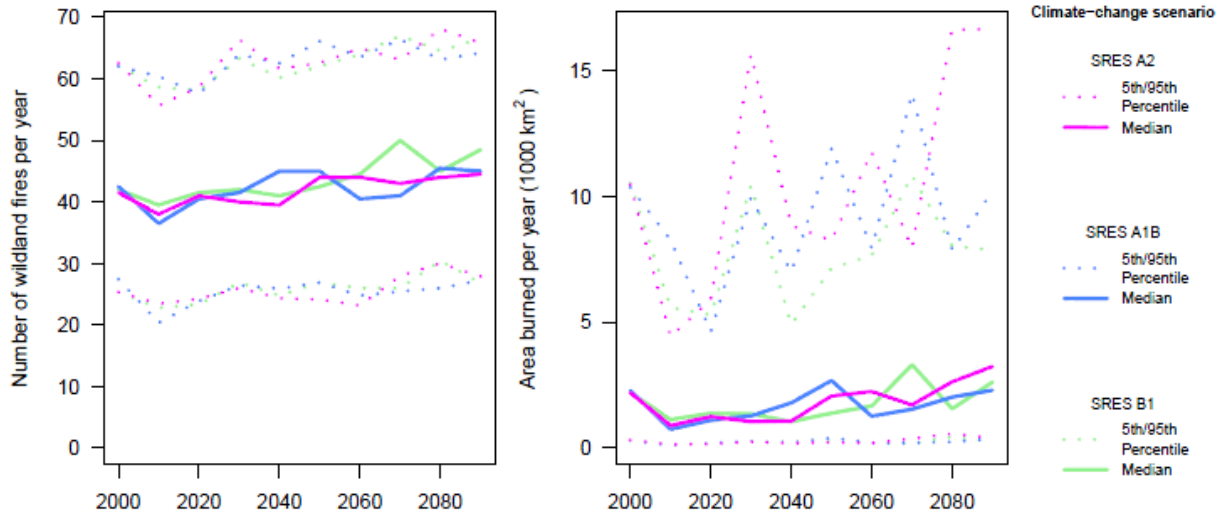

(b)

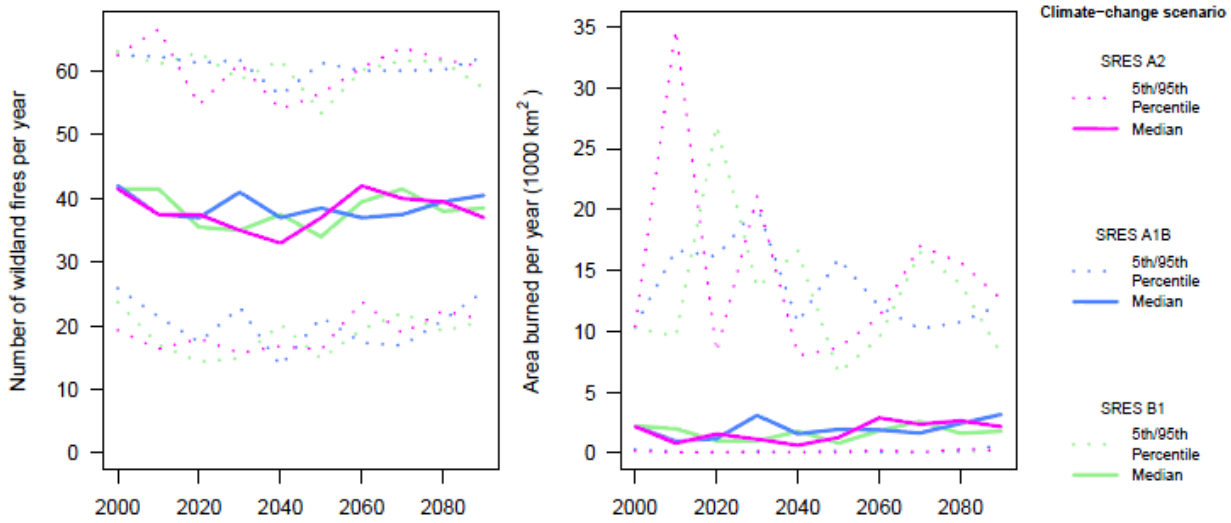

Figure 9.1. Simulated fire activity across the interior Alaska showing summaries of projected wildland-fire ignitions and area burned for each decade for (A) CCCMA and (B) ECHAM. Median, 5th and 95th percentiles reported across 200 simulations.

(a)

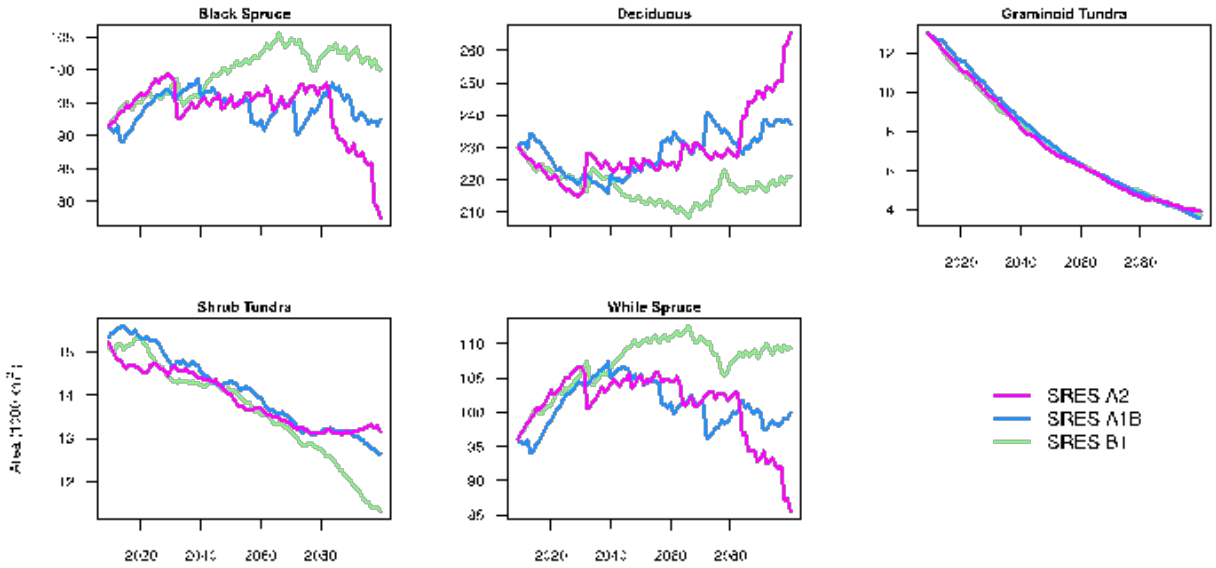

(b)

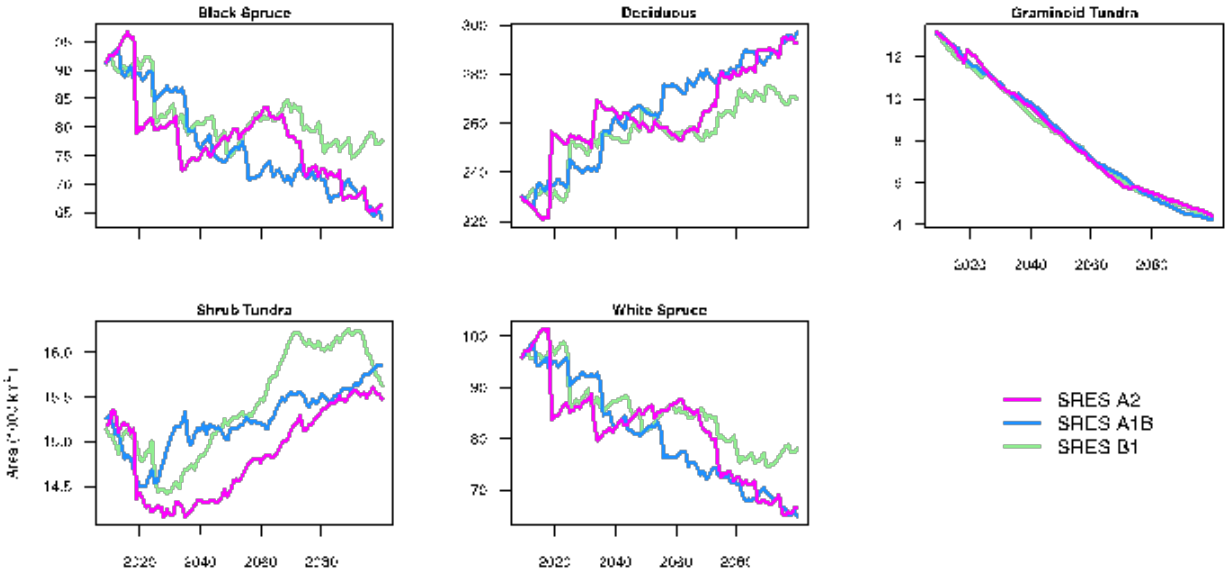

Figure 9.2. Projected land cover type change (in 1000 square km) across interior Alaska under the three emission scenarios. (A) changes from the CCCMA climate scenarios, and (B) changes from the ECHAM5 climate scenarios.

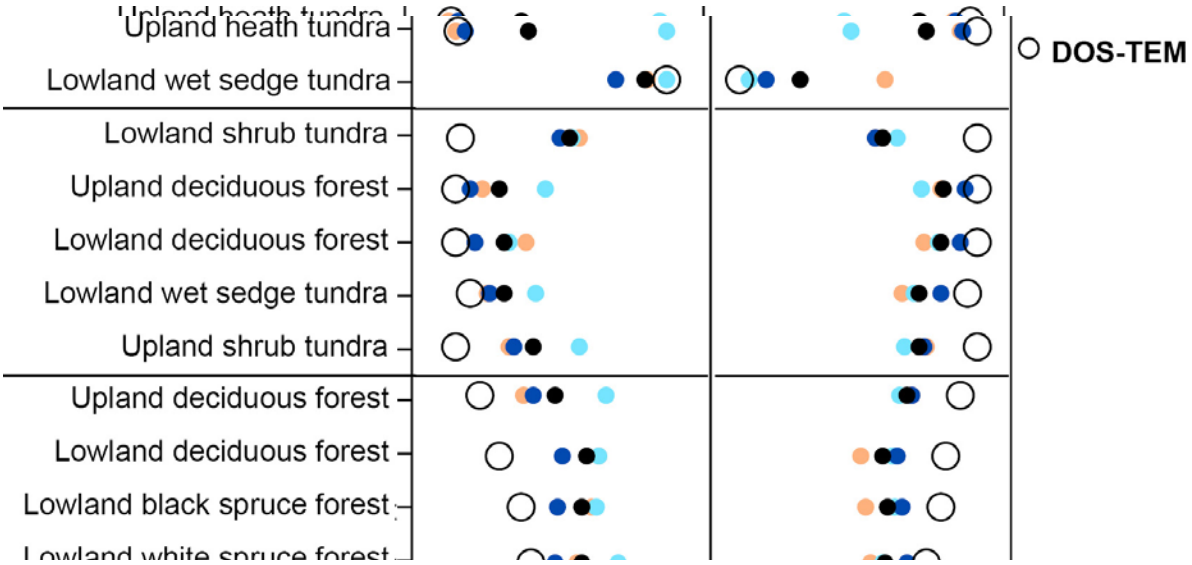

Figure 9.3. Extent of near-surface (within 1m) permafrost (NSP) and averaged active-layer depth (ALD) of major ecotypes in interior Alaska. Areas estimated to have ALDs greater than 1 m were given a value of 101 cm for direct comparison and to account for differences in investigation depths.

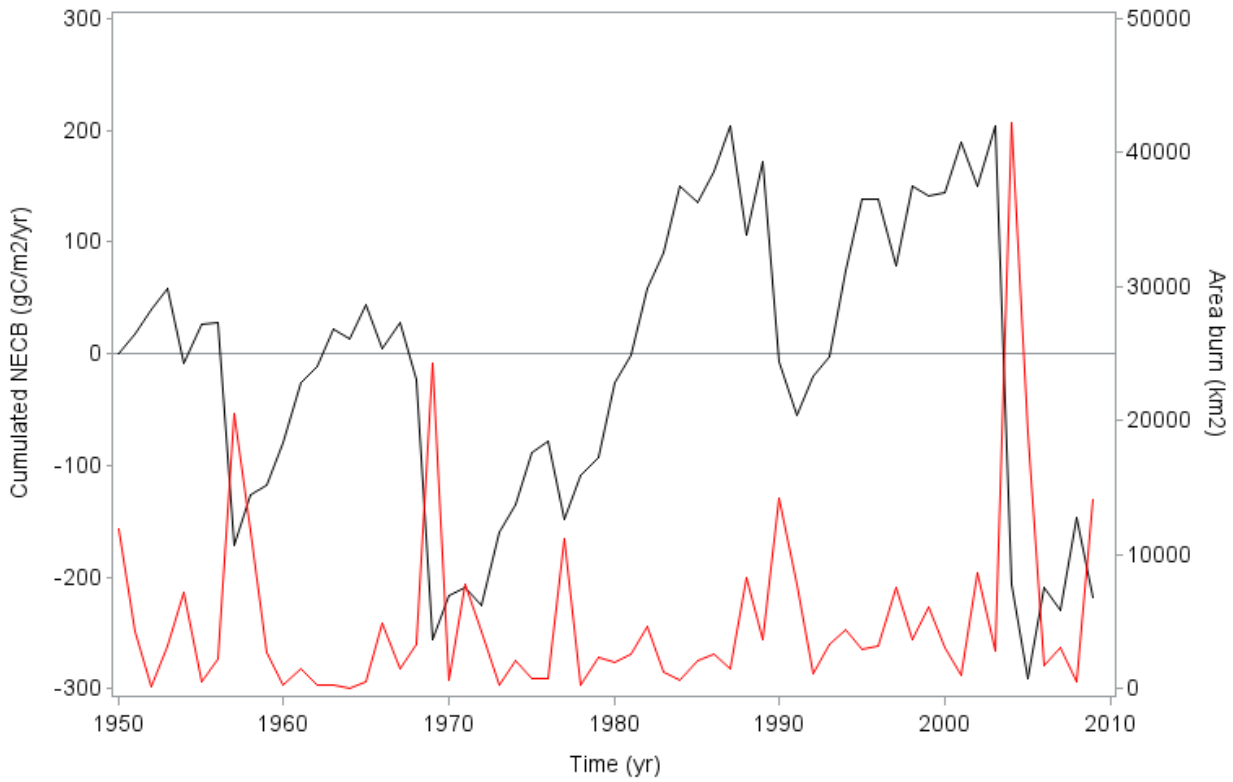

Figure 9.4. Time series of cumulated net ecosystem carbon balance (black solid line) and total annual area burn (red solid line) for the historical period [1950-2009].

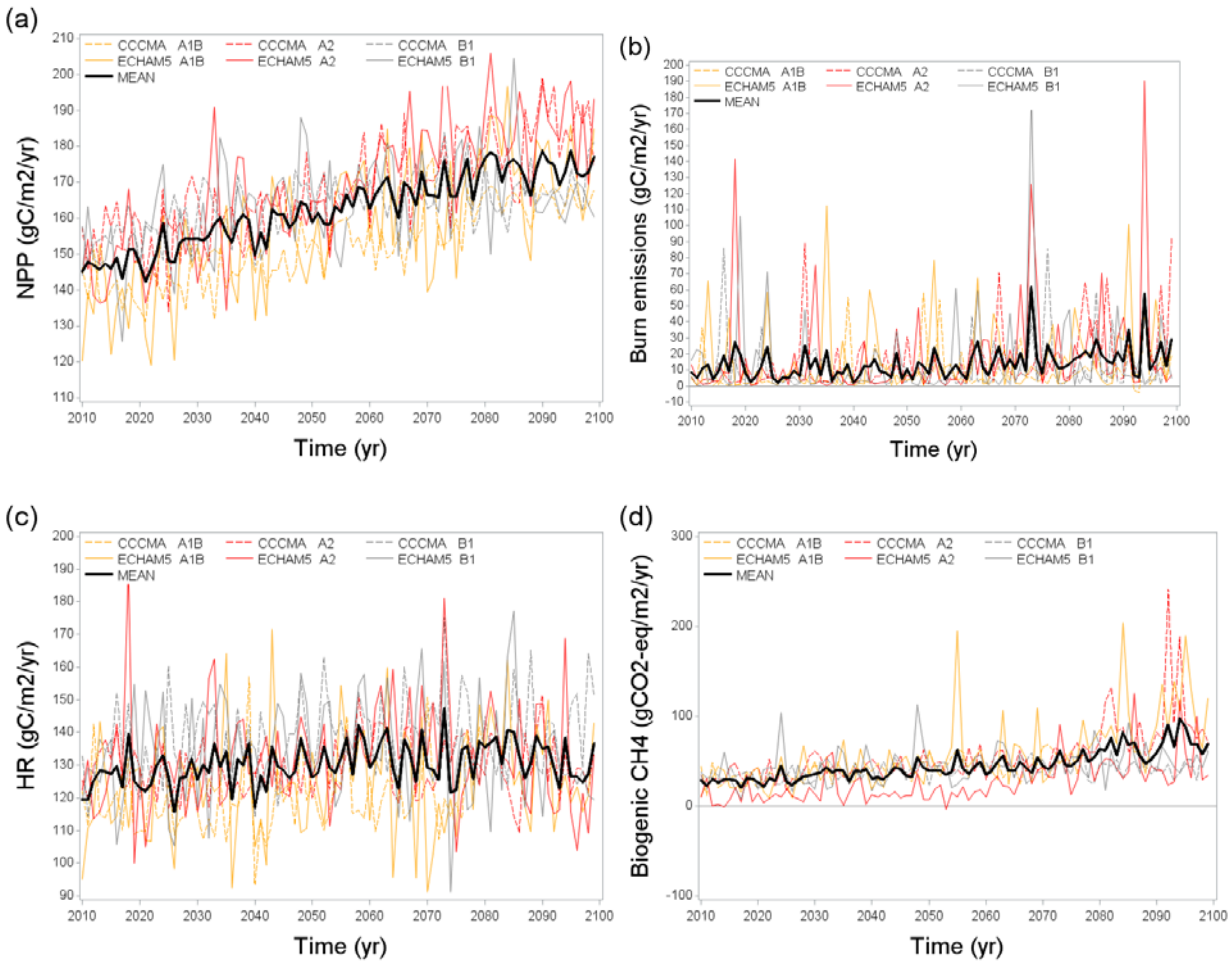

Figure 9.5. Time series of relative changes in carbon fluxes for the projection period (2010–2099) for the six climate simulations: (a) Net Primary Productivity (NPP), (b) Burn emission, (c) Heterotrophic respiration (HR) and (d) Biogenic methane emissions. Each thin line represents a scenario. The thick black line represents the mean annual fluxes among scenarios.

Task 10: Application Products Developed for Alaska Land Managers

T10: Materials and methods

To provide meaningful simulations to inform Alaska land managers about potential future impacts of climate change on wildland fire regimes at a landscape scale, a University of Alaska Fairbanks research team met multiple times with fire resource management groups that work on military lands in Interior Alaska. Fire management has the potential to influence the natural fire regime by determining the spatial patterning and timing of fire occurrence, and thus the successional state of an ecosystem within a managed area.

The groups discussed relevant fire management scenarios that could be used to explore their influence on future fire and vegetation dynamics. Recent wildfires such as the 2013 Stuart Creek fire in Interior Alaska, which was sparked by an explosive ordinance on an army weapons range, demonstrate the need to test alternate fire management scenarios, as one hypothesized method to reduce future large fires is to increase fire suppression. Consequently, together we chose to investigate how changing fire management planning options (FMPO) within military training lands would influence the future fire regime and concurrent boreal forest vegetation dynamics. Military lands, as are all lands in Alaska, are designated by FMPO that provide for a full range of suppression responses from aggressive control and extinguishment, to surveillance (AWFCG 2010). Results shown in this task were delivered to back to fire managers in a workbook format developed in concert with the Alaska Fire Science Consortium and the Scenarios Network for Arctic and Alaska Planning (Appendix C).

The framework for this task consisted singularly of the ALFRESCO vegetation-fire model. The methodology we used for this application was equivalent to that used for Task 9, with two exceptions. First, the pair of climate models (National Center for Atmospheric Research Community Climate System Model 4.0 (NCAR-CCSM4) and Meteorological Research Institute Coupled General Circulation Model v3.0 (MRI-CGCM3)) and single future emission scenario (representative concentration pathway, RCP 8.5) chosen to drive the model to bracket the uncertainty associated with forecasted landscape changes are derived from the more recent best performing CMIP5 models (Moss et al. 2010). Second, we chose to focus our modeling effort on the Upper Tanana Hydrologic Basin in Interior Alaska as it encompasses Fort Wainwright, Eielson Air Force Base, and Fort Greeley along with the larger urban communities on the road system in Interior Alaska (Figure 10.1). The specific questions addressed by this task include:

i. How might changes in fire management planning options within military training land boundaries influence the frequency and extent of wildfire activity on, and adjacent to, military lands in the Upper Tanana Hydrologic Basin during the 21st century?
ii. Does the frequency and extent of future wildfire activity vary depending on the driving climate scenario?

To simulate fire management scenarios, we created flammability maps as an input to ALFRESCO. We varied the level of fire suppression among FMPO using sensitivity values that

control how likely a fire is to spread after ignition. Sensitivity values were assigned from high to low, in decreasing order, for the critical, full, modified and limited protection options. For the purposes of the modeling effort, we lumped unclassified lands with the limited fire protection class. We then created two flammability maps for the Upper Tanana Hydrologic Basin depicting: 1) the current FMPO designation and 2) an experimental alternative FMPO designation in which we changed the protection status of all military lands that are currently designated as the modified protection option to the full protection option.

The timeline for implementation differs between the two fire management scenarios (Figure 10.2). After model spin-up, transition from a natural fire regime, equivalent to the limited fire protection class, to the current FMPO occurs in 1950. While we are aware FMPO were not implemented until the 1980s, fire suppression was commonplace in urban areas before this time so this early date to switch to the current FMPO is justified and is a better match to the historical record. The experimental fire management planning scenario was implemented in 2009 as this is the year the climate inputs switch from historical to future climate projections. We performed separate computer model runs with the two alternate fire management scenarios depicted in Fig. 10.1 and compared the results for fire and vegetation dynamics into the future to determine the effect of the experimental FMPO designation.

T10: Results and discussion

The model results show the experimental alternative FMPO we implemented, changing all military lands within the study area from limited to full protection, led to an increase in the number of fires per decade (Figure 10.3), yet a decrease in the cumulative area burned through 2100 compared to the status quo (Figure 10.4). The greatest difference between future fire regimes, however, is observed in the comparison between the two driving climate models. While the number of fires per decade is similar (~35) between the warmer and drier NCAR-CCSM4 and cooler and wetter MRI-CGCM3 model, the cumulative area burned is not. There is a difference in fire activity between the two models with the greatest difference observed at the end of the 21st century in where the cumulative area burned is over 10,000 km^2 greater for the NCAR-CCSM4 model compared to MRI-CGCM3 model.

These projected changes in fire regime led to concurrent increases in the amount of late successional coniferous forest present on the landscape in contrast to maintaining the current FMPO, which leads to more early successional deciduous forest on the landscape through the end of the century (Figure 10.5). Similar to fire regime, the greater difference in landscapes is between the driving climate models. Due to the greater fire activity in the warmer and drier NCAR-CCSM4 scenario, there is far less coniferous forest, both black (~7,000 km^2) and white spruce (~5,000 km^2), than deciduous forest (~23,000 km^2) at the end of the 21st century. This trend is the opposite for the cooler and wetter MRI-CGCM3 model where there is far less deciduous forest (~13,000 km^2) at the end of the 21st century than black (~12,000 km^2) and white spruce (~10,000 km^2) combined.

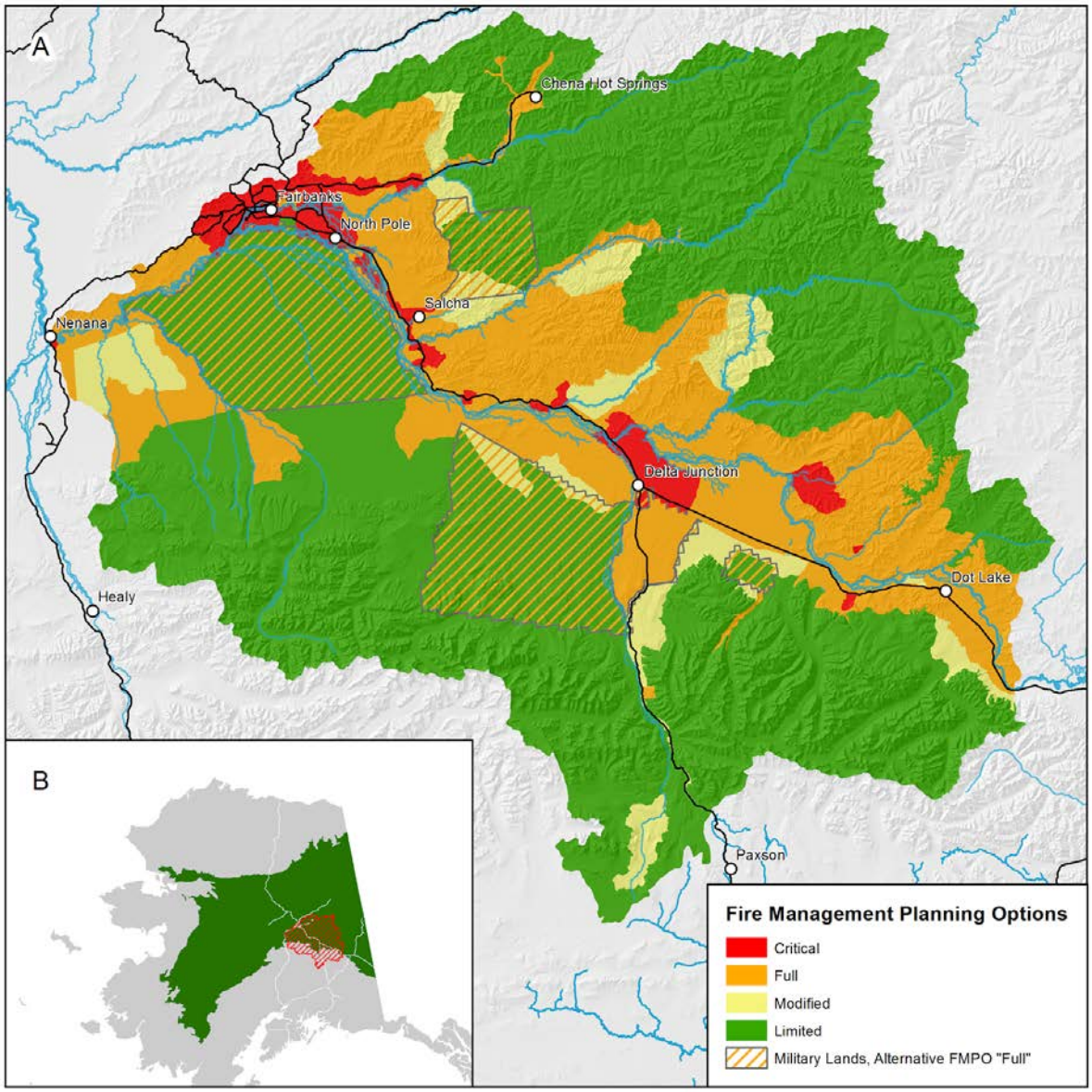

Figure 10.1. Map showing the A) Upper Tanana Hydrologic Basin study area in Interior Alaska and B) the location of the study area within Alaska. Fire management planning options are shown within the study area and military lands are outlined in gray. In the inset map, the Intermontane Boreal Ecoregion (Nowaki et al. 2001) over which the ALFRESCO model is calibrated is shown in green and the specific study area is outlined in red.

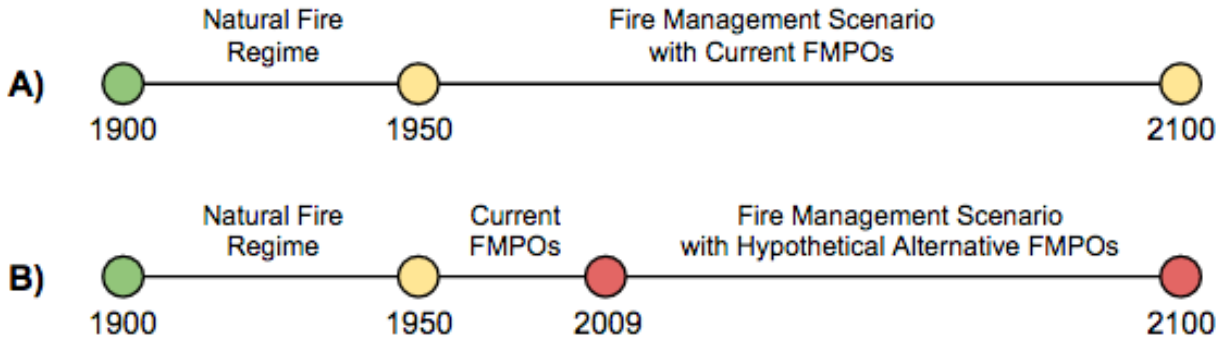

Figure 10.2. Timeline showing fire management scenarios implemented in the ALFRESCO computer model for A) current FMPO and B) alternative FMPO for the Upper Tanana Hydrologic Basin in Interior Alaska. The alternative FMPO changes all military lands within the study area to the full protection fire management planning option.

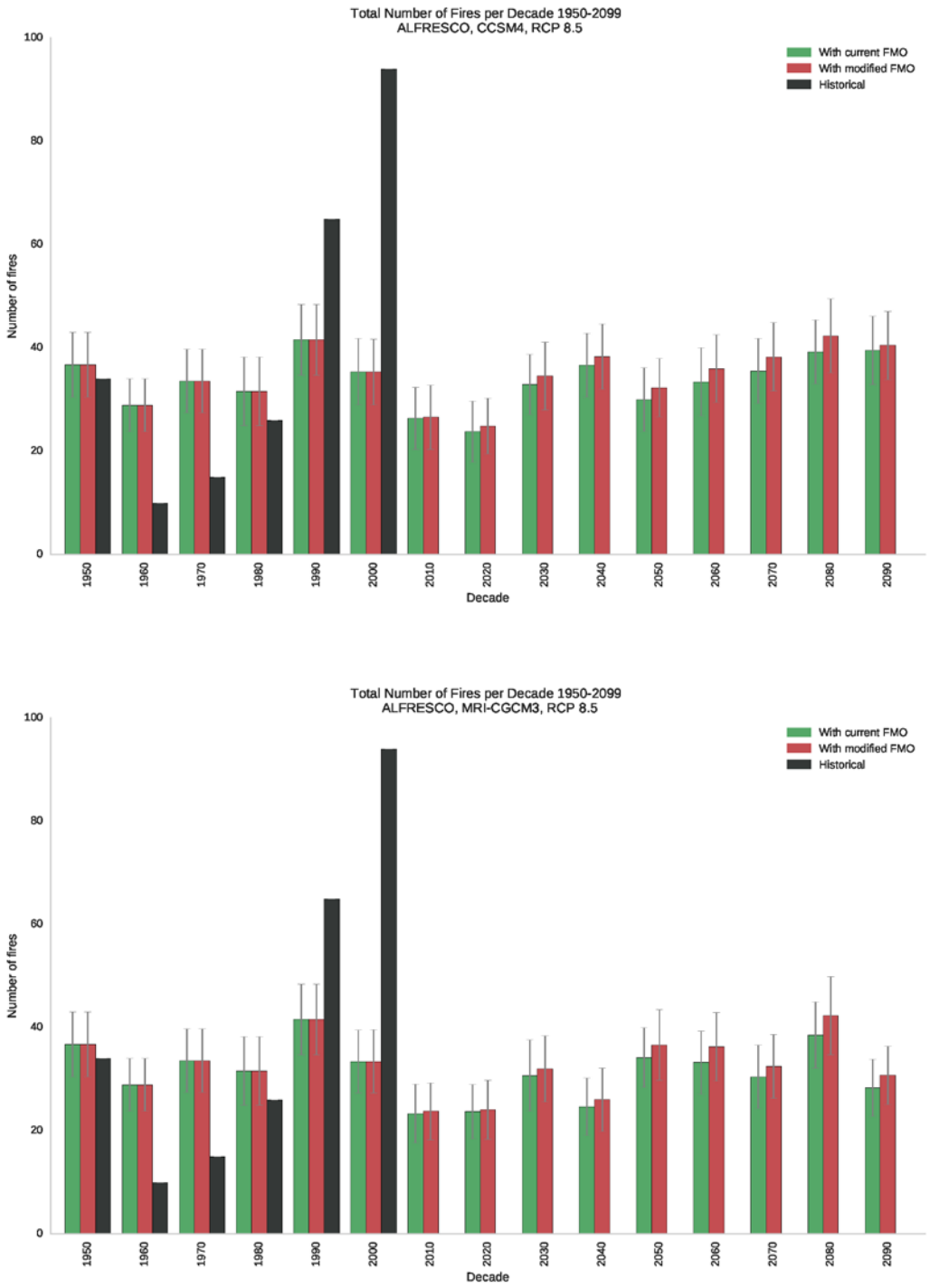

Figure 10.3. Total number of fires per decade in the Upper Tanana Hydrological Basin from 1950-2100. Total number of fires is reported from historical records, and from our modeling results with the current FMPO and the experimental FMPO in which the fire protection status of military lands within the study area is changed from limited to full. Model results are presented

for two global circulation models a) NCAR-CCSM4 and b) MRI-CGCM3 for the RCP 8.5 emission scenario. Data presented are means and standard errors from 200 model replicates.

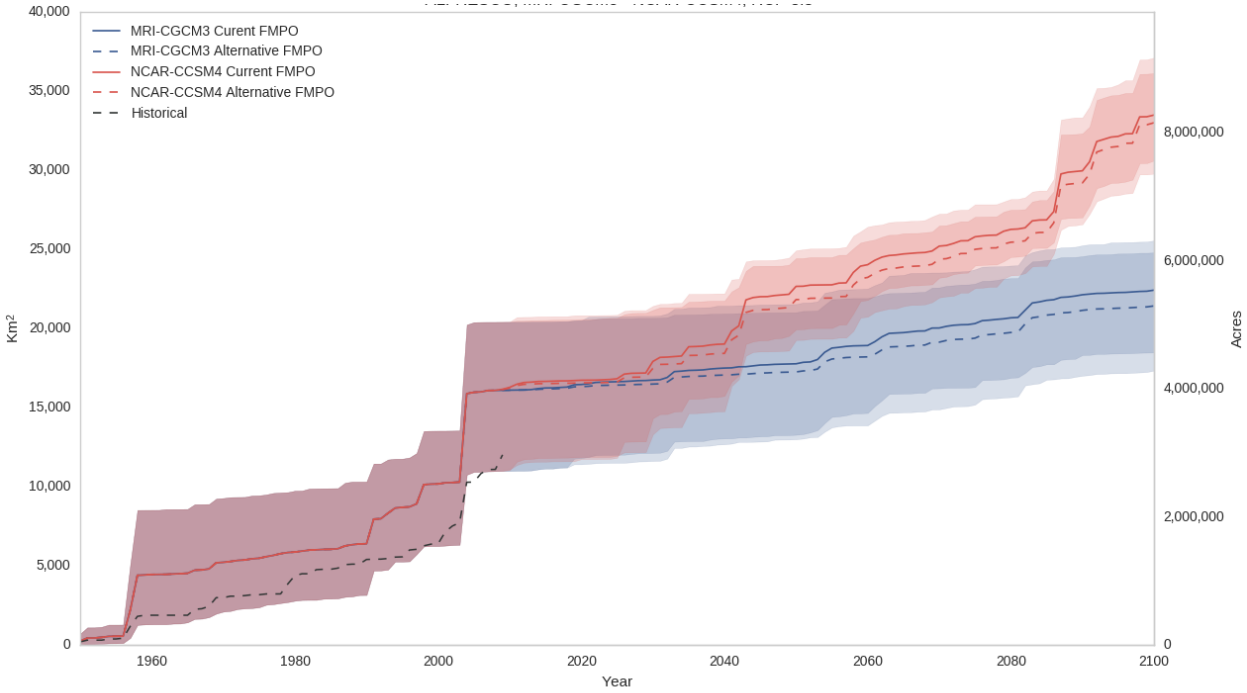

Figure 10.4. Cumulative area burned the historical (1950-2009) and projected (2010-2100) periods for the Upper Tanana Hydrological Basin in Interior Alaska. Model results are presented for fire management scenarios driven by the NCAR-CCSM4 and MRI-CGCM3 global circulation models for the RCP 8.5 emission scenario. Data presented are means and shading indicates results from 200 model replicates.

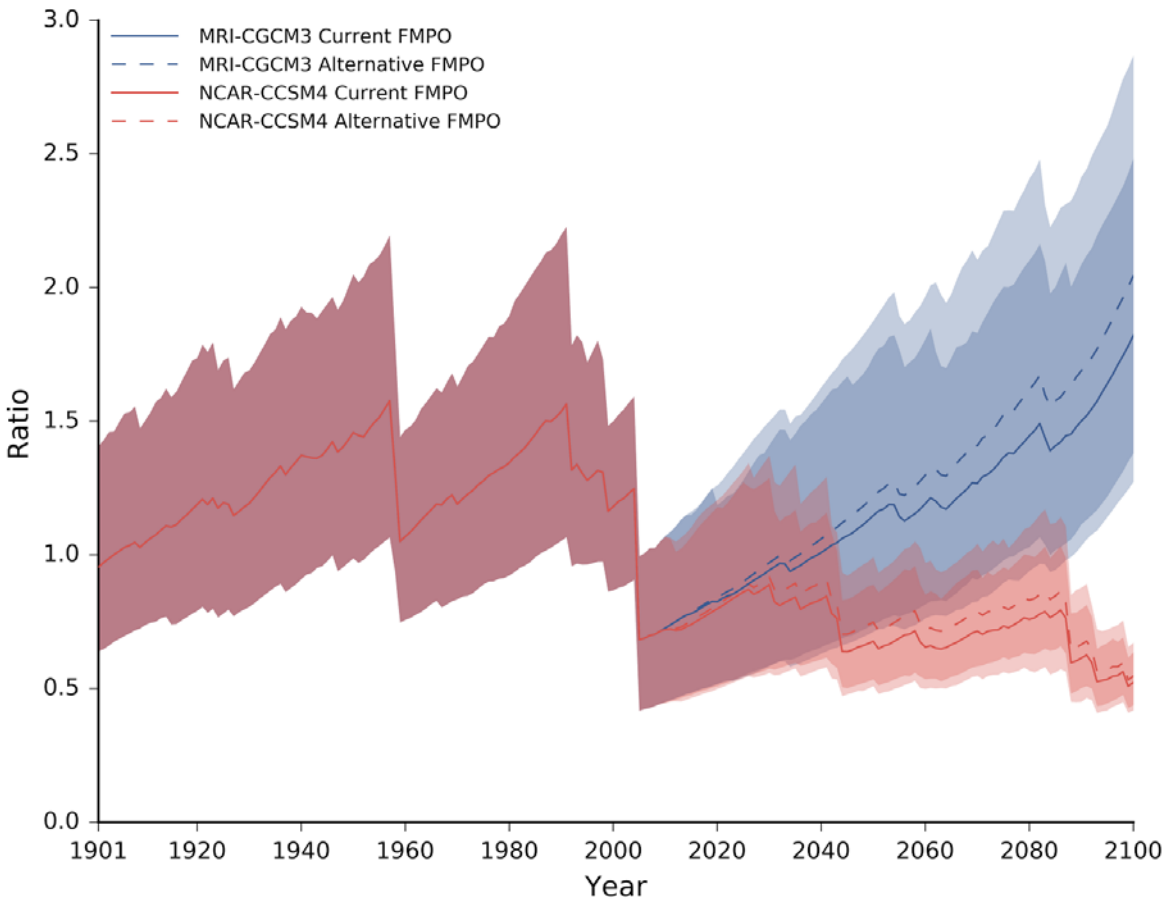

Figure 10.5. Conifer:Deciduous ratios for the model spin-up (1901-1949), historical (1950-2009) and projected (2010-2100) periods for the Upper Tanana Hydrological Basin in Interior Alaska. Model results are presented for fire management scenarios driven by the NCAR-CCSM4 and MRI-CGCM3 global circulation models for the RCP 8.5 emission scenario. Data presented are means and shading indicates results from 200 model replicates.

Conclusions and Implications for Future Research/Implementation

The diverse suite of observational studies, empirical experiments, and modeling activities supported by this grant resulted a comprehensive research plan that met the objectives outlined in the original proposal. First, we proposed to determine mechanistic links among fire, soils, permafrost, and vegetation succession in order to develop and test field-based ecosystem indicators that can be used to directly predict ecosystem vulnerability to state change. We approached this objective using a mixture focused study sites and an extensive network of burned sites of various ages and composition.

Across our location-specific, intensive studies and the broad network of sites we established, consistent patterns emerged. Fire disturbance and loss of the SOL have strong effects on species establishment, with last effects on forest succession, biogeochemical cycling, and soils, which have long-term implications for ecosystem structure and function, as well as permafrost thaw. Our seedling studies indicated that black spruce is more likely to self-replace and re-establish on sites when the SOL does not burn deeply. In contrast, when severe burns leave a shallow SOL, deciduous species may be more likely to establish, setting the ecosystem on a new successional trajectory. The long-term implications of shifting trajectories were studied extensively in our study of carbon and nutrient stocks and fluxes in mid-successional black spruce and Alaska paper birch forest at Murphy Dome. Our findings indicate that ecosystem C distribution between conifer and deciduous stands is dramatically different, with conifer forest storing large quantities of C in cooler soils comprised of long-term moss accumulation. In contrast, deciduous stands aboveground biomass was the predominant C pool, with little moss in the understory and relatively small SOL C pools. Additionally, nutrient cycling was much more rapid in deciduous stands. These findings suggest that fundamental shifts in biogeochemical cycling and nutrient availability are occurring across the boreal region as severe wildfire disturbances allow for greater deciduous tree species establishment post-fire. The long-term consequences of these shifts remain an active area of study, however it is likely that these changes will continue to affect ecosystem C sequestration and storage, as well as fire return intervals because of changes in flammability of the tree species present, and permafrost thaw, if SOL re-accumulation is inhibited in deciduous stands.

Our investigation of the relationship between tree species composition and mosses showed that deciduous litter inputs can reduce moss growth, and that moss communities and functional traits vary across deciduous and coniferous forest types. Divergence in moss cover and species composition seemed to occur during the mid-successional stage, between 20 and 40 years since fire. If moss growth is limited by deciduous litter inputs, soils are likely to warm, causing greater permafrost degradation and reducing the likelihood of permafrost recovery following fire.

Evaluation of the C losses from the SOL during fire showed that much of the C lost during fires is relatively young, and that the deeper SOL may survive multiple fire cycles. If fires continue to become more severe and deeper burning occurs, these C pools that are hundreds of years old may be at greater risk of loss from the ecosystem. Monitoring of the soil temperature post-fire showed that fire disturbance increases soil temperatures considerably, likely due to the reduction in the SOL. Continued monitoring of burned and unburned sites will improve our record of these relationships and allow for greater exploration of the linkage between SOL and permafrost thaw and recovery following fire events.

Consideration of topography, temperature and moisture impacts on tree growth showed that future warming, particularly in spring, is likely to result in drought stress and a reduction of black spruce growth that is independent of region, landscape position, or stand characteristics. Further, we identified the prominence of drought stress in northern black spruce ecosystems and suggest that if temperatures continue to warm, we can expect drought induced productivity declines across large regions of the boreal forest, even for trees located in cool and moist landscape positions. The largest changes in boreal vegetation will likely not be in direct response to climate warming, but indirectly through alterations in the fire regime, which will subsequently affect boreal forest regeneration and the successional trajectory.

In addition to shifting tree species composition, fire disturbances can facilitate non-native species establishment. Non-native plants were observed in recently burned and managed areas, but not in mature forest stands adjacent to roadside seed sources, indicating that mature forests are resistant to non-native plant colonization under current conditions. This observation is appears to be driven by the legacy effects of the thick organic layer found in mature forest stands. Similar to deciduous tree species establishment on thin SOLs post-fire, non-native species also prefer these conditions.

Our second study objective was to forecast landscape change in response to projected changes in climate, fire regime, and fire management. Integrating our empirical studies with new modeling efforts showed generally consistent linkages among fires, vegetation, soils, and permafrost as were observed in the field. The predictive model of fire severity, designed from the analysis of field observations, reproduces the effect of local topography, weather conditions and fire characteristics on the reduction of the SOL caused by fire and allows a better representation of the spatial variability of fire severity in boreal forest in process-based models. Post-fire SOL re-accumulation may attenuate the impact of fire disturbance on permafrost degradation. However, in upland black spruce forest, permafrost could completely degrade within 120 years of a severe fire in an unchanging climate. In contrast, in a lowland black spruce forest, permafrost is more resilient to disturbance and can persist under moderate burn severity. The distribution of near surface permafrost is projected to decrease in Interior Alaska for all climate scenarios tested. This decrease (between 60 and 70% compare to the end of the historical period) is mainly related to the effect of warming and fire disturbance on permafrost thaw. The conceptual model of post-fire vegetation succession, which is based on field observations and literature review, represents the importance of local drainage conditions, pre-fire biological legacies and fire severity. The representation of the effects of these drivers in disturbance models may be critical to reproduce spatial heterogeneity of post-fire vegetation succession across the boreal region of Alaska.

Late successional boreal forest cover types are also projected to decrease under almost all future climate scenarios. A concomitant increase in early successional deciduous vegetation is also projected. Wildfire frequency and extent are projected to increase across the majority of future climate combinations for the northern boreal forest region of Alaska, despite the increase of less flammable deciduous vegetation and the reduction of more flammable late successional spruce forest.

Forest management by the DoD and state agencies were shown to have similar impacts on successional trajectories to fire, in that removal of the SOL was associated with greater deciduous tree species establishment and increased permafrost thaw post-disturbance. Large C losses, especially from aboveground biomass removal were also identified. The use of thinning as a management strategy instead of shearblading however, can lessen these impacts considerably. Shifting forests to deciduous tree species however, may reduce the likelihood of fire in future, which may be an important consideration to managers making decisions on fire risk.

We also modeled an experimental alternative fire management planning scenario that changed all military lands within the study area from limited to full protection. This led to a consistent increase in the number of fires, yet a decrease in the amount of area burned through 2100 compared to the status quo. Projected changes in fire regime due to alternative management led to a concurrent increase in the amount of late successional coniferous forest present on the landscape in contrast to maintaining the current fire management scenario, which led to more early successional deciduous forest on the landscape through the end of the century. Additional research and economic analyses are necessary to determine if the cost of implementing such changes is warranted. However, these findings provide new insights for managers of DoD lands and a new tool to evaluate potential future changes to the fire regime and vegetation composition.

Literature Cited

Alaska Wildland Fire Coordinating Group (AWFCG). 2010. Alaska Interagency Wildland Fire Management Plan. http://fire.ak.blm.gov/content/planning/aiwfmp_2010.pdf

Alexander, H. D., M. C. Mack, S. Goetz, P. S. A. Beck, and E. F. Belshe. 2012. Implications of increased deciduous cover on stand structure and aboveground carbon pools of Alaskan boreal forests. Ecosphere 3:1-21.

Balshi M. S., A. D. McGuire, Q. Zhuang, J. Melillo, D. W. Kicklighter, E. Kasischke, C. Wirth, M. Flannigan, J. Harden, J. S. Clein, T. J. Burnside, J. McAllister, W. A. Kurz, M. Apps, and A. Shvidenko. 2007. The role of historical fire disturbance in the carbon dynamics of the pan-boreal region: A process-based analysis. Journal of Geophysical Research-Biogeosciences 112

Barber, V. A. et al. 2000. Reduced growth of Alaskan white spruce in the twentieth century from temperature-induced drought stress. - Nature 405: 668–673.

Bates, D. et al. 2009. lme4 package for R. in press.

Bennie, J., M.O. Hill, R. Baxter, and B. Huntley. 2006. Influence of slope and aspect on long-term vegetation change in British chalk grasslands. Journal of Ecology 94:355-368.

Benscoter, B.W. and D. H. Vitt. 2007. Evaluating feathermoss growth: a challenge to traditional methods and implications for the boreal carbon budget. Journal of Ecology 95:151-158.

Berner LT, Alexander HD, Loranty MM, Ganzlin P, Mack MC, Davydov SP, Goetz SJ. 2015. Biomass allometry for alder, dwarf birch, and willow in boreal forest and tundra ecosystems of far northeastern Siberia and north-central Alaska. Forest Ecology and Management 337: 110-118.

Berg, E. E. and Chapin III, F. S. 1994. Needle loss as a mechanism of winter drought avoidance in boreal conifers. - Can. J. For. Res. 24: 1144–1148.

Bernhardt, E., T. N. Hollingsworth, F. S. I. Chapin, and L. A. Viereck. 2011. Fire severity mediates climate driven shifts in understory composition of black spruce stands in interior Alaska. Journal of Vegetation Science 22:32–44.

Blanchet, F. G. et al. 2008. Forward selection of explanatory variables. - Ecology 89: 2623–2632.

Bracho R, Natali SM, Pegoraro E, Crummer KG, Schadel C, Celis G, Hale L, Wu L, Yin H, Tiedje JM, Konstantinidis K, Luo Y, Zhou J, Schuur EAG. 2016. Temperature sensitivity of the microbial soil organic matter decomposition in permafrost-region soils during laboratory incubations. Soil Biology and Biogeochemistry 97: 1-14.

Branch, C. A. C. R. et al. 1987. The Canadian system of soil classification. - Agriculture Canada.

Boby, L. A., E. A. G. Schuur, M. C. Mack, D. Verbyla, and J. F. Johnstone. 2010. Quantifying fire severity, carbon, and nitrogen emissions in Alaska's boreal forest. Ecological Applications 20:1633–1647.

Brown, C. D. 2011. Ecological responses to altered fire frequency in treeline forests of the North Yukon, Canada. Ph.D. thesis, University of Saskatchewan, Saskatoon, SK, Canada.

Brown, C. D., and J. F. Johnstone. 2012. Once burned, twice shy: Repeat fires reduce seed availability and alter substrate constraints on *Picea mariana* regeneration. Forest Ecology and Management 266:34–41.

Brown, C. D., J. Liu, G. Yan, and J. F. Johnstone. 2015. Disentangling legacy effects from environmental filters of post-fire assembly of boreal tree assemblages. Ecology 96:3023–3032.

Brown, J., O. J. F. Jr., J. A. Heginbottom, and E. S. Melnikov. 1998. Circum-Arctic map of permafrost and ground-ice conditions. National Snow and Ice Data Center/World Data Center for Glaciology, Boulder, CO.

Brown, J. K. 1974. Handbook for Inventorying Downed Woody Material. USDA Forest Service, Intermountain Forest and Range Experiment Station, Ogden, Utah, USA.

Bunn, A. G. 2010. Statistical and visual crossdating in R using the dplR library. Dendrochronologia 28:251-258.

Burnham, K. P. and Anderson, D. R. 2003. Model Selection and Multimodel Inference: A Practical Information-Theoretic Approach. - Springer Science & Business Media.

Burnham, K. P., and D. R. Anderson. 2002. Model selection and multimodel inference: a practical information-theoretic approach. Springer, New York, NY, USA.

Busby, J. R., L. C. Bliss, and C. D. Hamilton. 1978. Microclimate control of growth-rates and habitats of boreal forest mosses, *Tomenthypnum nitens* and *Hylocomium splendens*. Ecological Monographs **48**:95-110.

Calef, M. P., A. D. McGuire, H. E. Epstein, T. S. Rupp, and H. H. Shugart. 2005. Analysis of vegetation distribution in interior Alaska and sensitivity to climate change using a logistic regression approach. Journal of Biogeography 32:863–878.

Carrascal L. M., I. Galvan, and O. Gordo. 2009. Partial least squares regression as an alternative to current regression methods used in ecology Oikos 118 681–90

Chapin, F. S., A. D. McGuire, R. W. Ruess, D. A. Walker, R. D. Boone, M. E. Edwards, B. P. Finney, L. D. Hinzman, J. B. Jones, G. P. Juday, E. S. Kasischke, K. Kielland, A. H. Lloyd, M. W. Oswood, C. L. Ping, E. Rexstad, V. E. Romanovsky, J. P. Schimel, E. B. Sparrow, B. Sveinbjornsson, D. W. Valentine, K. VanCleve, D. L. Verbyla, L. A. Viereck, R. A. Werner, T. L. Wurtz, and J. Yarie. 2006. Summary and Synthesis:Past and future changes in the

Alaskan boreal forest. Oxford University Press, New York.

Chapin, F. S., S. F. Trainor, O. Huntington, A. L. Lovecraft, E. Zavaleta, D. C. Natcher, A. D. McGuire, J. L. Nelson, L. Ray, M. Calef, N. Fresco, H. Huntington, T. S. Rupp, L. Dewilde, and R. L. Naylor. 2008. Increasing wildfire in Alaska's boreal forest: Pathways to potential solutions of a wicked problem. Bioscience 58:531-540.

Conn, J. S., K. L. Beattie, M. A. Shephard, M. L. Carlson, I. Lapina, M. Hebert, R. Gronquist, R. Densmore, and M. Rasy. 2008. Alaska Melilotus invasions: Distribution, origin, and susceptibility of plant communities. Arctic Antarctic and Alpine Research 40:298-308.

Cook, E. R. and Kairiukstis, L. 1990. Methods of Dendrochronology: Applications in the Environmental Sciences. - Kluwer Academic Publishers.

Cook, E. R. and Briffa, K. R. 1990. A comparison of some tree-ring standardization methods. - In: Cook, E. R. and Kairiukstis, L. A. (eds), Methods of Dendrochronology. Kluwer Academic Publishers, in press.

Coplen, T. 1995. Reporting of stable carbon, hydrogen, and oxygen isotopic abundances. - Ref. Intercomp. Mater. Stable Isot. Light Elem. 825: 31–34.

Cumming, S. G. 2001. Forest type and wildfire in the alberta boreal mixedwood: What do fires burn? Ecological Applications 11:97-110.

Daly, C., G. Taylor, and W. Gibson. 1997. The PRISM approach to mapping precipitation and temperature. Pages 10-12 in Proceedings, 10th Conference on Applied Climatology, American Meteorology Society.

Dissing, D., and D. L. Verbyla. 2003. Spatial patterns of lightning strikes in interior Alaska and their relations to elevation and vegetation. Canadian Journal of Forest Research-Revue Canadienne De Recherche Forestiere 33:770-782.

Elith, J. et al. 2008. A working guide to boosted regression trees. - J. Anim. Ecol. 77: 802–813.

Ellison, A. M. 2004. Bayesian inference in ecology. Ecology Letters 7:509–520.

Euskirchen E.S., A. D. McGuire, F. S. Chapin III. 2007. Energy feedbacks of northern high-latitude ecosystems to the climate system due to reduced snow cover during 20th century warming. Global Change Biology 13:2425-2438

Euskirchen E.S., A. D. McGuire, D. W. Kicklighter, Q. Zhuang, J. S. Clein, R. J. Dargaville, D. G. Dye, J. S. Kimball, K. C. McDonald, J. M. Melillo, V. E. Romanovsky, and N. V. Smith. 2006. Importance of recent shifts in soil thermal dynamics on growing season length, productivity, and carbon sequestration in terrestrial high-latitude ecosystems. Global Change Biology 12:731-750

Flato, G.M., 2005. The third generation coupled global climate model (CGCM3) (and included links to the description of the AGCM3 atmospheric model): Canadian Centre for Climate Modelling and Analysis [WWW Document]. URL http://ec.gc.ca/ccmac-cccma/default.asp?lang=En&n=1299529F-1.

Forkel M., K. Thonicke, C. Beer, W. Cramer, S. Bartalev, and C. Schmullius. 2012. Extreme fire events are related to previous-year surface moisture conditions in permafrost-underlain larch forests of siberia. Environmental Research Letters 7

Fowler H.J., S. Blenkinsop, and C. Tebaldi. 2007. Linking climate change modelling to impacts studies: Recent advances in downscaling techniques for hydrological modelling. International Journal of Climatology 27:1547-1578

Fritts, H. C. 1976. Tree Rings and Climate. Academic Press, London.

Genet, H., Y. He, A.D. McGuire, Q. Zhuang, Y. Zhang, F. Biles, D.V. D'Amore, X. Zhou, and K.D. Johnson. 2016. Terrestrial carbon modeling: Baseline and projections in upland ecosystems. Chapter 6 (pages 105-132) in Z. Zhu and A.D. McGuire, eds., *Baseline and projected future carbon storage and greenhouse-gas fluxes in ecosystems of Alaska.* U.S. Geological Survey Professional Paper 1826, 196 p., http://dx.doi.org/10.3133/pp1826.

Genet, H., McGuire, A.D., Barrett, K., Breen, A., Euskirchen, E.S., Johnstone, J.F., Kasischke, E.S., Melvin, A.M., Bennett, A., Mack, M.C., Rupp, T.S., Schuur, A.E.G., Turetsky, M.R., Yuan, F., 2013. Modeling the effects of fire severity and climate warming on active layer thickness and soil carbon storage of black spruce forests across the landscape in interior Alaska. Environmental Research Letters 8, 045016. doi:10.1088/1748-9326/8/4/045016

Gessler P.E., I. D. Moore, N. J. McKenzie, and P. J. Ryan. 1995. Soil-landscape modeling and spatial prediction of soil attributes. International Journal of Geographical Information Systems 9:421-432

Goodall, D. 1952. Some considerations in the use of point quadrats for the analysis of vegetation. Australian Journal of Biological Sciences 5:1-41.

Greene, D. F., and E. A. Johnson. 2000. Tree recruitment from burn edges. Canadian Journal of Forest Research 30:1264–1274.

Greene, D. F., J. C. Zasada, L. Sirois, D. Kneeshaw, H. Morin, I. Charron, and M. J. Simard. 1999. A review of the regeneration dynamics of North American boreal forest tree species. Canadian Journal of Forest Research 29:824–839.

Grissino-Mayer, H. D. 2001. Evaluating Crossdating Accuracy: A Manual and Tutorial for the Computer Program COFECHA. Tree Ring Research 57:205-221.

Harden J.W., C. D. Koven, C-L. Ping, G. Hugelius, A. D. McGuire, P. Camill, T. Jorgenson, P. Kuhry, G. J. Michaelson, J. A. O'Donnell, E. A. G. Schuur, C. Tarnocai, K. Johnson, and G.

Grosse. 2012a. Field information links permafrost carbon to physical vulnerabilities of thawing. Geophysical Research Letters 39

Harden J.W., K. L. Manies, M. R. Turetsky, and J. C. Neff. 2006. Effects of wildfire and permafrost on soil organic matter and soil climate in interior alaska. Global Change Biology 12:2391-2403

He, Y., H. Genet, A.D. McGuire, Q. Zhuang, B.K. Wylie, and Y. Zhang. 2016. Terrestrial carbon modeling: Baseline and projections in lowland ecosystems of Alaska. Chapter 7 (pages 133-158) in Z. Zhu and A.D. McGuire, eds., *Baseline and projected future carbon storage and greenhouse-gas fluxes in ecosystems of Alaska.* U.S. Geological Survey Professional Paper 1826, 196 p., http://dx.doi.org/10.3133/pp1826.

Hesketh, M., D. F. Greene, and E. Pounden. 2009. Early establishment of conifer recruits in the northern Rocky Mountains as a function of postfire duff depth. Canadian Journal of Forest Research 39:2059–2064.

Higuera, P. E., L. B. Brubaker, P. M. Anderson, F. S. Hu, and T. A. Brown. 2009. Vegetation mediated the impacts of postglacial climate change on fire regimes in the south-central Brooks Range, Alaska. Ecological Monographs 79:201-219.

Hijmans, R. J. et al. 2013. Package "dismo." - Circles 9: 1.

Hinzman, L. D., N. D. Bettez, W. R. Bolton, F. S. Chapin, M. B. Dyurgerov, C. L. Fastie, B. Griffith, R. D. Hollister, A. Hope, H. P. Huntington, A. M. Jensen, G. J. Jia, T. Jorgenson, D. L. Kane, D. R. Klein, G. Kofinas, A. H. Lynch, A. H. Lloyd, A. D. McGuire, F. E. Nelson, W. C. Oechel, T. E. Osterkamp, C. H. Racine, V. E. Romanovsky, R. S. Stone, D. A. Stow, M. Sturm, C. E. Tweedie, G. L. Vourlitis, M. D. Walker, D. A. Walker, P. J. Webber, J. M. Welker, K. Winker, and K. Yoshikawa. 2005. Evidence and implications of recent climate change in northern Alaska and other arctic regions. Climatic Change 72:251-298.

Hogg, E. H. 1997. Temporal scaling of moisture and the forest-grassland boundary in western Canada. - Agric. For. Meteorol. 84: 115–122.

Jafarov, E.E., Romanovsky, V.E., Genet, H., McGuire, A.D., Marchenko, S.S., 2013. The effects of fire on the thermal stability of permafrost in lowland and upland black spruce forests of interior Alaska in a changing climate. Environmental Research Letters 8, 035030. doi:10.1088/1748-9326/8/3/035030

Johnson K. D., J. Harden, A. D. McGuire, N. B. Bliss, J. G. Bockheim, M. Clark, T. N. Hollingsworth, M. T. Jorgenson, E. S. Kane, M. Mack, J. O'Donnell, C-L. Ping, E. A. G. Schuur, M. R. Turetsky, and D. W. Valentine. 2011. Soil carbon distribution in Alaska in relation to soil-forming factors Geoderma 167/68 71–84

Johnstone, J. F., C. D. Allen, J. F. Franklin, L. E. Frelich, B. D. Harvey, P. E. Higuera, M. C. Mack, R. K. Meentemeyer, M. R. Metz, G. L. W. Perry, T. Schoennagel, and M. G. Turner. 2016. Changing disturbance regimes, ecological memory, and forest resilience. Frontiers in Ecology and the Environment in press.

Johnstone, J.F., Chapin, F.S., III, Hollingsworth, T.N., Mack, M.C., Romanovsky, V., Turetsky, M., 2010a. Fire, climate change, and forest resilience in interior Alaska. Canadian Journal of Forest Research-Revue Canadienne De Recherche Forestiere 40, 1302–1312. doi:10.1139/x10-061

Johnstone, J.F., Hollingsworth, T.N., Chapin, F.S.I., and Mack, M.C. 2010b. Changes in fire regime break the legacy lock on successional trajectories in Alaskan boreal forest. Glob.ChangeBiol. 16: 1281–1295. doi:10.1111/j.1365-2486.2009.02051.x.

Johnstone, J. F., L. Boby, E. Tissier, M. Mack, D. Verbyla, and X. Walker. 2009. Postfire seed rain of black spruce, a semiserotinous conifer, in forests of interior Alaska. Canadian Journal of Forest Research 39:1575–1588.

Johnstone, J. F. et al. 2008. A key for predicting postfire successional trajectories in black spruce stands of interior Alaska. - Gen. Tech. Rep. - Pac. Northwest Res. Stn. USDA For. Serv.: i + 37 pp.

Johnstone, J. and Chapin, F. 2006. Effects of soil burn severity on post-fire tree recruitment in boreal forest. - Ecosystems 9: 14–31.

Johnstone, J.F., Kasischke, E.S., 2005. Stand-level effects of soil burn severity on postfire regeneration in a recently burned black spruce forest. Canadian Journal of Forest Research-Revue Canadienne De Recherche Forestiere 35, 2151–2163. doi:10.1139/x05-087

Jorgenson, M.T., Racine, C.H., Walters, J.C., Osterkamp, T.E., 2001. Permafrost degradation and ecological changes associated with a warming climate in central Alaska. Climatic Change 48, 551–579.

Kasischke E. 2013. Organic layer thickness measurements from burned and unburned black spruce forests in Alaska collected between 1994 and 2012 BNZ-LTER Data Catalog

Kasischke E.S., D. L. Verbyla, T. S. Rupp, A. D. McGuire, K. A. Murphy, R. Jandt, J. L. Barnes, E. E. Hoy, P. A. Duffy, M. Calef, and M. R. Turetsky. 2010. Alaska's changing fire regime - implications for the vulnerability of its boreal forests. Canadian Journal of Forest Research-Revue Canadienne De Recherche Forestiere 40:1313-1324

Kasischke E.S., M. R. Turetsky, R. D. Ottmar, N. H. F. French, E. E. Hoy, and E. S. Kane. 2008. Evaluation of the composite burn index for assessing fire severity in Alaskan black spruce forests. International Journal of Wildland Fire 17:515-526

Kasischke E.S., and M. R. Turetsky. 2006. Recent changes in the fire regime across the north american boreal region - spatial and temporal patterns of burning across Canada and Alaska. Geophysical Research Letters 33

Kasischke E.S., D. Williams, and D. Barry. 2002. Analysis of the patterns of large fires in the boreal forest region of alaska. International Journal of Wildland Fire 11:131-144

Kuo, S. 1996. Phosphorus. In: *Methods for soil Analysis- Part 3-Chemical Methods.* Editor: D.L. Sparks. SSS Book Series: 5. 893 p.

Legendre, P. and L. Legendre. 1998. Numerical ecology, second English edition. Elsevier, Amsterdam.

Lewkowicz, A. G. 2008. Evaluation of miniature temperature-loggers to monitor snowpack evolution at mountain permafrost sites, northwestern Canada. Permafrost and Periglacial Processes 19:323–331.

Lloyd, A. H. and A. G. Bunn. 2007. Responses of the circumpolar boreal forest to 20th century climate variability. Environmental Research Letters 2: 045013

Mack, M. C., M. S. Bret-Harte, T. N. Hollingsworth, R. R. Jandt, E. A. G. Schuur, G. R. Shaver, and D. L. Verbyla. 2011. Carbon loss from an unprecedented Arctic tundra wildfire. Nature 475:489-492.

Mack M.C., Treseder K.K., Manies K.L., Harden J.W., Schuur E.A.G., Vogel J.G., Randerson J.T., Chapin F.S., III. 2008. Recovery of aboveground plant biomass and productivity after fire in mesic and dry black spruce forests of interior alaska. Ecosystems 11: 209-225.

Manies K. L., J. W. Harden, B. P. Bond-Lamberty, and K. P. O'Neill. 2005. Woody debris along an upland chronosequence in boreal manitoba and its impact on long-term carbon storage. Canadian Journal of Forest Research-Revue Canadienne De Recherche Forestiere 35:472-482

Manies K. L., J. W. Harden, H. Veldhuis, and S. E. Trumbore. 2006. Soil data from a moderately well and somewhat poorly drained fire chronosequence near Thompson, Manitoba, Canada. In: Survey USG (ed), vol. 1291, v. 1.1, p 8

McCune, B. and Keon, D. 2002. Equations for potential annual direct incident radiation and heat load. - J. Veg. Sci. 13: 603–606.

McFarlane, N.A., Boer, G.J., Blanchet, J.-P., Lazare, M., 1992. The Canadian Climate Centre Second-Generation General Circulation Model and Its Equilibrium Climate. J. Climate 5, 1013–1044. doi:10.1175/1520-0442(1992)005<1013:TCCCSG>2.0.CO;2

McGuire A.D., J. M. Melillo, L. A. Joyce, D. W. Kicklighter, A. L. Grace, B. Moore III, and C. J. Vorosmarty. 1992. Interactions between carbon and nitrogen dynamics in estimating net

primary productivity for potential vegetation in North America. Global Biogeochemical Cycles 6:101-124

Melvin A.M., Mack M.C., Johnstone J.F., McGuire A.D., Genet H., Schuur E.A.G. 2015. Differences in Ecosystem Carbon Distribution and Nutrient Cycling Linked to Forest Tree Species Composition in a Mid-Successional Boreal Forest. Ecosystems 18: 1472-1488.

Miyanishi K. and E. A. Johnson. 2002. Process and patterns of duff consumption in the mixed wood boreal forest Can. J. Forest Res. 32 1285–95

Moss, R. H., Edmonds, J. A., Hibbard, K. A., Manning, M. R., Rose, S. K., van Vuuren, D. P., Carter, T.R., Emori, S., Kainuma, M., Kram, T., Meehl, G. A., Mitchell, J. F., Nakicenovic, N., Riahi, K., Smith, S. J., Stouffer, R. J., Thomson, A. M., Weyant, J. P., Wilbanks, T. J. (2010). The next generation of scenarios for climate change research and assessment. *Nature* 463 (7282):747-56.

Murphy J., J. P. Riley. 1962. A modified single solution method for determination of phosphate in natural waters. Anal Chim Acta 26:31-36

Nalder I.A., Wein R.W., Alexander M.E., deGroot W.J. 1997. Physical properties of dead and downed round-wood fuels in the boreal forests of Alberta and Northwest Territories. Canadian Journal of Forest Research-Revue Canadienne De Recherche Forestiere 27: 1513-1517.

Ohse, B., F. Jansen, and M. Wilmking. 2012. Do limiting factors at Alaskan treelines shift with climatic regimes? Environmental Research Letters 7:015505.

Økland, R. H. 1995. Population biology of the clonal moss *Hylocomium splendens* in Norwegian boreal spruce forests. I. Demography. Journal of Ecology **83**:697-712.

Osterkamp, T. E. and V. E. Romanovsky. 1999. Evidence for warming and thawing of discontinuous permafrost in Alaska. Permafrost and Periglacial Processes 10:17-37.

Osterkamp, T. E., T. Zhang, and V. E. Romanovsky. 1994. Thermal regime of permafrost in Alaska and predicted global warming. Journal of Cold Regions Engineering 4:38-42.

Ott R.A., Jandt R. 2005. Fuels treatment demonstration sites in the boreal forests of interior Alaska. Joint Fire Science Program.

Ottmar R. D. and D. V. Sandberg. 2003. Predicting forest floor consumption from wildland fire in boreal forests of Alaska - preliminary results. In: Galley KEM, Klinger RC, Sugihara NG (eds) Proceedings of fire conference 2000: The first national congress on fire ecology, prevention, and management. , vol Miscellaneous Publication No. 13. , Tallahassee, FL: Tall Timbers Research Station, pp 218-224

R Core Team. 2014. R: A language and environment for statistical computing. R Foundation for Statistical Computing, Vienna, Austria.

R Development Core Team. 2011. R: A language and environment for statistical computing. R Foundation for Statistical Computing, Vienna, Austria.

Raich J.W., E. B. Rastetter, J. M. Melillo, D. W. Kicklighter, P. A. Steudler, B. J. Peterson, A. L. Grace, B. Moore, C. J. Vorosmarty. 1991. Potential net primary productivity in South-America - application of a global-model. Ecological Applications 1:399-429

Randerson J.T., Liu H., Flanner M.G., Chambers S.D., Jin Y., Hess P.G., Pfister G., Mack M.C., Treseder K.K., Welp L.R., Chapin F.S., Harden J.W., Goulden M.L., Lyons E., Neff J.C., Schuur E.A.G., Zender C.S. 2006. The impact of boreal forest fire on climate warming. Science 314: 1130-1132.

Rasband, W. S. 2012. ImageJ. U.S. National Institutes of Health, Bethesda, Maryland, USA.

Ridgeway, G. et al. 2013. Package “gbm.” - Viitattu 10: 2013.

Robertson, G. P., D. C. Coleman, C. S. Bledsoe, and P. Sollins, editors. 1999. Standard Soil Methods for Long-Term Ecological Research. Oxford University Press, New York.

Roeckner, E., Brokopf, R., Esch, M., Giorgetta, M., Hagemann, S., Kornblueh, L., Manzini, E., Schlese, U., Schulzweida, U., 2004. The atmospheric general circulation model ECHAM5 Part II: Sensitivity of simulated climate to horizontal and vertical resolution, Report / Max-Planck-Institut für Meteorologie. Max Planck Institut für Meteorologie, Hamburg.

Roland, C. A., J. H. Schmidt, and E. F. Nicklen. 2013. Landscape-scale patterns in tree occupancy and abundance in subarctic Alaska. Ecological Monographs 83:19–48.

Rupp T. S., F. S. Chapin III, and A. M. Starfield. 2001. Modeling the influence of topographic barriers on treeline advance at the forest-tundra ecotone in northwestern Alaska. Climatic Change 48:399-416

Rupp T.S., A. M. Starfield, F. S. Chapin III, and P. Duffy. 2002. Modeling the impact of black spruce on the fire regime of Alaskan boreal forest. Climatic Change 55:213-233
Scenarios Network for Alaska and Arctic Planning (SNAP). 2013. University of Alaska. www.snap.uaf.edu.

Schuur, E. A. G., J. G. Vogel, K. G. Crummer, H. Lee, J. O. Sickman, and T. E. Osterkamp. 2009. The effect of permafrost thaw on old carbon release and net carbon exchange from tundra. Nature 459:556-559.

Schuur, E. A. G., J. Bockheim, J. G. Canadell, E. Euskirchen, C. B. Field, S. V. Goryachkin, S. Hagemann, P. Kuhry, P. M. Lafleur, H. Lee, G. Mazhitova, F. E. Nelson, A. Rinke, V. E. Romanovsky, N. Shiklomanov, C. Tarnocai, S. Venevsky, J. G. Vogel, and S. A. Zimov. 2008. Vulnerability of permafrost carbon to climate change: Implications for the global carbon cycle. Bioscience 58:701-714.

Schuur, E. A. G., K. G. Crummer, J. G. Vogel, and M. C. Mack. 2007. Plant species composition and productivity following permafrost thaw and thermokarst in alaskan tundra. Ecosystems 10:280-292.

Shur, Y. L., and M. T. Jorgenson. 2007. Patterns of permafrost formation and degradation in relation to climate and ecosystems. Permafrost and Periglacial Processes 18:7-19.

Speer, J. H. 2010. Fundamentals of tree ring research. - University of Arizona Press.

Tamm, C. O. 1953. Growth, yield and nutrition in carpets of a forest moss (Hylocomium splendens). Meddeland Statens Skogsforsok Inst 43:1-140.

Tenenhaus M., V. E. Vinzi, Y. M. Chatelin, and C. Lauro. 2005. PLS path modeling Computational Statistics and Data Analysis. 48 159–205

Ter-Mikaelian M.T., Colombo S.J., Chen J.X. 2008. Amount of downed woody debris and its prediction using stand characteristics in boreal and mixedwood forests of Ontario, Canada. Canadian Journal of Forest Research-Revue Canadienne De Recherche Forestiere 38: 2189-2197.

Tibshirani, R. 1996. Regression shrinkage and selection via the Lasso. Journal of the Royal Statistical Society. Series B (Methodological) 58:267–288.

Turetsky, M. R., B. Bond-Lamberty, E. Euskirchen, J. Talbot, S. Frolking, A. D. McGuire, and E. S. Tuittila. 2012. The resilience and functional role of moss in boreal and arctic ecosystems. New Phytologist **196**:49-67.

Turetsky M.R., E. S. Kane, J. W. Harden, R. D. Ottmar, K. L. Manies, E. Hoy, and E. S. Kasischke. 2011. Recent acceleration of biomass burning and carbon losses in Alaskan forests and peatlands. Nature Geoscience 4:27-31

Turetsky, M. R., M. C. Mack, T. N. Hollingsworth, and J. W. Harden. 2010. The role of mosses in ecosystem succession and function in Alaska's boreal forest. Canadian Journal of Forest Research 40:1237-1264.

Turetsky, M. R. 2003. The role of bryophytes in carbon and nitrogen cycling. Bryologist **106**:395-409.

Turetsky, M., K. Wieder, L. Halsey, and D. Vitt. 2002. Current disturbance and the diminishing peatland carbon sink. Geophysical Research Letters 29:-.

Turner, M. G., W. H. Romme, and R. H. Gardner. 1999. Prefire heterogeneity, fire severity, and early postfire plant reestablishment in subalpine forests of Yellowstone National Park, Wyoming. International Journal of Wildland Fire 9:21–36.

Turner, M. G. et al. 1997. Effects of Fire Size and Pattern on Early Succession in Yellowstone National Park. - Ecol. Monogr. 67: 411–433.

Underwood AJ. 1997. Experiments in ecology. Cambridge: Cambridge University Press. 504p.

Van Cleve, K., F. S. Chapin, III, C. T. Dryness, and L. A. Viereck. 1991. Element cycling in taiga
forest: State-factor control. Bioscience 41:78-88.

Van Cleve, K., and L. A. Viereck. 1981. Forest succession in relation to nutrient cycling in the boreal forest of Alaska. Pages 184–211 Forest Succession, Concepts and Application. Springer-Verlag, New York.

Van Cleve, K. and C. T. Dyrness. 1983. Introduction and overview of a multidisciplinary research project: The structure and function of a black spruce forest in relation to other fire-affected taiga ecosystems. Canadian Journal of Forest Research 13:695-916.

Viereck, L. A., C. T. Dyrness, K. Vancleve, and M. J. Foote. 1983. Vegetation, Soils, and Forest Productivity in Selected Forest Types in Interior Alaska. Canadian Journal of Forest Research-Revue Canadienne De Recherche Forestiere 13: 703-720.

Viglas, J. N., C. D. Brown, and J. F. Johnstone. 2013. Age and size effects on seed productivity of northern black spruce. Canadian Journal of Forest Research 43:534–543.

Wilmking, M. and I. Myers-Smith. 2008. Changing climate sensitivity of black spruce (Picea mariana Mill.) in a peatland-forest landscape in Interior Alaska. Dendrochronologia 25:167-175.

Wold, S. 1994. PLS for multivariate linear modeling. In: van de Waterbeemd H (ed) Chemometric methods in molecular design. VHC, pp 195-218

Wylie, B., Pastick, N., Johnson, K.D., Genet, H., 2016. Soil Carbon and Permafrost Estimates and1 Susceptibility in Alaska In: Baseline and Projected Future Carbon Storage and Greenhouse-Gas Fluxes in Ecosystems of Alaska., Zhu, Z., and McGuire, A. D. ed, Professional Paper. U.S. Geological Survey.

Yi S., M. A. Arain, and M-K.Woo. 2006. Modifications of a land surface scheme for improved simulation of ground freeze-thaw in northern environments. Geophysical Research Letters 33

Yi S., K. Manies, J. Harden, and A. D. McGuire. 2009a. Characteristics of organic soil in black spruce forests: Implications for the application of land surface and ecosystem models in cold regions. Geophysical Research Letters 36

Yi S., A. D. McGuire, J. Harden, E. Kasischke, K. Manies, L. Hinzman, A. Liljedahl, J. Randerson, H. Liu, V. Romanovsky, S. Marchenko, and Y. Kim. 2009b. Interactions between

soil thermal and hydrological dynamics in the response of alaska ecosystems to fire disturbance. Journal of Geophysical Research-Biogeosciences 114

Yoshikawa K, Bolton WR, Romanovsky VE, Fukuda M, Hinzman LD. 2002. Impacts of wildfire on the permafrost in the boreal forests of Interior Alaska. Journal of Geophysical Research-Atmospheres 108.

Yuan F.M., S. H. Yi, A. D. McGuire, K. D. Johnson, J. Liang, J. W. Harden, E. S. Kasischke, and W. A. Kurz. 2012. Assessment of boreal forest historical C dynamics in the Yukon River Basin: Relative roles of warming and fire regime change. Ecological Applications 22:2091-2109

Zang, C. 2010. bootRes: Bootstrapped response and correlation functions. R package version 0.3. http://cran.r-project.org/web/packages/bootRes/. in press.

Zhuang Q., A. D. McGuire, J. M. Melillo, J. S. Clein, R. J. Dargaville, D. W. Kicklighter, R. B. Myneni, J. Dong, V. E. Romanovsky, J. Harden, and J. E. Hobbie. 2003. Carbon cycling in extratropical terrestrial ecosystems of the northern hemisphere during the 20th century: A modeling analysis of the influences of soil thermal dynamics. Tellus Series B-Chemical and Physical Meteorology 55:751-776

Zhuang Q., A. D. McGuire, K. P. O'Neill, J. W. Harden, V. E. Romanovsky, and J. Yarie. 2002. Modeling soil thermal and carbon dynamics of a fire chronosequence in interior Alaska. Journal of Geophysical Research-Atmospheres 108

Zhuang Q., V. E. Romanovsky, and A. D. McGuire. 2001. Incorporation of a permafrost model into a large-scale ecosystem model: Evaluation of temporal and spatial scaling issues in simulating soil thermal dynamics. Journal of Geophysical Research-Atmospheres 106:33649-33670

Zuur, A., E. N. Ieno, N. J. Walker, A. A. Saveliev, and G. M. Smith. 2009. Mixed Effects Models and Extensions in Ecology with R. Springer, New York.

Appendices

Appendix A. Supporting Data

All data generated as a result of this grant is intended for archiving. Data has been archived for many of the tasks (see below). Some projects/tasks are still ongoing and the datasets are in preliminary form and will be archived once they are finalized.

Datasets currently archived in the Bonanza Creek Long-Term Ecological Research data catalog are available at the following URLs:
https://portal.lternet.edu/nis/mapbrowse?packageid=knb-lter-bnz.591.2
https://portal.lternet.edu/nis/mapbrowse?packageid=knb-lter-bnz.592.2
https://portal.lternet.edu/nis/mapbrowse?packageid=knb-lter-bnz.590.2
http://www.lter.uaf.edu/data/data-detail/id/639/inline/data/data-detail/id/639
http://www.lter.uaf.edu/data/data-detail/id/640
http://www.lter.uaf.edu/data/data-detail/id/641
http://www.lter.uaf.edu/data/data-detail/id/639
http://www.lter.uaf.edu/data/data-detail/id/641
http://www.lter.uaf.edu/data/data-detail/id/640

Datasets currently archived in the Scenarios Network for Alaska + Arctic Planning catalog ar available at the following URLs:
http://ckan.snap.uaf.edu/dataset/time-series-of-terrestrial-ecosystem-carbon-stocks-and-fluxes-snow-cover-and-organic-layer-mois
http://ckan.snap.uaf.edu/dataset/decadal-averages-of-ecosystem-carbon-balance-snow-cover-and-soil-moisture-by-landscape-conserva
http://ckan.snap.uaf.edu/dataset/alfresco-model-outputs-linear-coupled-annual
http://ckan.snap.uaf.edu/dataset/alfresco-model-outputs-linear-coupled-relative-spatial-fire-and-vegetation
http://ckan.snap.uaf.edu/dataset/fire-and-vegetation-plots-csvs-alfresco-model-outputs-linear-coupled

Appendix B. List of Scientific/Technical Publications

Articles in peer-reviewed journals:

Breen, A. L., Bennett, A., Jandt, R., Kurkowski, T., Lindgren, M., McGuire, A. D., Rupp, T. S. (2016) Forecasting landscape change in response to projected changes in climate, fire regime, and fire management. Alaska Fire Science Consortium Research Brief 2016-1.

Brown C.D., Liu J., Yan G., and Johnstone J.F. 2015. Disentangling legacy effects from environmental filters of post-fire assembly of boreal tree assemblages. *Ecology* **96**: 3023–32.

Genet, H., McGuire, A.D., Barrett, K., Breen, A., Euskirchen, E.S., Johnstone, J.F., Kasischke, E.S., Melvin, A.M., Bennett, A., Mack, M.C., Rupp, T.S., Schuur, A.E.G., Turetsky, M.R., Yuan, F., 2013. Modeling the effects of fire severity and climate warming on active layer thickness and soil carbon storage of black spruce forests across the landscape in interior Alaska. Environmental Research Letters 8, 045016. doi:10.1088/1748-9326/8/4/045016.

Jafarov E.E., Romanovsky V.E., Genet H., McGuire A.D., Marchenko S.S. 2013. The effects of fire on the thermal stability of permafrost in lowland and upland black spruce forests of interior Alaska in a changing climate. Environmental Research Letters 8, 035030. doi:10.1088/1748-9326/8/3/035030

Johnstone J.F., Allen C.D., Franklin J.F., *et al.* 2016. Changing disturbance regimes, ecological memory, and forest resilience. *Frontiers in Ecology and the Environment. In press.*

Melvin, A.M., Mack, M.C., Johnstone, J.F., McGuire, A.D., Genet, H., Schuur, E.A.G. 2015. Differences in ecosystem carbon distribution and nutrient cycling linked to forest tree species composition in a mid-successional boreal forest. *Ecosystems* 18: 1472-1488.

Rupp, T.S., P. Duffy, M. Leonawicz, M.Lindgren, A. Breen, T. Kurkowski,1A. Floyd, A. Bennett, and L. Krutikov. 2016. Climate simulations, land cover, and wildfire. Chapter 2 (pages 17-52) in Z. Zhu and A.D. McGuire, eds., *Baseline and projected future carbon storage and greenhouse-gas fluxes in ecosystems of Alaska.* U.S. Geological Survey Professional Paper 1826, 196 p., http://dx.doi.org/10.3133/pp1826.

Walker X., Mack M., Johnstone J.F., 2015 “Stable carbon isotope analysis reveals widespread drought stress in boreal black spruce forests” Global Change Biology, DOI: 0.1111/gcb.12893

Walker X., Johnstone J.F., 2014 “Widespread negative correlations between black spruce growth and temperature across topographic moisture gradients in the boreal forest” Environmental Research Letters 9:064016

Technical reports – published

Genet, H., Y. He, A.D. McGuire, Q. Zhuang, Y. Zhang, F. Biles, D.V. D'Amore, X. Zhou, and K.D. Johnson. 2016. Terrestrial carbon modeling: Baseline and projections in upland ecosystems. Chapter 6 (pages 105-132) in Z. Zhu and A.D. McGuire, eds., *Baseline and projected future carbon storage and greenhouse-gas fluxes in ecosystems of Alaska.* U.S. Geological Survey Professional Paper 1826, 196 p., http://dx.doi.org/10.3133/pp1826.

He, Y., H. Genet, A.D. McGuire, Q. Zhuang, B.K. Wylie, and Y. Zhang. 2016. Terrestrial carbon modeling: Baseline and projections in lowland ecosystems of Alaska. Chapter 7 (pages 133-158) in Z. Zhu and A.D. McGuire, eds., *Baseline and projected future carbon storage and greenhouse-gas fluxes in ecosystems of Alaska.* U.S. Geological Survey Professional Paper 1826, 196 p., http://dx.doi.org/10.3133/pp1826.

McGuire, A.D., B.K. Wylie, D.V. D'Amore, X. Zhou, T.S. Rupp, H. Genet, Y. He, S. Stackpoole, and Z. Zhu. 2016. Executive Summary-Baseline and Projected Future Carbon Storage and Greenhouse-Gas Fluxes in Ecosystems of Alaska. Pages 1-3 in Z. Zhu and A.D. McGuire, eds., *Baseline and projected future carbon storage and greenhouse-gas fluxes in ecosystems of Alaska.* U.S. Geological Survey Professional Paper 1826, 196 p., http://dx.doi.org/10.3133/pp1826.

McGuire, A.D., T.S. Rupp, T. Kurkowski, and S. Stackpoole. 2016. Introduction. Chapter 1 (pages 5-16) in Z. Zhu and A.D. McGuire, eds., *Baseline and projected future carbon storage and greenhouse-gas fluxes in ecosystems of Alaska.* U.S. Geological Survey Professional Paper 1826, 196 p., http://dx.doi.org/10.3133/pp1826.

McGuire, A.D., H. Genet, Y. He, S. Stackpoole, D.V. D'Amore, T.S. Rupp, B.K. Wylie, X. Zhou, and Z. Zhu. 2016. Alaska Carbon Balance. Chapter 9 (pages 189-196) in Z. Zhu and A.D. McGuire, eds., *Baseline and projected future carbon storage and greenhouse-gas fluxes in ecosystems of Alaska.* U.S. Geological Survey Professional Paper 1826, 196 p., http://dx.doi.org/10.3133/pp1826.

Wylie, B.K., N.J. Pastick, K.D. Johnson, N. Bliss, and H. Genet. 2016. Soil carbon and permafrost estimates and susceptibility to climate change in Alaska. Chapter 3 (pages 53-76) in Z. Zhu and A.D. McGuire, eds., *Baseline and projected future carbon storage and greenhouse-gas fluxes in ecosystems of Alaska.* U.S. Geological Survey Professional Paper 1826, 196 p., http://dx.doi.org/10.3133/pp1826.

Zhu, Z., and McGuire, A.D., eds. 2016. *Baseline and projected future carbon storage and greenhouse-gas fluxes in ecosystems of Alaska.* U.S. Geological Survey Professional Paper 1826, 196 p., http://dx.doi.org/10.3133/pp1826.

Conference and symposium abstracts

Genet H., He Y., McGuire A.D., Zhuang Q., Zhu Z., Pastick N.J., Wylie B., Johnson K., Rupp S.T., Breen A., Bennett A. 2016. Quantifying the impact of permafrost dynamics on soil carbon accumulation in response to climate change and wildfire intensification in Alaska. International Conference On Permafrost meeting, Postdam, Germany.

Genet H., Zhang Y., McGuire A.D., He Y., Johnson K., D'Amore D., Zhou X., Bennett A., Biles F., Bliss N., Breen A., Euskirchen E.S., Kurkowski T., Pastick N., Rupp S., Wylie B., Zhu Z., Zhuang Q. 2015. The importance of permafrost thaw, fire and logging disturbances as driving factors of historical and projected carbon sequestration in Alaskan terrestrial ecosystems. North American Carbon Program annual meeting, Washington DC, USA.

Genet H., Zhang Y., McGuire A.D., He Y., Johnson K., D'Amore D., Zhou X., Bennett A., Biles F., Bliss N., Breen A., Euskirchen E.S., Kurkowski T., Pastick N., Rupp S., Wylie B., Zhu Z., Zhuang Q. 2014. The importance of permafrost thaw, fire and logging disturbances as driving factors of historical and projected carbon dynamics in Alaskan ecosystems. American Geophysical Union annual meeting, San Francisco, USA.

Genet H., Barrett K., McGuire A.D., Kasischke E.S., Turetsky M., Rupp S., Euskirchen E., Yuan F.M. 2013. Modeling the effects of fire severity on soil organic horizons and its effects on permafrost and vegetation composition in Interior Alaska. International Boreal Forest Research Association meeting, Edmonton, Alberta, CAN.

Genet H., McGuire A.D., Johnstone J.F., Breen A.L., Euskirchen E.S., Mack M.C., Melvin A.M., Rupp T.S., Schuur E.A., Yuan F. 2013. Modeling post-fire vegetation succession and its effect on permafrost vulnerability and carbon balance. American Geophysical Union annual meeting, San Francisco, CA, USA.

Genet H., Barrett K.M., Johnstone J.F., McGuire A.D., Yuan F., Euskirchen E.S., Kasischke E.S., Rupp S.T., Turetsky M.T. 2013. Modeling the effects of changes in fire severity on soil organic horizons and forest composition in Interior Alaska. North American Carbon Program annual meeting. Albuquerque, NM, USA.

Genet H., McGuire A.D., Johnstone J.F., Breen A.L., Euskirchen E.S., Mack M.C., Melvin A.M., Rupp T.S., Schuur E.A., Yuan F. 2013. Modeling post-fire vegetation succession and its effect on permafrost vulnerability and carbon balance. American Geophysical Union annual meeting, San Francisco, USA.

Genet H., McGuire A.D., He Y., Johnson K., Wylie B., Pastick N., Zhuang Q., Zhu Z., Zhang Y. 2015. Identifying the main drivers of soil carbon response to climate change in arctic and boreal Alaska. American Geophysical Uniong annual meeting, San Francisco, USA.

Jafarov E.E., Genet H., Romanovsky V.E., McGuire A.D., Marchenko S.S. 2012. The effects of forest fire on the frozen soil thermal state. American Geophysical Union annual meeting San Francisco, CA, USA.

Jean M., Alexander H.D., Mack M.C., Johnstone J.F. 2015. Diverging patterns of moss succession in deciduous and coniferous trajectories in boreal Alaska. Association of Canadian Universities for Northern Science (ACUNS) student meeting, Calgary, Alberta, CAN.

Jean M., Johnstone J.F., Mack M.C., Melvin A.M. 2015. Effects of environmental conditions and leaf litter on boreal feather mosses: Implications for ecosystem processes. Ecology and Evolution of Managed Landscapes, 10th annual meeting of the Canadian Society for Ecology and Evolution (CSEE), Montreal, Quebeca, CAN.

Jean M., Johnstone J.F., Mack M.C., Alexander H.D. 2014. How does variation in moss communities and functional traits across forest types influence successional trajectories among deciduous, coniferous and mixed stands in interior Alaska? Genomes to/aux biomes, 9th annual meeting of the Canadian Society for Ecology and Evolution (CSEE), Montreal, Quebec, CAN.

Jean M., Johnstone J.F., Alexander H.D., Melvin A.M., and Mack M.C. 2013. What are the roles of mosses in stabilizing ecosystem processes among alternate types of boreal forests? Long Term Ecological Research (LTER) group symposium, Fairbanks, Alaska, USA (poster presented by Jill Johnstone).

Johnson K.D., Bliss N., D'Amore D., Genet H., Mishra U., Pastick N.J., Wylie B.K. 2015. Multiple Soil Carbon Maps Facilitate Comparisons with Modeled Outputs. American Geophysical Union annual meeting, San Francisco, USA.

Johnstone, J.F., C.D. Brown, S. Kuleza. 2014. At the burning edge: Potential tree recruitment after fire at high latitude treelines. Genomes to Biomes: Canadian Society for Ecology and Evolution and Canadian Society of Zoologists joint conference, Montréal, Quebec, CAN.

Johnstone, J. F. 2013. Disturbance, resilience, and inertia of boreal forests under climate change. Invited keynote speaker, 16th Conference of the International Boreal Forest Research Association meeting, Edmonton, Alberta, CAN.

Johnstone, J.F. 2012. Mechanisms of resilience in boreal forests. 2012 Krajina Lecture, Botany Department, University of British Columbia, British Columbia, CAN.

Mack, M.C., H.D. Alexander, A.M. Melvin, M. Jean, and J.F. Johnstone, 2014. Plant functional traits reinforce alternate successional trajectories in Alaskan boreal forest. Ecological Society of America annual meeting, Sacramento, CA, USA.

McGuire A.D., Genet H. and Members of the Alaska Land Carbon Assessment Team. 2015. A synthesis of terrestrial carbon balance of Alaska and projected changes in the 21st Century: Implications for climate policy and carbon management at local, regional, national, and

international scales. International Boreal Forest Research Association annual meeting, Rovaniemi, Finland.

Melvin, A.M., Mack, M.C., Johnstone, J.F., Schuur, E.A.G. 2013. Nutrient cycling in mid-successional Alaskan boreal forest. American Geophysical Union annual meeting, San Francisco, CA, USA.

Melvin, A.M., Mack, M.C., Frey, M., Johnstone, J.F., Schuur, E.A.G. 2013. Forest management effects on carbon, permafrost, and plant successional trajectories in interior Alaska. International Boreal Forest Research Association meeting, Edmonton, Alberta, CAN.

Melvin, A. M. 2013. Effects of fire management on vegetation, carbon storage, and permafrost thaw. Alaska Fire Science Consortium webinar.

Melvin, A.M., Mack, M.C., Johnstone, J.F., Schuur, E.A.G. 2012. Investigating tree species effects on plant-soil-microbial feedbacks in Alaskan boreal forest. Long Term Ecological Research All Scientists Meeting, Estes Park, CO, USA.

Pastick N.J., Jorgenson M.T., Minsley B.J., Wylie B.K., Brown D.R.N., Genet H., Johnson K.D., McGuire A.D., Kass M.A., Knight J.F. 2015. Towards a better understanding of the sensitivity of permafrost and soil carbon to climate and disturbance-induced change in Alaska. American Geophysical Union annual meeting, San Francisco, USA.

Rupp, T. S. 2015. Climate and Wildfire (Keynote Address). Alaska Wildland Fire Coordinating Group, Interagency Fall Fire Review Fairbanks, AK, USA.

Rupp, T. S. 2015. Projections of climate and vegetation change. Feedbacks of Alaska's Boreal Forest to the Climate System. Bonanza Creek Long-Term Ecological Research Symposium, Fairbanks, AK, USA.

Turner, M.G. and Johnstone, J. F. 2014. Changing climate and novel fire regimes alter tree recruitment and postfire succession in northern conifer forests. Invited presentation, organized oral session on Climate Warming, Changing Disturbance Regimes, and Forest Resilience at the Ecological Society of America annual meeting, Sacramento, CA, USA.

Appendix C. Draft User Guide

Research Summary: Projecting vegetation and wildfire response to changing climate and fire management in interior Alaska

Amy L. Breen, Alec Bennett, Tom Kurkowski, Michael Lindgren, Julien Schroder, A. David McGuire, and T. Scott Rupp, University of Alaska Fairbanks

Project Summary

The extent and frequency of wildfires in Alaska's boreal forest are predicted to increase in the coming century. In addition to natural sources of ignition, military lands in Interior Alaska are vulnerable to human ignitions due to their proximity to the road system and training activities. Recent wildfires such as the 2013 Stuart Creek fire, sparked by an explosive ordinance on an army weapons range, demonstrate the need to test alternative fire management scenarios. One method that might reduce future large fires is to increase the level of fire suppression by changing the fire management planning options (FMPOs) for these areas from mostly Limited to Full protection. But will that method work well long-term?

We used the Alaska Frame-based Ecosystem Code (ALFRESCO) vegetation-fire computer model to investigate how increasing fire suppression on military training lands could influence the extent and frequency of wildfire activity within the Upper Tanana Hydrologic Basin through the 21st century. ALFRESCO simulates wildfire, vegetation establishment, and succession—the dominant landscape-scale processes in boreal ecosystems in Alaska. We used a pair of climate models to bracket the uncertainty associated with projecting landscape changes. To simplify outputs, we focused on a single Representative Concentration Pathway (RCP) for greenhouse gases to drive the ALFRESCO model.

Changing all military lands within the study area to Full protection led to an increased number of fires, but a decrease in the total area burned, through 2100 compared to the status quo (mostly Limited protection). These projected changes in fire regime also increased the amount of late successional coniferous forest present on the landscape. In contrast, keeping the areas in mostly Limited protection leads to more early successional deciduous forest on the landscape through the end of the century.

The two climate models, however, drive the greater difference in results. Both models project future conditions warmer than today, but NCAR-CCSM4 projects a much warmer and drier future than MRI-CGCM3. Thus, ALFRESCO outputs using NCAR-CCSM4 predict greater fire activity and a declining conifer:deciduous ratio through the end of the 21st century. In contrast, ALFRESCO outputs using the MRI-CGCM3 model show an increase in the conifer:deciduous ratio over time. The effects of the alternative fire management planning options are subtle, so we recommend an economic study to determine if the cost of implementing such changes is warranted. Furthermore, we caution the results of this study are specific to a limited area within Interior Alaska. Future work will investigate whether modeling more large-scale fire suppression yields similar results.

Acknowledgements: This work evolved from discussions between researchers and land managers at Fort Wainwright during multiple meetings at University of Alaska Fairbanks from 2013-2015. Our research was supported by the Department of Defense Strategic Environmental Research and Development Program through the funded project "Identifying indicators of state change and forecasting future vulnerability in Alaska boreal forest" (Grant No. RC-2109). We thank Nancy Fresco, Hélène Genet, Randi Jandt, and Alison York for comments that greatly improved this research summary.

Where can I learn more about wildfire and wildfire management in Alaska?

Alaska Wildland Fire Information:
https://akfireinfo.com/

Alaska Interagency Coordination Center:
fire.ak.blm.gov

Alaska Division of Forestry, Wildland Fire & Aviation:
http://forestry.alaska.gov/wildland

Alaska Fire Science Consortium:
www.akfireconsortium.uaf.edu

Figure 1. Map showing the A) Upper Tanana Hydrologic Basin study area in Interior Alaska and B) the location of the study area within Alaska. Fire management planning options are shown within the study area, and military lands are outlined in gray. In the inset map, the Intermontane Boreal Ecoregion (Nowacki et al. 2001) over which the ALFRESCO model is calibrated is shown in green and the specific study area is outlined in red. The military lands within the study area comprise about 16% of the total land area.

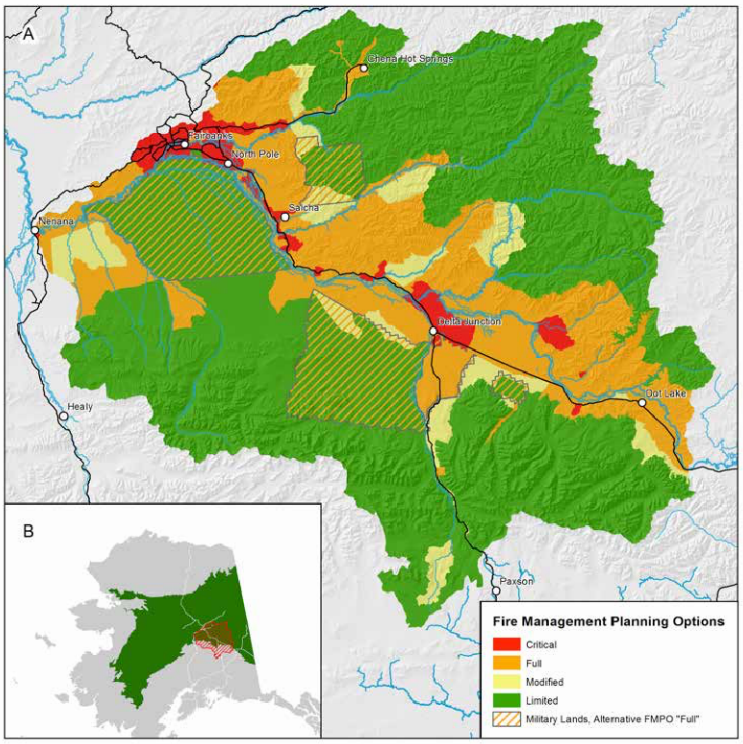

Where are U.S. Department of Defense lands located in Alaska?

The U.S. Department of Defense (DoD) manages approximately 70,000 km^2 (~17,300,000 acres) of land in Alaska. Over 95% of military land is located in the boreal forest of Interior Alaska, associated with Fort Wainwright and Eielson Air Force Base near Fairbanks, and with Fort Greely near Delta Junction. These lands cross two ecologically, economically, and culturally important regions within the Intermontane Boreal Ecoregion – the Tanana-Kuskokwim Lowlands, which covers about 520,000 km^2 (~128,500,000 acres), and the Yukon-Tanana Uplands, which covers about 1020,000 km^2 (~252,050,000 acres)(Nowacki et al. 2001, Fig. 1).

Wildfire is the most widespread natural disturbance in these ecoregions. The Yukon-Tanana Uplands have the third highest incidence of lightning strikes in Interior Alaska (Dissing & Verbyla 2003). In addition to high natural sources of ignition, these military lands also experience high human ignition pressures due to their proximity to the road system and urban areas, and the frequency of military testing and training activities. Thus, the Alaska Fire Service designates these military lands in a distinct fire management zone so local fire managers can address the unique needs of military land management.

All lands in Alaska, including military lands, are designated by Fire Management Planning Options (FMPO) that provide for a full range of initial suppression responses from aggressive control and extinguishment to surveillance (sidebar). We chose to focus our modeling effort on the Upper Tanana Hydrologic Basin study area, as it encompasses Fort Wainwright, Eielson Air Force Base, and Fort Greeley, along with the larger urban communities on the road system in Interior Alaska (Fig. 1). The military lands within the study area comprise about 16% of the total land area.

What are the four Fire Management Planning Options designated in Alaska?

Fire management planning options (FMPOs) in Alaska designate different levels of protection (AWFCG 2010). Values-at-risk, ecological considerations, and suppression costs were all considered to develop the management option criteria. These options include:

1) **Critical Protection** - suppression action provided on a wildland fire that threatens human life, inhabited property, designated physical developments and structural resources such as those designated as National Historic Landmarks. The suppression objective is to provide complete protection to identified sites and control the fire at the smallest acreage reasonably possible. The allocation of suppression resources to fires threatening critical sites is given the highest priority.
2) **Full Protection**- suppression action provided on a wildland fire that threatens uninhabited private property, high-valued natural resource areas, and other high-valued areas such as identified cultural and historical sites. The suppression objective is to control the fire at the smallest acreage reasonably possible. The allocation of suppression resources to fires receiving the full protection option is second in priority only to fires threatening a critical protection area.
3) **Modified Protection** - suppression action provided on a wildland fire in areas where values to be protected do not justify the expense of full protection. The suppression objective is to reduce overall suppression costs without compromising protection of higher-valued adjacent resources. The allocation of suppression resources to fires receiving the modified protection option is of a lower priority than those in critical and full protection areas. A higher level of protection may be given during the peak burning periods of the fire season than early or late in the fire season.
4) **Limited Protection** - lowest level of suppression action provided on a wildland fire in areas where values to be protected do not justify the expense of a higher level of protection, and where opportunities can be provided for fire to help achieve land and resource protection objectives. The suppression objective is to minimize suppression costs without compromising protection of higher-valued adjacent resources. The allocation of suppression resources to fires receiving the limited protection option is of the lowest priority. Surveillance is an acceptable suppression response as long as higher valued adjacent resources are not threatened.

Fire is a natural part of the boreal forest—an ecosystem dominated by black and white spruce. (T. S. Rupp)

How do vegetation and wildfire interact to create the landscape mosaic found in Interior Alaska?

The boreal region of Interior Alaska is comprised of a mosaic of coniferous, deciduous, and mixed forest ecosystems interspersed with herbaceous or shrub-by wetlands. Coniferous stands dominated by black spruce, or *Picea mariana*, are the most abundant forest type in Interior Alaska, and are frequently underlain by permanently frozen, or permafrost, soils. Black spruce forests are highly flammable and typically burn during stand-replacing fires every 70-130 years. Stable cycles of fire disturbance and spruce self-replacement have persisted for over 8,000 years since black spruce came to dominate the evergreen forests of Interior Alaska.

White spruce, or *Picea glauca*, is less flammable than black spruce, as illustrated by a long history during the Holocene of white spruce dominance (8-10,000 years before present) with concurrent low fire frequency. However, the juxtaposition of black and white spruce forest stands on the landscape means that white spruce often burns in tandem within the fire regime of black spruce, as do shrubby or herbaceous wetlands where surface organic soils can serve as a ground fuel to carry fire during dry months.

In contrast, deciduous early successional stands have less ground fuel, and while they can burn—especially in warm spring seasons before green-up—they often reduce the spread of fire relative to other ecosystem types during the height of the growing season. Projected changes in future climate, however, could affect the stability of boreal ecosystems through an increase in fire size, frequency and severity.

Why simulate an altered fire management scenario using the ALFRESCO computer model? How did we alter the current fire management planning designations?

To provide meaningful information to fire managers about the potential future impacts of climate change on fire regimes at a landscape scale, a University of Alaska Fairbanks research team met multiple times with fire and resource management groups that work on military lands in Interior Alaska. Fire management can influence the natural fire regime by affecting the spatial patterning and timing of fire occurrence, and thus the successional state of an ecosystem within a managed area.

The groups discussed relevant fire management scenarios that could be used to alter current wildfire trends on DoD training lands and to explore their influence on future fire and vegetation dynamics. Recent wildfires demonstrate the need to test alternate FMPOs as one potential method to reduce future large fires and/or manage associated smoke impacts to communities. We investigated how changing these FMPOs within military training lands would influence the future fire regime and concurrent boreal forest vegetation dynamics.

To simulate fire management scenarios, we used the Alaska Frame-based Ecosystem Code (ALFRESCO, Fig. 2) vegetation-fire model. Since one important aspect of fire spread is suppression effort, we modified ALFRESCO's fire routine to include the general effects of fire suppression by influencing the likelihood of fire to spread after it has started. We informed the fire routine with information on acreage burned ratios across the different FMPOs reported by Calef et al. (2015). We then simulated two different FMPO scenarios:

1) the current FMPO designation, and
2) a hypothetical alternative FMPO designation in which we changed the protection status of all military lands that are currently designated as either Modified or Limited protection to Full protection (Fig. 1).

Based on these two model scenarios we then analyzed the difference, and ultimately the potential effects on fire regime and vegetation dynamics, of an altered FMPO scenario.

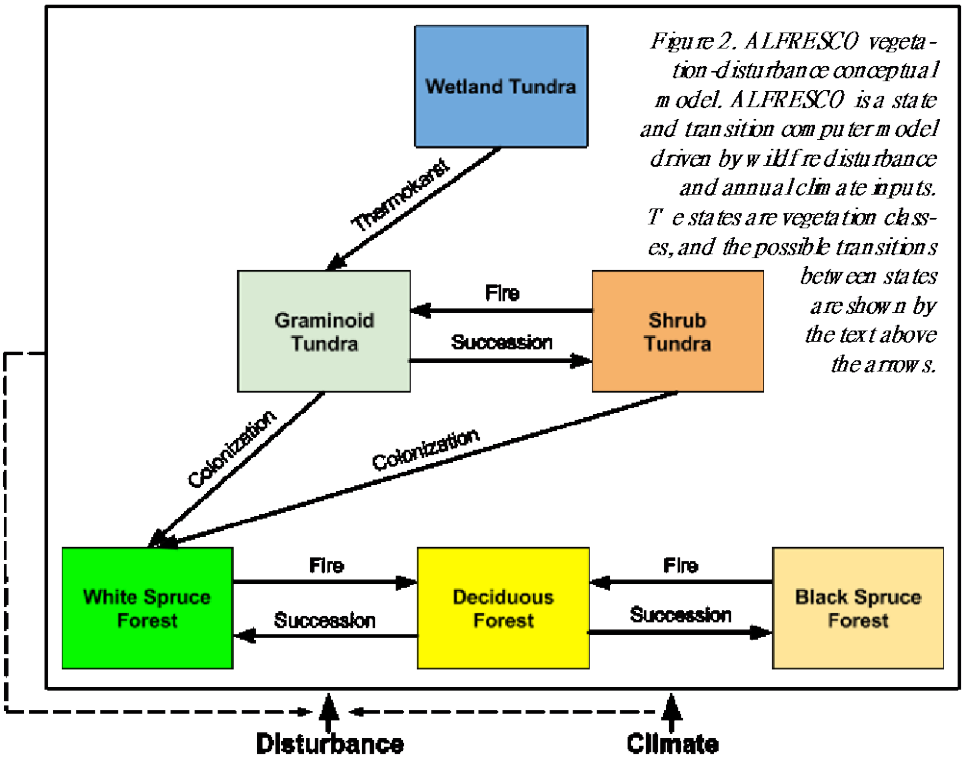

Figure 2. ALFRESCO vegetation-disturbance conceptual model. ALFRESCO is a state and transition computer model driven by wildfire disturbance and annual climate inputs. The states are vegetation classes, and the possible transitions between states are shown by the text above the arrows.

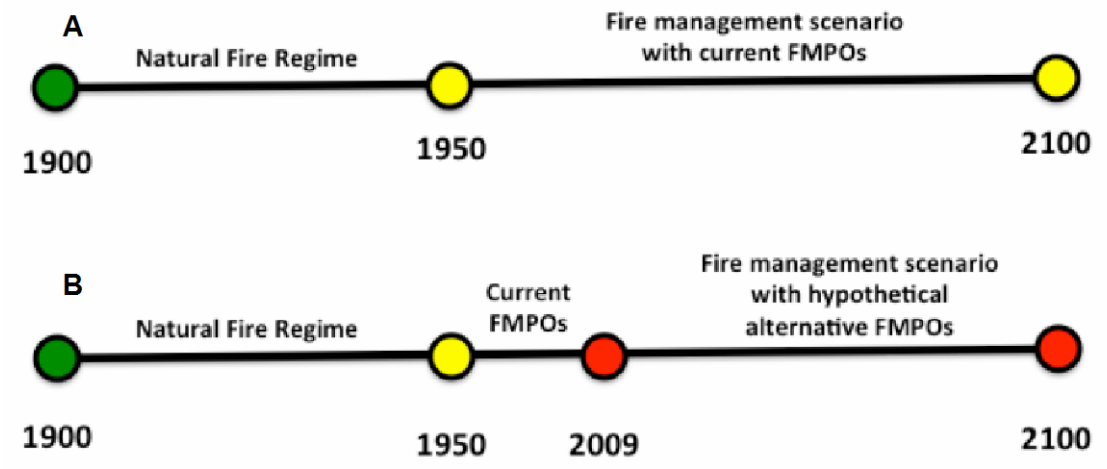

Figure 3. Timeline showing fire management scenarios implemented in the ALFRESCO computer model for A) current FMPOs and B) hypothetical alternative FMPOs for the Upper Tanana Hydrologic Basin in Interior Alaska. The hypothetical alternative fire management scenario changes all military lands within the study area to the full protection fire management planning option.

The timeline for implementation of the FMPOs differs (Fig. 3). After model spin-up, transition from a natural fire regime, equivalent to the limited fire protection class, to the current FMPOs occurs in 1950. While we are aware FMPOs were not implemented until the mid-1980s, fire suppression was commonplace in urban areas before this time, so this early date to switch to the current FMPOs is justified and is a better match to the historical record. The hypothetical future FMPO scenario is implemented in 2009 because this is the year the climate data switches from observed to projected.

Model calibration was performed over the Intermontane Boreal Ecoregion in Interior Alaska. The FMPO simulations were analyzed for the Upper Tanana Hydrologic Basin study area only. For each model run, 200 replicates were generated. All model data inputs and outputs are at a 1 x 1 km spatial resolution.

What were the specific questions addressed in this research?

We used ALFRESCO to investigate how altering FMPOs within military training lands influences the extent and frequency of wildfire activity within the Upper Tanana Hydrologic Basin through the 21st century.

We performed separate model simulations using two alternative fire management scenarios. The first scenario uses the current FMPO designation for the Upper Tanana Hydrologic Basin, and the second scenario represents a hypothetical scenario in which military lands within the study area are changed from primarily Limited and Modified to 100% Full protection (Figs. 2 & 4).

We addressed the following questions:

1) How might increasing fire suppression within military training land boundaries influence the frequency and extent of wildfire activity and vegetation dynamics on, and adjacent to, military lands in the Upper Tanana Hydrologic Basin during the 21st century?
2) How does the frequency and extent of future wildfire activity and vegetation dynamics vary depending on the driving climate scenario?

What climate models and greenhouse gas scenarios are used to drive the ALFRESCO computer model?

ALFRESCO requires mean monthly temperature and precipitation inputs. The source of this information can either be historical data or future climate scenarios generated by General Circulation Models (GCMs). We used a new generation of GCMs and projections (AR5; IPCC 2013) that use representative concentration pathways, or RCPs. RCPs are defined by varying degrees of "radiative forcing", or the balance between incoming and outgoing radiation. A positive forcing (more incoming radiation) tends to warm the system, while a negative forcing (more outgoing energy) tends to cool the system. Increasing concentrations of greenhouse gases, such as carbon dioxide, cause a positive forcing.

Two GCMs, operating under the anticipated RCP 8.5 emissions scenario, were chosen to represent the range of warming and precipitation expected to occur across Alaska:

- the Community Climate System Model, v. 4.0 (NCAR-CCSM4), and
- the Meteorological Research Institute-Coupled General Circulation Model v. 3.0 (MRI-CGCM3)

These were chosen among a suite of AR5 GCMs ranked among the top five best performing models across Alaska and the Arctic using the methods described in Walsh et al. (2008). These two climate models were selected because they produce the largest differences in simulated future area burned, where NCAR-CCSM4 burns the most and MRI-CGCM3 burns the least (Fig. 4).

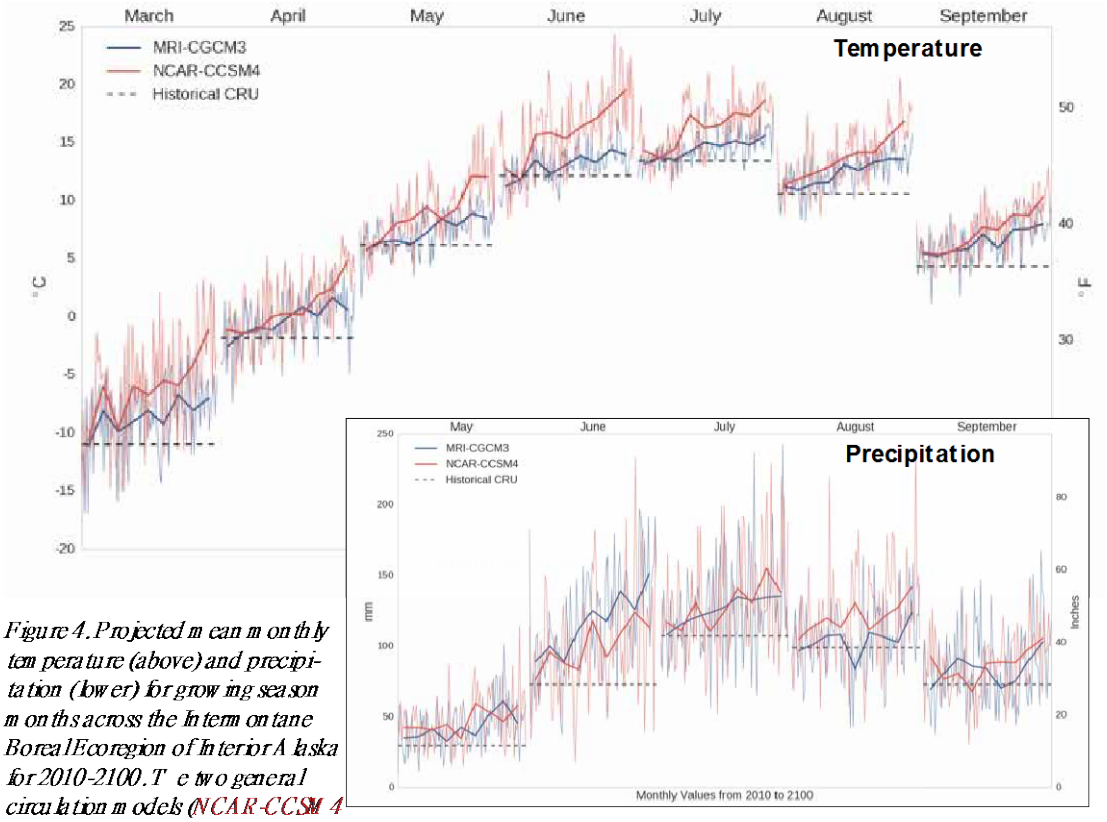

Figure 4. Projected mean monthly temperature (above) and precipitation (lower) for growing season months across the Intermontane Boreal Ecoregion of Interior Alaska for 2010-2100. The two general circulation models (NCAR-CCSM4 and MRI-CGCM3) and single scenario (RCP 8.5) used to drive the ALFRESCO computer model are presented. Narrow lines are yearly monthly averages showing the annual variability, bold lines are decadal monthly averages, and the dashed line shows the historical average from 1980-2010.

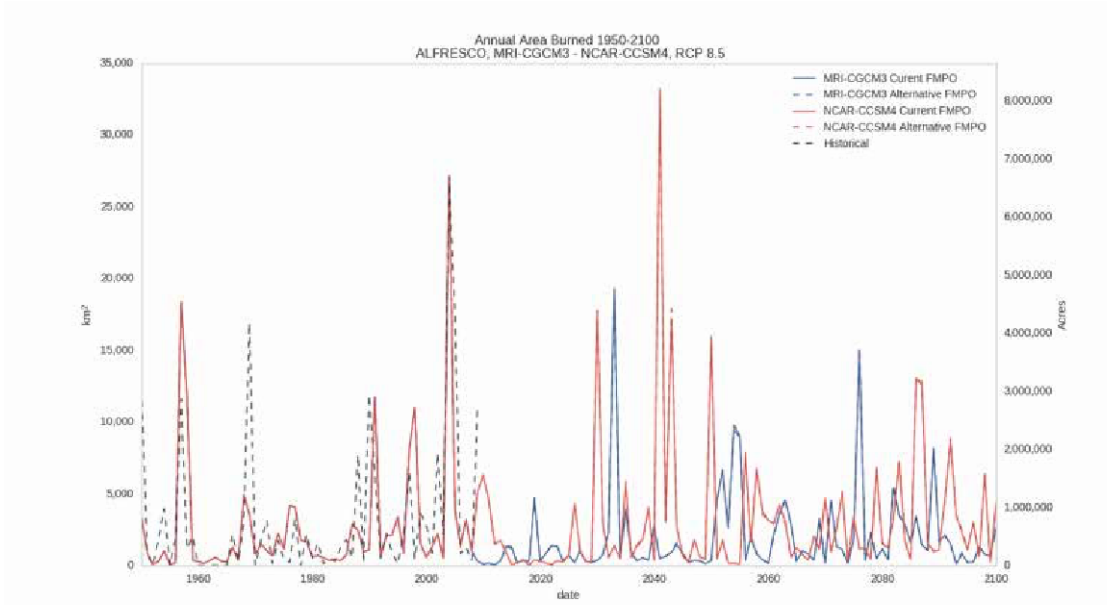

Figure 5. Annual area burned over the historical (1950-2009) and projected (2010-2100) periods for the Interm ontane Boreal Ecoregion in Interior Alaska. Model results are presented for fire management scenarios driven by the NCAR-CCSM 4 and MRI-CGCM 3 global circulation models for the RCP 8.5 scenario. Data presented are the average from 200 model replicates. Dashed lines indicating the alternative FMPO scenarios are essentially indistinguishable from the current FMPO scenarios (solid red and blue).

What do the ALFRESCO model results tell us about potential future fire regimes and landscape dynamics in Interior Alaska?

The ALFRESCO results show that changing all military lands within the study area to full protection led to a modest increase in the number of fires per decade, while decreasing the annual area and cumulative area burned through 2100 compared to the status quo (Figs. 5 & 6).

The greatest difference between the scenarios, however, is observed not in the comparison between FMPOs but between the two driving climate models. While the number of fires per decade is similar (~35) between the very warm and drier NCAR-CCSM 4 and the moderately warm and wetter MRI-CGCM 3 model, the annual and cumulative area burned is not. Projected fire activity differs significantly between the two models, with the greatest difference observed at the end of the 21st century, when the cumulative area burned is over 10,000 km² (2,470,000 acres) greater for the NCAR-CCSM 4 model compared to MRI-CGCM 3 model (Fig. 6).

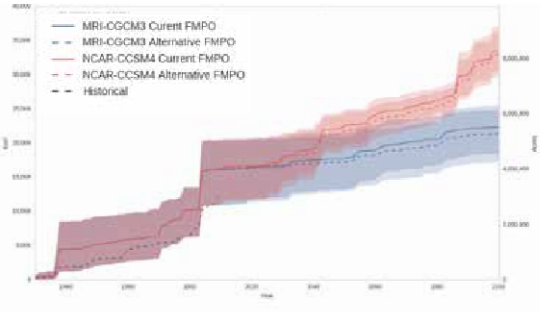

Figure 6. Cumulative area burned during the historical (1950-2009) and projected (2010-2100) periods for the Upper Tanana Hydrological Basin in Interior Alaska. Model results are presented for fire management scenarios driven by the NCAR-CCSM 4 and MRI-CGCM 3 global circulation models for the RCP 8.5 scenario. Data presented are means and shading indicates results from 200 model replicates.

These projected changes in fire regime also led to concurrent changes in the amount of late successional coniferous forest and early-successional deciduous forest present on the landscape in contrast to the current FMPOs (Fig. 7). Similar to the fire regime, the greater difference in vegetation distribution and composition is more attributable to the driving climate models than to differences in suppression activity. The greater fire activity in the warmer and drier NCAR-CCSM4 scenario leads to a declining conifer:deciduous ratio through the end of the 21st century, regardless of suppression regime, although suppression slows the shift. The moderately warm and wetter MRI-CGCM3 model projects the opposite trend– an increase in the conifer:deciduous ratio over time, again with suppression favoring a coniferous-dominated landscape. The driving climate models bracket the projected conifer:deciduous ratio from 0.5-2.0.

Overall, the simulated effects of the increased fire suppression scenario (i.e., the hypothetical alternative FMPOs) were subtle, and warrant additional analysis and research that could assess cost/benefit considerations and whether such changes to the FMPOs are warranted.

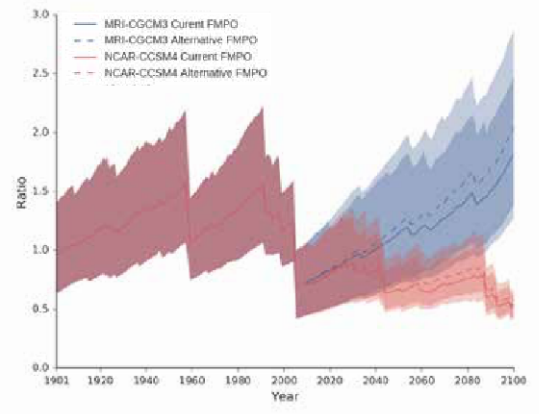

Figure 7. Conifer:Deciduous ratios for the model spin-up (1901-1949), historical (1950-2009) and projected (2010-2100) periods for the Upper Tanana Hydrological Basin in Interior Alaska. Model results are presented for fire management scenarios driven by the NCAR-CCSM4 and MRI-CGCM3 global circulation models for the RCP 8.5 emission scenario. Data presented are means and shading indicates results from 200 model replicates.

References

Alaska Wildland Fire Coordinating Group (AWFCG). 2010. Alaska Interagency Wildland Fire Management Plan. http://fire.ak.blm.gov/content/planning/aiwfmp_2010.pdf

Calef, M.P., A.V. Varvak, A.D. McGuire, F.S. Chapin III, and K.B. Reinhold. 2015. Recent Changes in Annual Area Burned in Interior Alaska: The Impact of Fire Management. Earth Interactions 19(5): 1-17.

Dissing, D., and Verbyla, D.L. 2003. Spatial patterns of lightning strikes in interior Alaska and their relations to elevation and vegetation. Canadian Journal of Forest Research (33): 770-782.

IPCC. 2013. Climate Change 2013: The Physical Science Basis. Contribution of Working Group I to the Fifth Assessment Report of the Intergovernmental Panel on Climate Change [Stocker, T.F., D. Qin, G.-K. Plattner, M. Tignor, S.K. Allen, J. Boschung, A. Nauels, Y. Xia, V. Bex and P.M. Midgley (eds.)]. Cambridge University Press, Cambridge, United Kingdom and New York, NY, USA, 1535 pp, doi:10.1017/CBO9781107415324.

Moss, R.H., Edmonds, J.A., Hibbard, K.A., Manning, M.R., Rose, S.K., van Vuuren, D.P., Carter, T.R., Emori, S., Kainuma, M., Kram, T., Meehl, G.A., Mitchell, J.F., Nakicenovic, N., Riahi, K., Smith, S.J., Stouffer, R.J., Thomson, A.M., Weyant, J.P. & Wilbanks, T.J. (2010). The next generation of scenarios for climate change research and assessment. Nature 463 (7282): 747-56.

Nowacki, G.; Spencer, P., Fleming, M., Brock, T. & Jorgenson, T. Ecoregions of Alaska: 2001. U.S. Geological Survey Open-File Report 02-297 (map).

Walsh, J.E., Chapman, W.L., Romanovsky V., Christensen, J.H. & Stendel, M. 2008. Global Climate Model Performance over Alaska and Greenland. Journal of Climate 21 (23): 6156-74.

For more information on this project, contact Amy Breen at albreen@alaska.edu